Title
CRL4-AMBRA1 Negatively Regulates CRL5 Ubiquitin E3 Ligases by Targeting Elongin C for Polyubiquitination and Proteasomal Degradation

Author
Chen, Si-Han

Publication Date
2016

Peer reviewed|Thesis/dissertation

CRL4-AMBRA1 negatively regulates CRL5 ubiquitin E3 ligases by targeting Elongin C for polyubiquitination and proteasomal degradation

by

Si-Han Chen

DISSERTATION

Submitted in partial satisfaction of the requirements for the degree of

DOCTOR OF PHILOSOPHY

in

Biophysics

in the

GRADUATE DIVISION

of the

UNIVERSITY OF CALIFORNIA, SAN FRANCISCO

[redacted]

Preface

This thesis describes my close-to-seven year scientific journey in the Krogan lab. These findings are an extension of our previous HIV-1-human proteomic study in which HIV-1 VIF was found to associate with the human protein AMBRA1 (Activating Molecule In BECN1-Regulated Autophagy Protein 1).

Until now our understanding of AMBRA1 has been limited to its role in autophagy regulation, which was my first hypothesis in testing VIF-AMBRA1 connection — I hypothesized that HIV-1 VIF might perturb host autophagy pathway via VIF-AMBRA1 protein-protein interaction. Despite much effort, I found that VIF expression does not affect autophagy in the absence and in the presence of autophagy stimuli. Surprisingly, VIF interacts with another poorly understood AMBRA1 protein complex, $CRL4^{AMBRA1}$, in which AMBRA1 serves as a substrate receptor in a CRL4 ubiquitin E3 ligase. Through a series of rigorous hypothesis testing in combination with discovery-based proteomics, I found that $CRL4^{AMBRA1}$ has a previously unknown function in negatively regulating CRL5 and CRL2 ubiquitin E3 ligases including the viral $CRL5^{VIF}$ complex; this underlies the interaction we found with VIF and AMBRA1.

Driven by the proposed mechanism supported by the biochemical data, I sought to understand the functional importance of $CRL4^{AMBRA1}$ in human and viral CRL5 regulation, specifically to investigate its impact on CRL^{SOCS3}-regulated and $CRL5^{VIF}$-regulated pathways. In CRL^{SOCS3}-regulated IL-6/STAT3 signaling, I found that $CRL4^{AMBRA1}$ has a prominent and straightforward effect that appears to correlate with attenuation of CRL^{SOCS3} ubiquitin E3 ligase

activity by $CRL4^{AMBRA1}$. I also showed that AMBRA1 modulates $CRL5^{VIF}$-mediated degradation of the antiviral factor APOBEC3G in co-transfection experiments; it however remains to be explored to what extent $CRL4^{AMBRA1}$ influences HIV-1 replication kinetics by modulating $CRL5^{VIF}$ function, as the results from my HIV-1 infection experiments indicate that AMBRA1 may play multiple roles at different stages of HIV-1 life cycle.

Nevertheless, from uncovering the substrates of $CRL4^{AMBRA1}$ to studying the mechanism and functional relevance of one substrate targeted by $CRL4^{AMBRA1}$, I am pleased to end this chapter of my professional life. I am grateful to my thesis advisor, Nevan Krogan, for giving me plenty of room to explore and grow as a scientist. It is such a privilege to be able to study my PhD at UCSF, a stimulating and nurturing environment for scientists. Although it is unavoidable to have a few hiccups in every research project, I enjoy my research work and every little piece of evidence I collected from numerous experiments. Hereby, I share the graphical abstract art of my thesis — in this CRL puzzle, AMBRA1 as the red ghost pursues the PAC-MAN VIF and SOCS3, which consume the substrates Cherry and Strawberry, respectively. AMBRA1 also acts as an avatar of myself who needs to obtain her PhD before stepping into the bomb which might terminate her scientific career. As intimidating as it sounds, you will find out in chapter one that the bomb acts as a re-activation mechanism that allows ghosts and PAC-MAN alike to function properly even if they are unable to fulfill their goals in this particular stage of their lives.

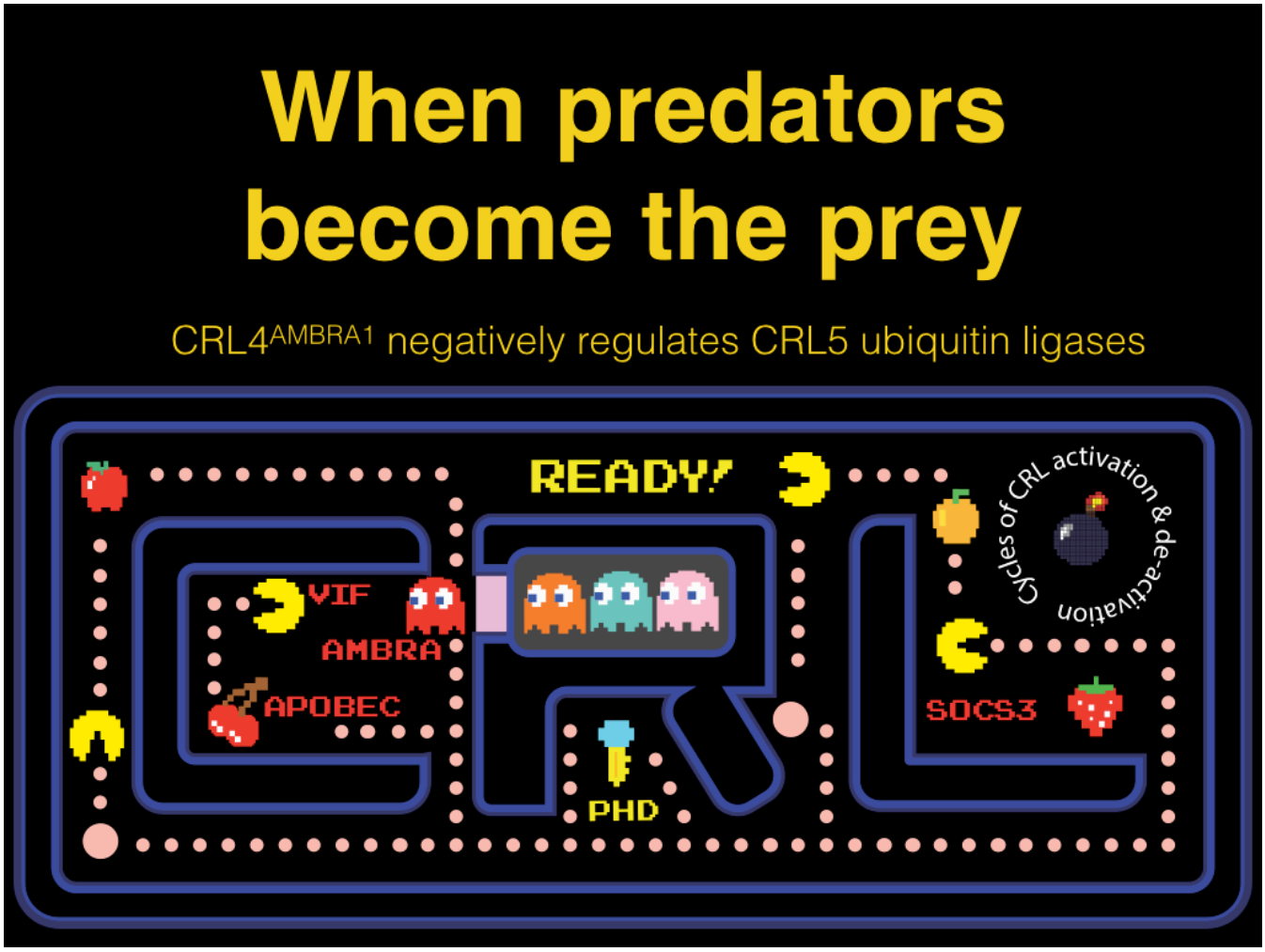
When predators become the prey
CRL4AMBRA1 negatively regulates CRL5 ubiquitin ligases
READY!
VIF
AMBRA
APOBEC
PHD
SOCS3
Cycles of CRL activation & de-activation

Table of Contents

List of Figures

List of Figures (Continued)

List of Figures (Continued)

List of Tables

Acknowledgements

I would like to thank my thesis advisor, Nevan Krogan, for giving me the opportunity to work on this challenging project, which has helped me reflect on strategies I have taken to approach scientific questions. It can be a bitter pill to swallow when a hypothesis failed, but it is also important to quickly synthesize new hypotheses and reset my priorities. I have learned to become a better scientist with those experiences. With federal funding becomes more and more limited every year, I can only imagine how Nevan can be so successful in acquiring funding to maintain such a big laboratory. It can be a huge investment on a risky project with long turnaround time. I really appreciate Nevan for keeping his faith and continue supporting this project.

I also thank my thesis committee John Gross and Jay Debnath for spending time to discuss my research progress regularly at committee meetings and one-on-one meetings. My first-year lab rotation advisors Yifan Cheng and Matt Jacobson introduced me to different aspects structural biology, which has laid the foundation for me to continue working on mechanistic studies in different contexts. I am also grateful to my graduate program iPQB/Biophysics for years of training, and especially to our program administrator Rebecca Brown for making sure that I get my monthly stipends and helping me with VISA renewal from time to time.

I want to thank members of Krogan laboratory for being supportive both research-wise and recreationally. I especially appreciate Gwen Jang for helping me collect the final data set when I was trying to finish my manuscript in a timely manner. Gwen is an exquisitely detailed person in

performing and book-keeping experiments, and she has been my go-to person when I need to troubleshoot or design new affinity purification protocols. I also want to thank Ruth Hüttenhain for teaching me the protocols of quantitative mass spectrometry. Ruth is a technology-driven scientist and fond of solving problems with her expertise in mass spectrometry. It was a fun collaboration as we exchanged knowledge of molecular biology and protein science. Meanwhile, I have learned a slightly different philosophy of doing science from her that would be valuable to me in the future. Priya Shah had helped me shape the manuscript from very early on and I am very grateful for that. Priya quickly recognized the novelty of my research and help me highlight the important points while minimize superfluous data that could stray from the main storyline. Manon Eckhardt is my virology mentor who got me familiar to with BSL-3 laboratory procedures. She also had helped me with bench work during my recovery from thumb ligament surgery. I also want to thank Dan Du for helping me with IL-6/STAT3 signaling experiments. It was a risky but necessary step. With Dan's assistance, I was able to quickly determine an ideal cell line for the experiments and obtained the first set of data within three months. I would also like to thank our lab manager Kathy Franks-Skiba. Kathy plays a pivotal role in keeping the lab running, and has helped me numerous times with ordering issues and rush packages. Last but not least, I want to thank many other current and former lab members who provided helpful discussions, including Stefanie Jäger, Cathal Mahon, Jeff Johnson, Billy Newton, Assen Roguev, John von Dollen, Joshua Kane, Robyn Kaake, Judd Hultquist, David Gordon, and Jason Wojcechowskyj.

Finally, I want to thank my family and friends for supporting me throughout the graduate school. I am grateful to my parents Jien-An Chen and Yu-Wen Huang, my sister Wei-Ling Chen,

and my brother Ying-Chuan Chen for understanding and supporting my decision to pursue my PhD training in the US, and to my dearest friends Chin-Yu Lin, I-Chin Wang, Julia Lu, Xuan Gao, Shujun Yuan, Rahel Woldeyes, Yi-Liang Liu, and Jen-Hsuan Wei. I would like to share this little accomplishment with all of you.

Published Materials and Author Contributions

Chapters 1-6 contain materials that will soon be submitted for publication:

Chapter 1: Introduction

Chapter 2-4: Experimental Results

Chapter 5: Discussion Sections pertinent to results shown in Chapter 2-4

Chapter 6: Materials and Methods

Chapter 7: Future Directions (unpublished materials)

Chen SH, Jang G, Hüttenhain R, Du D, Newton BW, Johnson JR, Johnson LT, Ye J, Debnath J, Gross JD, Krogan NJ. $CRL4^{AMBRA1}$ negatively regulates CRL5 ubiquitin E3 ligases by targeting Elongin C for polyubiquitination and proteasomal degradation.

Author contributions in the manuscript:

S.H.C. and N.J.K. conceived the project. S.H.C. designed and performed the experiments, and N.J.K. supervised the research. S.H.C. and G.J. performed comparative proteomics on $CRL4^{AMBRA1}$ with the assistance from R.H. on scoring. J.R.J, B.W.N, and T.L.J. performed MS sample preparation, machine runs, and database searching. J.Y. generated ATG knockout lines. S.H.C. generated stable cell lines, performed tandem IPs, single IPs, cell-based ubiquitination assays, Western blotting, and co-transfection experiments. S.H.C. and D.D. conducted IL-6 stimulation experiments. S.H.C. generated AMBRA knockout lines with the assistance from D.D. on genotyping. S.H.C. wrote the manuscript with input from N.J.K., D.J., and J.D.G. S.H.C, G.J., R.H., and D.D. edited the manuscript for publication.

$CRL4^{AMBRA1}$ Negatively Regulates CRL5 Ubiquitin E3 Ligases by Targeting Elongin C for Polyubiquitination and Proteasomal Degradation

Si-Han Chen

SUMMARY

Multi-subunit Cullin-RING ligases (CRLs) comprise the largest family of ubiquitin E3 ligases in humans. Although some CRLs attenuates substrate degradation, it remains unclear whether their modularity can be targeted to regulate CRL subfamilies. With proteomics, we discovered cross talk between $CRL4^{AMBRA1}$ and $CRL5^{VIF}$. We also found that $CRL4^{AMBRA1}$ targets Elongin C (ELOC), the essential adapter protein of CRL5 and CRL2 complexes, for polyubiquitination and proteasomal degradation. Depletion of AMBRA1 promotes accumulation of ELOC, which enhances ligase activity and autocatalysis of CRL5 and CRL2 substrate receptors. We also found that $CRL4^{AMBRA1}$ reduces the assembly and ligase activity of both $CRL5^{SOCS3}$ and HIV-1 $CRL5^{VIF}$ complexes. Furthermore, AMBRA1 depletion blunts IL-6-induced STAT3 phosphorylation and enhances the degradation of the antiviral APOBEC3G protein, which are regulated by $CRL5^{SOCS3}$ and $CRL5^{VIF}$, respectively. Thus, we revealed that $CRL4^{AMBRA1}$ negatively regulates CRL5 ubiquitin E3 ligases by targeting their shared ELOC for degradation.

Chapter 1

Cullin-RING Ubiquitin E3 Ligases (CRL)

Overview of Ubiquitination

Ubiquitination is a versatile post-translational modification regulating diverse cellular processes such as protein degradation, intracellular trafficking, and protein localization (reviewed by [1]). The modification involves transferring ubiquitin molecules from an activating enzyme E1 to a conjugating enzyme E2, and subsequently to a ligase enzyme E3 **(Figure 1.1)**. The latter contains a substrate-recognizing moiety or substrate receptor (SR) that confers specificity for substrate recognition and ubiquitination. Proteins can be either mono- or polyubiquitinated. The primary function of polyubiquitination is to direct substrates to 26S proteasome for timely degradation, also known as the ubiquitin-proteasome pathway. Deficiency in ubiquitin-mediated degradation has been linked to neurodegenerative diseases, aberrant cell differentiation, viral pathogenesis, and tumorigenesis [2, 3].

Cullin-RING Ubiquitin E3 Ligase Family and the Regulatory Mechanisms

Cullin-RING ligases (CRLs) are the largest family of ubiquitin E3 ligases, sharing similar molecular architecture — a cullin scaffold, a RING-box protein (RBX1 and/or RBX2) for recruiting an E2, one or more adapter proteins, and a SR [4, 5] **(Figure 1.2)**. More than seven human CRL subfamilies, commonly referred to by their constituent cullins, have been defined,

including CUL1, CUL2, CUL3, CUL4A/B, CUL5, and CUL7. Members of the same subfamily share the same cullin, adaptors, and the RING-box protein, whereas the SRs within a subfamily are interchangeable **(blue colored in Figure 1.2)**. The multi-subunit nature of CRLs results in a wide variety of distinct complexes and allows for fine-tuning E3 ligase activity by regulating complex formation.

CRL complexes are activated when the ubiquitin-like protein NEDD8 covalently attaches to the cullins, also known as neddylation [6]. Hyperactivation of CRL complexes is often associated with autocatalytic degradation of SRs, particularly in the absence of their substrates, which creates an intramolecular mechanism of autodownregulation [7, 8]. On a global scale, CRL activity is controlled by negative regulators, such as the de-neddylator COP9 signalosome (CSN), the cullin-associated protein CAND1, and the RBX1-binding protein Glomulin, all of which prevent premature disassembly of CRL complexes or unintended degradation of substrates [9-12]. Additionally, certain CRL complexes selectively regulate the activity of other CRLs by targeting their subunits for polyubiquitination and degradation, as heterologous regulation, which can control the timing of cell cycle progression [13-16]. These findings implicate that we need to better understand the complexity and heterologous regulation of CRL activity.

AMBRA1: an Autophagy Regulator Implicated in the Beclin1-Vps34 Complex and a Substrate Receptor of CRL4 Complex

AMBRA1 (Activating Molecule In Beclin1-Regulated Autophagy Protein 1) was initially identified as an autophagy regulator and as part of the Beclin1-Vps34 autophagy initiation

complex **(Figure 1.3A)**. The role of AMBRA1 in autophagy signaling has been relatively well-studied. AMBRA1 deficiency inhibits basal autophagy in mouse embryos and results in severe neural tube defects, which seem to correlate with dysregulation of Beclin1-dependent autophagy [17]. AMBRA1 was also reported a ULK1 kinase substrate that regulates the dissociation of AMBRA1-Beclin1-Vps34 complex from the dynein motor complex upon autophagy induction [18]. Additionally, AMBRA1 interacts with the ubiquitin E3 ligase TRAF6, which supports ULK1 ubiquitination via K63-linked chains and autophagy upregulation, acting as a positive feedback mechanism [19]. The positive feedback loop can be disrupted when mTOR inhibits ULK1 ubiquitination by AMBRA1 phosphorylation. These findings connect AMBRA1 to different aspects of autophagy signaling that seem to account for its physiological importance in embryonic development and the balance of cell proliferation and death [17, 20, 21]. However, AMBRA1 is also a member of DDB1 and CUL4-associated factors (DCAFs), which serve as SRs for CRL4 [22], its function as a SR of CRL4 (denoted by $CRL4^{AMBRA1}$) remains largely unexplored **(Figure 1.3B)**.

CRL4 ubiquitin E3 ligases regulate DNA-damage repair and cell cycle progression. Many CRL4 SRs recognize DNA lesions/repairing factors and cell cycle regulators for ubiquitination and degradation [23-25], and other CRL4 complexes regulate cellular processes in the cytoplasm [26-28]. AMBRA1 is primarily a cytoplasmic protein and the full range of $CRL4^{AMBRA1}$ substrates has not been systematically interrogated. The autophagy factor Beclin1 is the only known ubiquitination target to date [29]. $CRL4^{AMBRA1}$ mediates non-degradative ubiquitination of Beclin1, which is important for initiating autophagy signaling [29, 30], but it is unclear what

proteolytic substrate(s) AMBRA1 targets for polyubiquitination and degradation. We do not yet know to what extent $CRL4^{AMBRA1}$ is connected to the physiological roles of AMBRA1.

AMBRA1 may be Involved in CRL Crosstalk

Previously, we identified AMBRA1 in association with HIV-1 VIF, a viral SR that hijacks CRL5 for the degradation of APOBEC3 proteins, in our HIV-1-human proteomic study [31-34]. More recently, another HIV-1 proteomic study identified that VIF associates with DDB1 in addition to AMBRA1 in the context of infection [35]. Interestingly, AMBRA1 was found to regulates autophagy via CRL5-mediated DEPTOR degradation [36]. These data implicate that AMBRA1 may influence CRL crosstalk. How AMBRA1 regulates CRL5-DEPTOR function, and whether a similar mechanism is important for other CRL5 complexes, including $CRL5^{VIF}$, is unclear.

HIV-1 Hijacking of Human Cullin-RING Ligases

HIV-1 has a small genome of less than 10kb and employs differential RNA splicing and proteolytic maturation to obtain 18 viral proteins. To achieve successful infection, HIV-1 extensively interacts with host protein machineries with these 18 proteins as well as its genetic material at different stages of its life cycle. Notably, several HIV-1 accessory proteins hijack or repurpose human CRL complexes to evade immune responses and to enhance viral replication **(Figure 1.4)**. For example, VPU repurposes $CRL1^{\beta TRCP}$ to target viral restriction factor Tetherin/BST-2 for polyubiquitination and degradation [37]. $CRL1^{\beta TRCP\text{-}VPU}$ can also target the

cytoplasmic domain of CD4 receptor for polyubiquitination and degradation, possibly at the late stage of HIV-1 life cycle since CD4 is required for initial infection [38]. VPR interacts with $CRL4^{DCAF1}$ and causes G2 cell cycle arrest, which has been recently linked to degradation of MUS81 by the rewired CRL4 complex [39]. In both VPU- and VPR-implicated CRL complexes, the presence of viral proteins seem to extend the surface area of existing SRs to recruit the novel substrates. Similar idea of viral-dependent substrate recruitment was demonstrated in SIV VPX-mediated degradation of SAMHD1 via $CRL4^{DCAF1}$[40], although there is no structure available yet for VPU and VPR in complex with their CRL components and the substrates. However, it is different in the case of HIV-1 VIF. VIF itself serves as a *bona fide* SR that targets the antiviral APOBEC3 proteins for polyubiquitination and degradation via $CRL5^{VIF}$ complex.

Figure 1.1

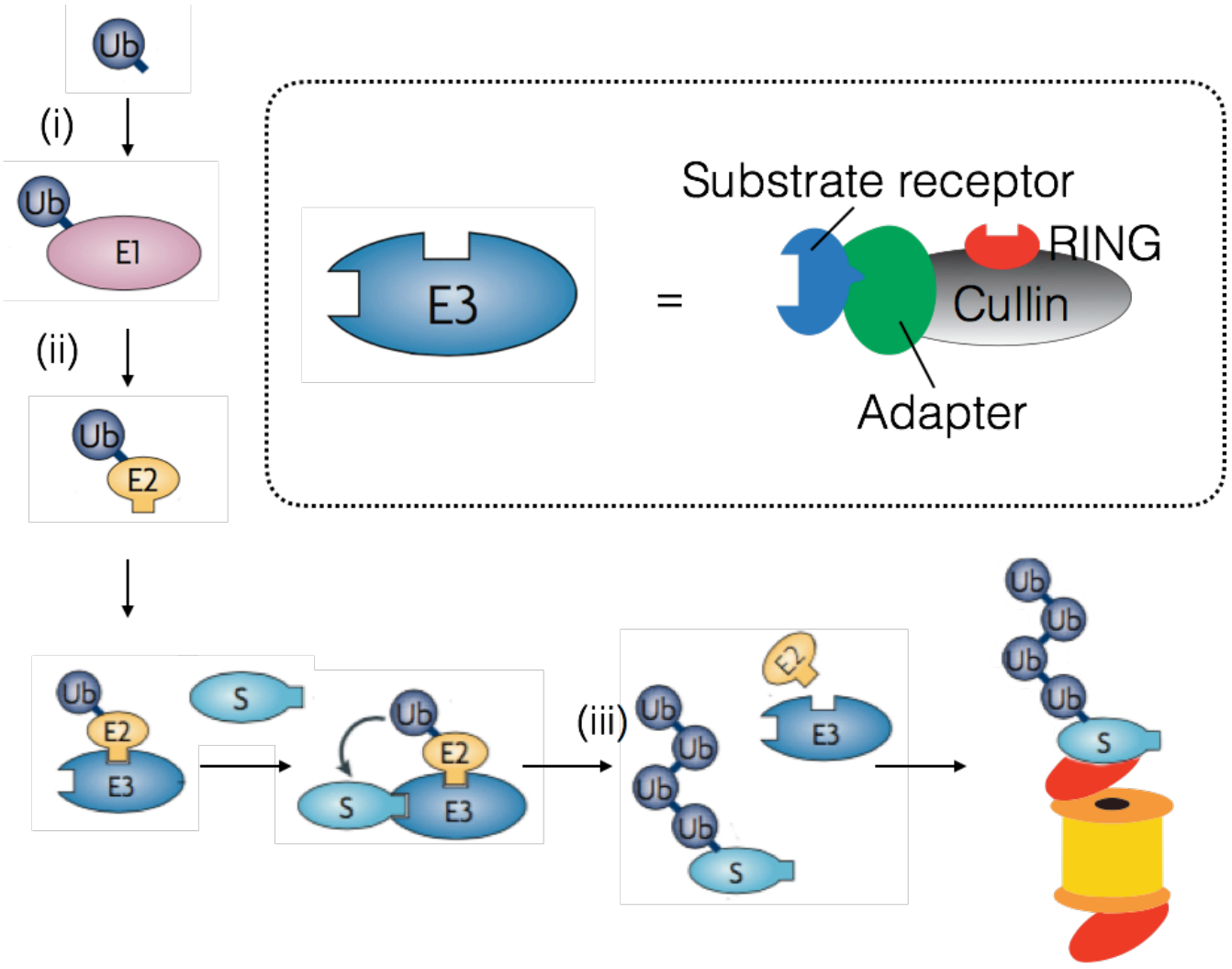

Figure 1.1 Ubiquitination Cascade and Schematics of Cullin-RING Ubiquitin E3 Ligase (Adapted from [41]).

Attachment of ubiquitin to protein substrates requires three major steps — activation (i), conjugation (ii), and ligation (iii), carried out by E1, E2, and E3 enzymes, respectively. E2 enzymes are important for ubiquitin chain assembly and determine ubiquitin linkage specificity.

After attaching a mono-ubiquitin to target lysine residue of the substrate, E2 enzymes may transfer another ubiquitin molecule to accessible lysine on the existing ubiquitin, resulting in a polyubiquitin chain. Ubiquitin E3 ligases contain a substrate receptor subunit for substrate recognition and catalyze the transfer of ubiquitin (from E2 or from Ub-E3 intermediate) to the target substrate. In the CRL family (as highlighted in the dashed rectangle), ubiquitin molecules are transferred indirectly from E2 which is in complex with E3 via a RING-box protein to the substrate which is in complex with the substrate receptor. CRL family members contain a cullin scaffold protein, one or several adapters, in addition to the above mentioned substrate receptor and RING-box protein.

Figure 1.2

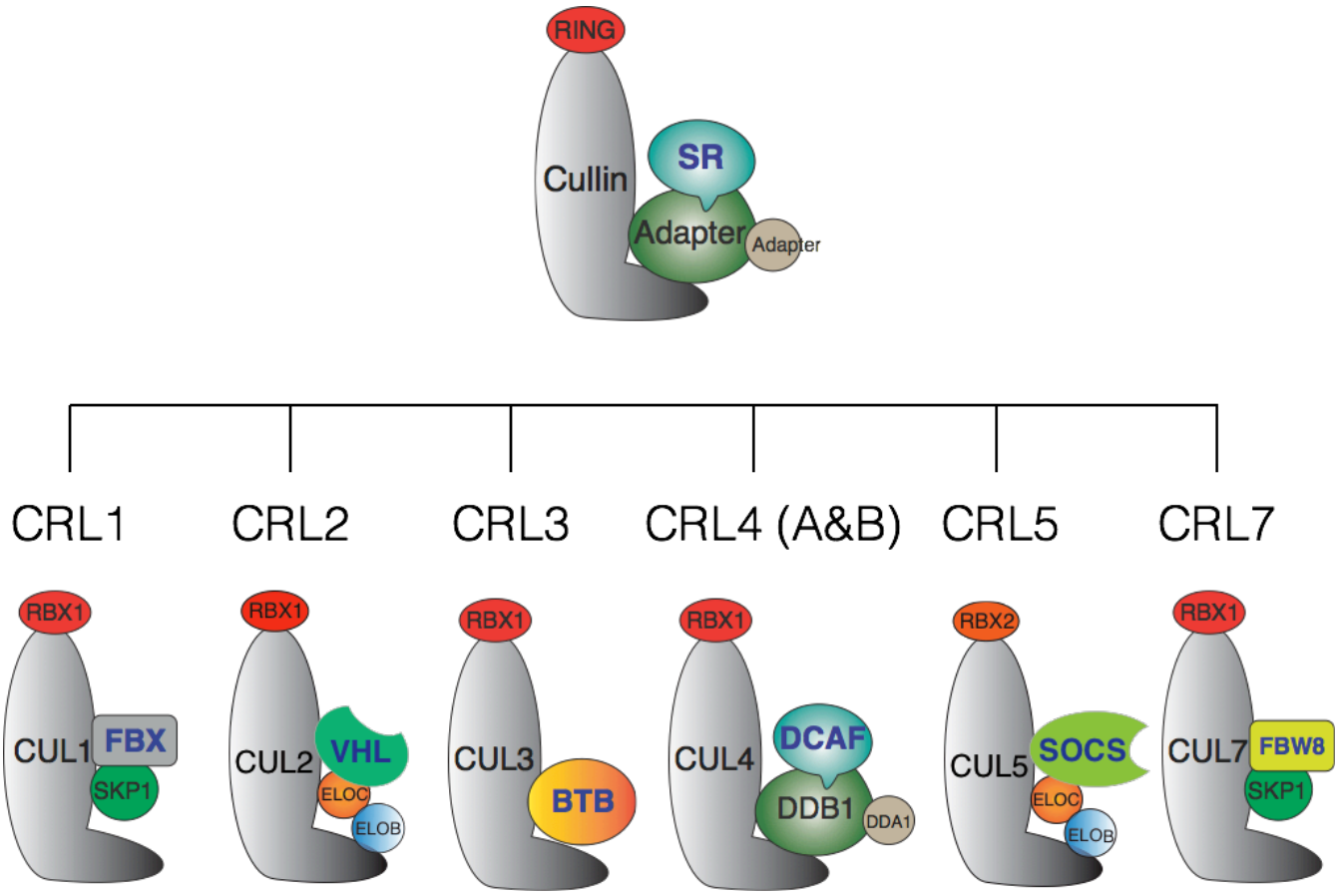

Figure 1.2 Schematics of CRL Family Members.

Listed are seven distinctive CRL subfamilies. Blue-colored proteins represent substrate receptors (SRs).

Figure 1.3

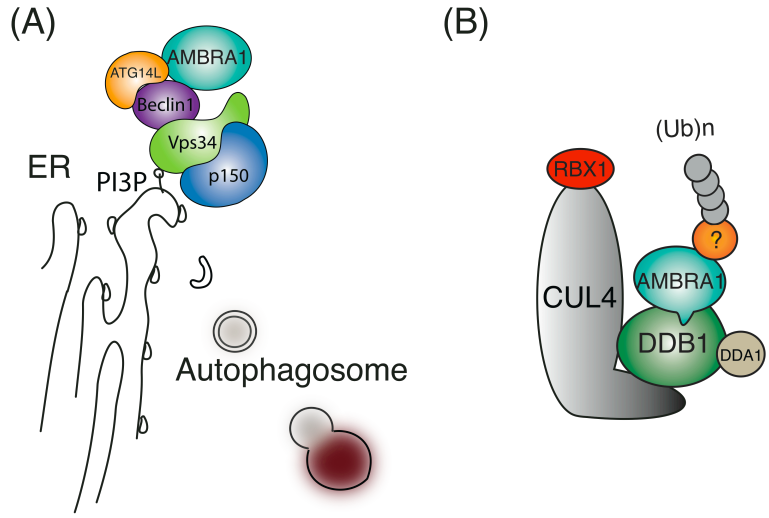

Figure 1.3 AMBRA1 Protein Complexes.

(A) AMBRA1 is a regulatory component of autophagy initiation complex (also known as class III PI3K complex), which contains Beclin1, Vps34, ATG14-like protein (ATG14L or BARKOR), and p150.

(B) In addition, AMBRA1 serves as a substrate receptor of CRL4 complex containing RBX1, CUL4A/B, DDB1, and DDA1. It remains mostly unknown what substrates AMBRA1 targets for polyubiquitination.

Figure 1.4

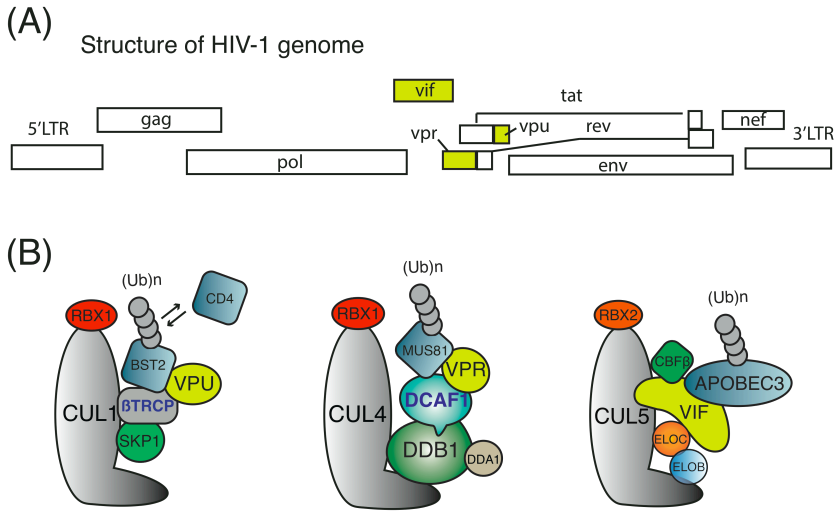

Figure 1.4 HIV-1 Hijacking of Cullin-RING Ubiquitin E3 Ligases.

(A) HIV-1 genome encodes 9 polypeptides which are synthesized by differential splicing. Additional 9 viral proteins are produced by the cleavage of precursor polypeptides GAG, POL, and ENV via viral or host proteases. Highlighted are HIV-1 accessory proteins that are known to interact with human CRL complexes.

(B) HIV-1 hijacking of CRL complexes. VPU repurposes $CRL1^{\beta TRCP}$ to degrade BST2 and CD4. VPR rewires $CRL4^{DCAF1}$ to degrade MUS81. VIF hijacks CRL5 to degrade APOBEC3 proteins. Of note, CBFβ is another host protein that is recruited to CRL5 in a VIF-dependent manner. CBFβ stabilizes VIF and is essential for CRL^{VIF} complex assembly.

Chapter 2

Proteomic Analysis of CRL4-CRL5 Crosstalk and $CRL4^{AMBRA1}$ Substrates

Crosstalk Between $CRL5^{VIF}$ and $CRL4^{AMBRA1}$ Complexes

Our previous HIV-1-human proteomic study identified a strong and specific interaction between the viral VIF protein and the human protein AMBRA1, which was preserved in both HEK293 and Jurkat T cells **(Figure 2.1)** [31]. Notably, AMBRA1 is the only other VIF-human interaction identified in both cell types that is seemingly not part of the $CRL5^{VIF}$ complex. We confirmed the specificity of AMBRA1 for VIF by reciprocal immunoprecipitations (IPs) **(Figure 2.2)**. VIF was recently reported by another group that it interacts with DDB1 and AMBRA1 in the context of HIV-1 infection [35]. Despite much experimental evidence confirming the VIF-AMBRA1 interaction, the underlying biology remained unclear. In addition, we found that autophagy, in which AMBRA1 has a well-established regulatory role, was not affected by VIF expression **(Figure 2.3)**.

To initially understand AMBRA1 biology, we sought to define AMBRA1 interactome by AP-MS. Therefore, we purified exogenously expressed, affinity-tagged AMBRA1 from 293T cells and subjected it to mass spectrometric analysis. In addition to CRL4 complex components in which AMBRA1 serves as a SR, we found that AMBRA1 interacts with two adapter proteins required for CRL5 and CRL2 (CRL5/2) complexes, ELOB and ELOC **(Figure 2.4; Appendix Table 1)**. Next, we performed tandem IPs of VIF and AMBRA1 not only to verify the

interaction between VIF and AMBRA1, but also to identify co-purified proteins **(Figures 2.5)**. We found that adapter proteins of both $CRL5^{VIF}$ and $CRL4^{AMBRA1}$ including ELOB, ELOC and DDB1 were enriched in the tandem IPs, whereas neither the scaffold proteins nor the RING-box proteins were co-purified with VIF and AMBRA1 (Figure 1D; Table S2). The result is in contrast with what previously suggested that AMBRA1-DDB1 and AMBRA1-ELOBC are mutually exclusive complexes [36]. Our data indicated a crosstalk between $CRL5^{VIF}$ and $CRL4^{AMBRA1}$ complexes, and we decided to further investigate $CRL4^{AMBRA1}$ functions.

Comparative Proteomics Reveals ELOC is a Substrate for $CRL4^{AMBRA1}$

In a CRL4 complex, DDB1 mediates the interaction between CUL4A/B and the DCAF SR [42]. DCAF-bound proteolytic substrates can be stabilized by abolishing the association with the CRL4 catalytic core **(Figure 2.6A)**[43]. DCAFs share a semi-conserved helical region that directly binds to the DDB1 double β-propeller pocket [24, 44]. We delimited AMBRA's DDB1-binding region to a 43 amino acid N-terminal helix motif that aligns with the DDB1-binding region of other DCAFs [45, 46]. Using IP-WB, we showed that deletion of either partial (1~22 amino acids; AMBRA1 ΔH22) or complete (1~43 amino acids; AMBRA1 ΔH43) region of the predicted DDB1-binding sequence abolished AMBRA1 binding to DDB1 and CUL4A; the same result was demonstrated in the presence of VIF expression **(Figure 2.6B)**.

Subsequently, we performed an AP-MS experiment quantitatively comparing the interactors of wild type AMBRA1 and DDB1-binding defective AMBRA1 mutants (AMBRA1 ΔH22 and ΔH43) in the presence of VIF, as we hypothesized that VIF may sensitize $CRL4^{AMBRA1}$ to

degradation of certain substrates. Deletion of the predicted helical region of AMBRA1 resulted in both the loss and gain of specific protein interactions **(Figures 2.6C and 2.6D; Appendix Table 3)**. AMBRA1 ΔH mutants lost interactions with CUL4A/B and RBX1, which constitute the catalytic core of CRL4, as well as the CRL4 adapter proteins DDB1 and DDA1 [47], and subunits of COP9 signalosome including CSN1, CSN2, and CSN4, which directly contact cullins [48, 49]. Furthermore, we found a small number of stabilized interactions by the ΔH mutations that are potentially proteolytic substrates of $CRL4^{AMBRA1}$, among them ELOC showing more than 1.5-fold stronger binding to both ΔH mutants compared to the wild type (WT). ELOB, another adapter protein of CRL5/2 complexes, did not show significant change in the proteomic data. We confirmed the differential ELOC binding by immunoblot and quantification of band intensity **(Figure 2.6E)**; consistent with the proteomic data, ELOC showed enhanced co-purification with ΔH mutants, whereas ELOB displayed noisier fold change. In contrast to AMBRA1, DCAF1 does not associate with ELOC, demonstrating specific binding of ELOC to AMBRA1 **(Figure 2.6B)**.

Notably, while the ΔH22 AMBRA1 could not bind to DDB1 and CUL4A/B, another helical region with degenerate nucleotides may be required for their interactions, as reported for other DCAFs [27, 50]. Thus, we chose to use ΔH43 or ΔH34 (abbreviated ΔH; **Figure 2.7**) for subsequent functional experiments.

Figure 2.1

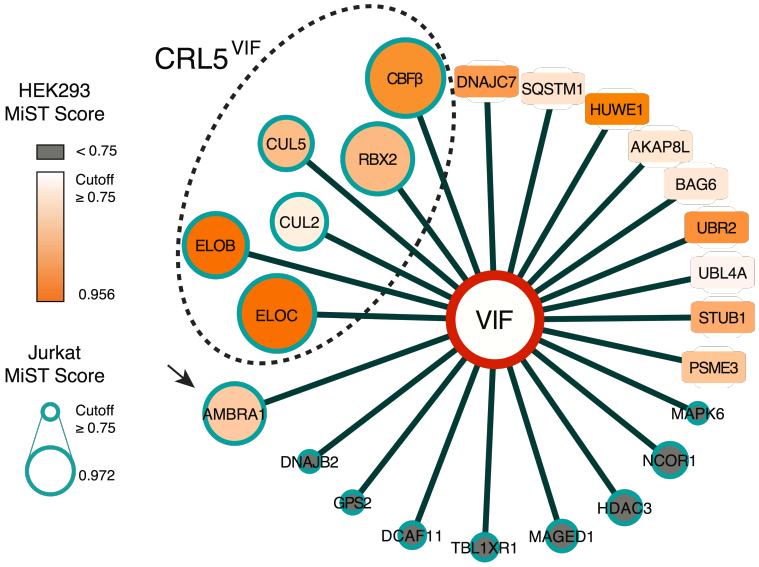

Figure 2.1 Network Representation of VIF-Human Protein-Protein Interactions, Recreated from Our Published Data Set [31].

VIF AP-MS was performed in HEK293 cells and Jurkat leukemia T cells, scored by Mass spectrometry interaction STatistics (MiST) which was optimally designed for host-pathogen protein-protein interactions. The orange color range and the size of green nodes represent MiST scores of identified Vif-human interactions in HEK293 and Jurkat, respectively. The red node denotes the affinity-tagged bait protein, which is VIF in this case. Interactors with HEK293 MiST scores below 0.75 were colored in grey, whereas interactors with Jurkat MiST scores below 0.75 were rendered in rectangles. Dash-line-circled interactors represent $CRL5^{VIF}$ complex, with CUL2 being another cullin scaffold that may replace CUL5. As noted, AMBRA1 was identified a strong interactor in both HEK293 and Jurkat cells.

Figure 2.2

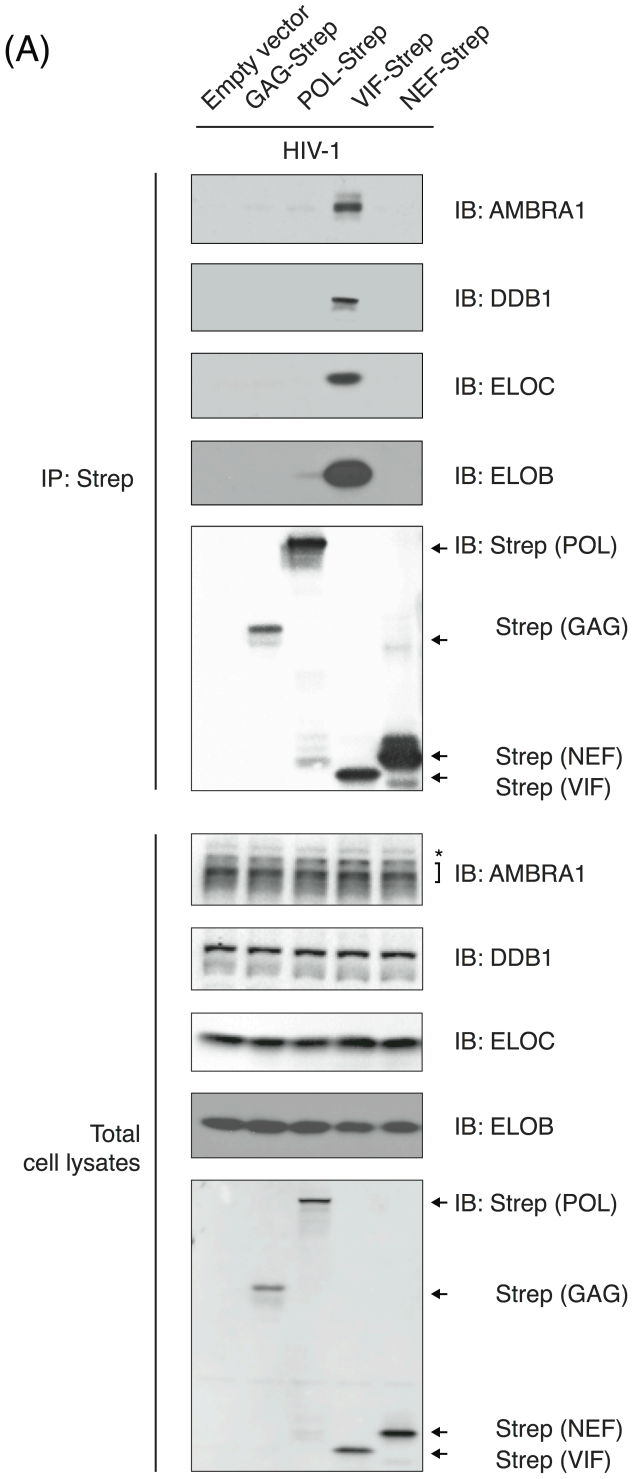
(A)
Empty vector
GAG-Strep
POL-Strep
VIF-Strep
NEF-Strep
HIV-1
IP: Strep
IB: AMBRA1
IB: DDB1
IB: ELOC
IB: ELOB
IB: Strep (POL)
Strep (GAG)
Strep (NEF)
Strep (VIF)
Total
cell lysates
IB: AMBRA1
IB: DDB1
IB: ELOC
IB: ELOB
IB: Strep (POL)
Strep (GAG)
Strep (NEF)
Strep (VIF)

(B)

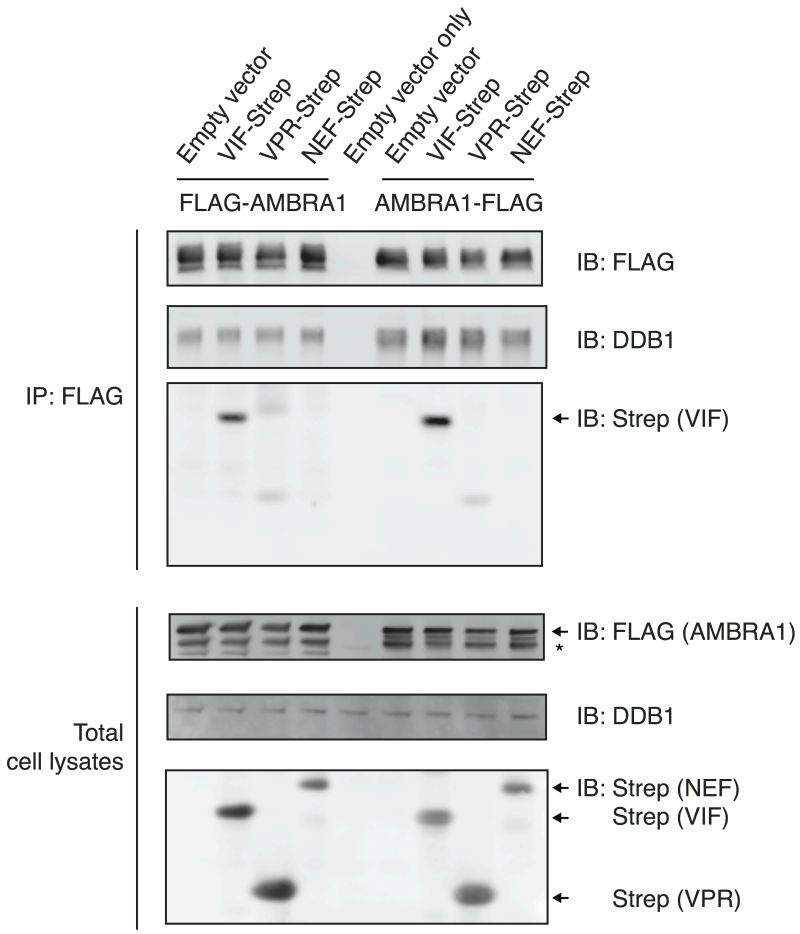

Figure 2.2 Specific Binding of AMBRA1 to HIV-1 VIF.

(A) HIV-1 VIF co-purified with AMBRA1 and DDB1, as well as ELOBC. 293T transfected with Empty vector or Strep-tagged HIV-1 constructs was affinity purified with Strep-Tactin beads and analyzed by immunoblot. Asterisk denotes nonspecific bands.

(B) Reciprocal IP confirmed AMBRA1-VIF interaction. N-terminally or C-terminally FLAG-tagged AMBRA1 along with Empty vector or Strep-tagged HIV-1 constructs were co-

transfected in 293T and was subjected to FLAG IP. IP and input lysates were analyzed by immunoblot. Asterisk denotes nonspecific bands.

Figure 2.3

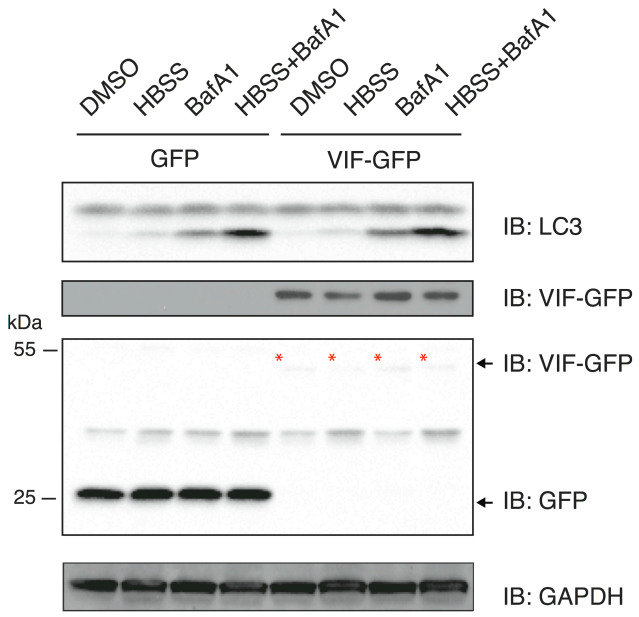

Figure 2.3 HIV-1 VIF Expression in HEK293 Cells Does Not Affect Autophagy Responses.

HEK293 stably expressing tet-on GFP or VIF-GFP was treated with 1 µg/mL of doxycycline overnight for protein expression, followed by the addition of DMSO, 100 nM Bafilomycin A1 (BafA1), or replaced with the starvation media HBSS supplemented with DMSO or BafA1. Red asterisks denote VIF-GFP.

Figure 2.4

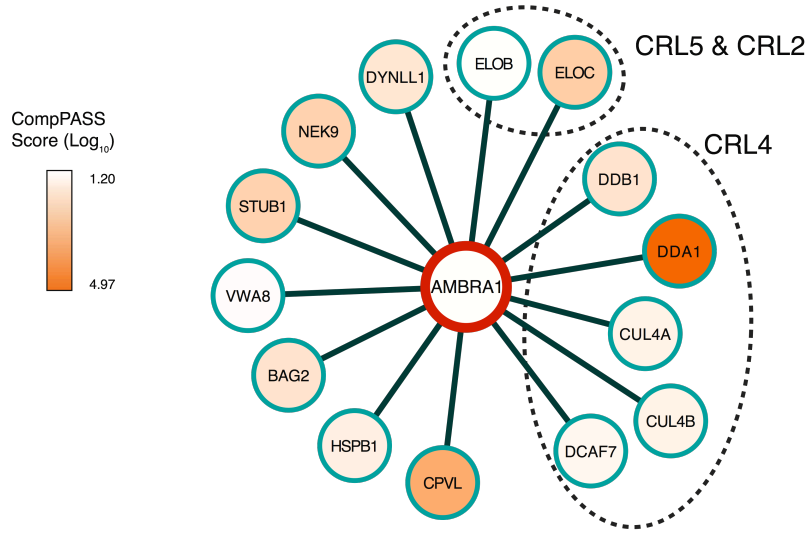

Figure 2.4 Network Representation of AMBRA1-Interacting Proteins.

Network representation of AMBRA1-interacting proteins from 12 independent AP-MS experiments performed in 293T cells transfected with FLAG-tagged AMBRA1. AP-MS scoring was performed with Comparative Proteomic Analysis Software Suite (CompPASS), which is ideal for non-pathogenic interactions. The orange color range represents CompPASS scores of individual interactions. Dash line enclosed components of CRL5/2 complexes and CRL4 complex, respectively. See also **Appendix Table 1**.

Figure 2.5

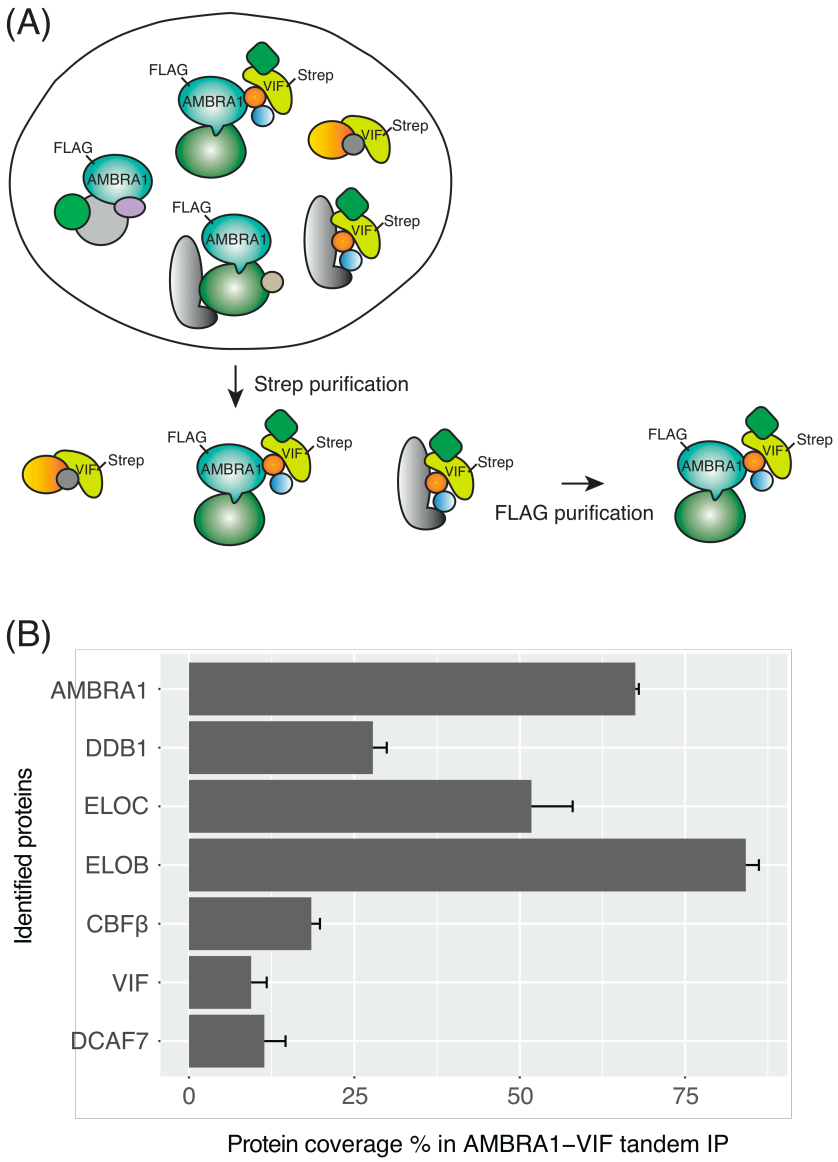

Figure 2.5 VIF-AMBRA1 Tandem IP.

(A) Schematic view of VIF-AMBRA1 tandem IP. Strep-tagged Vif and FLAG-tagged AMBRA1 were co-expressed in 293T, and the cell lysate was subjected to Strep and then followed by FLAG affinity purifications.

(B) Proteins identified in VIF-AMBRA1 tandem IPs in three independent experiments. Protein abundance was represented by the percentage of identified peptides over the length of protein sequence (protein coverage %). Of note, DDA1 was only identified in one of the three experiments. Bar graph represented mean + sem, n=3. See also **Appendix Table 2**.

Figure 2.6

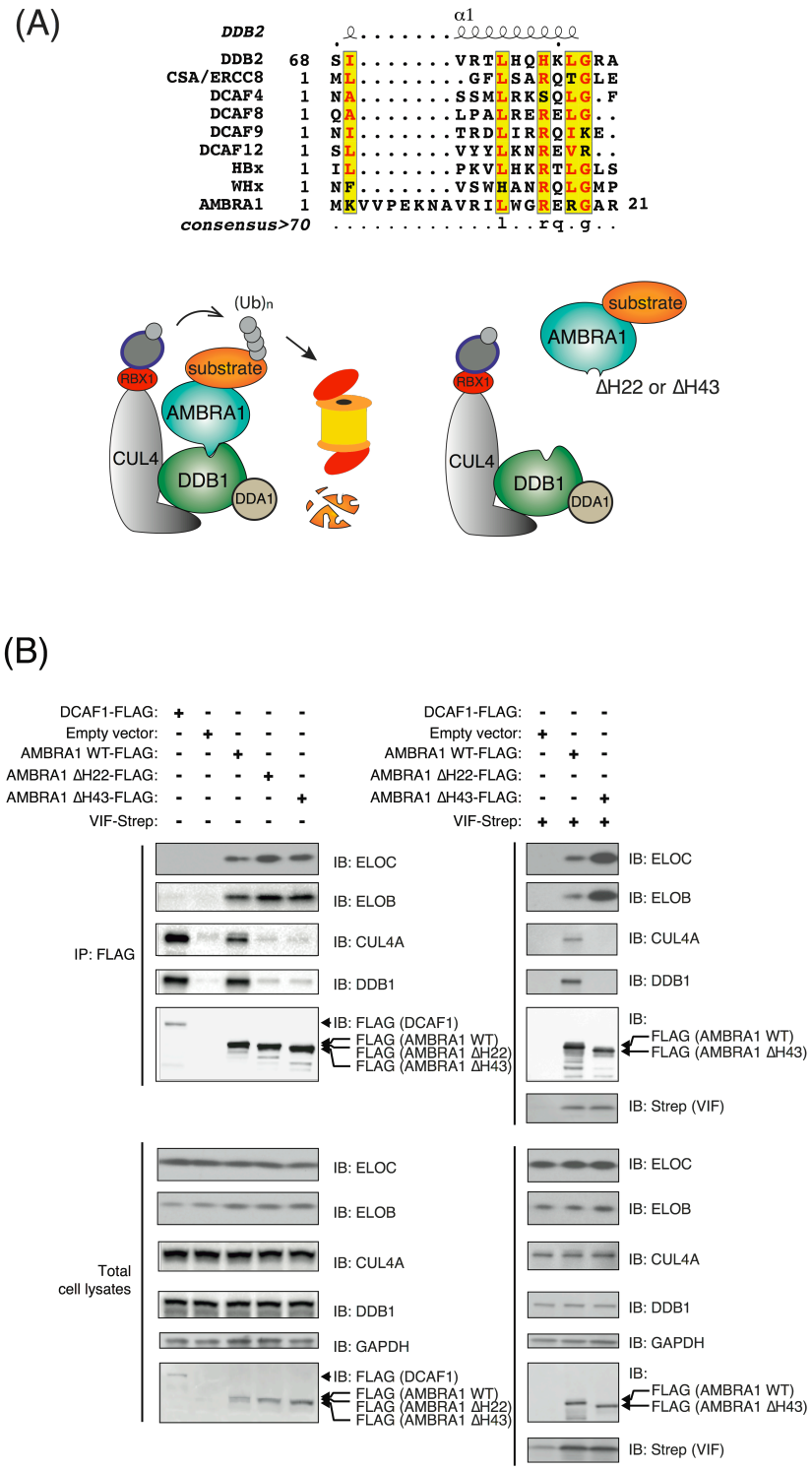
(A)
α1
DDB2
DDB2 68 SI.....VRTLHQHKLGRA
CSA/ERCC8 1 ML.....GFLSARQTGLE
DCAF4 1 NA.....SSMLRKSQLG.F
DCAF8 1 QA.....LPALRERELG..
DCAF9 1 NI.....TRDLIRRQIKE.
DCAF12 1 SL.....VYYLKNREVR..
HBx 1 IL.....PKVLHKRTLGLS
WHx 1 NF.....VSWHANRQLGMP
AMBRA1 1 MKVVPEKNAVRILWGRERGAR 21
consensus>70 .....l..rq.g..
(Ub)n
RBX1
substrate
AMBRA1
CUL4
DDB1
DDA1
ΔH22 or ΔH43
(B)
DCAF1-FLAG:
Empty vector:
AMBRA1 WT-FLAG:
AMBRA1 ΔH22-FLAG:
AMBRA1 ΔH43-FLAG:
VIF-Strep:
IP: FLAG
Total cell lysates
IB: ELOC
IB: ELOB
IB: CUL4A
IB: DDB1
IB: GAPDH
IB: FLAG (DCAF1)
FLAG (AMBRA1 WT)
FLAG (AMBRA1 ΔH22)
FLAG (AMBRA1 ΔH43)
IB: Strep (VIF)

(C)

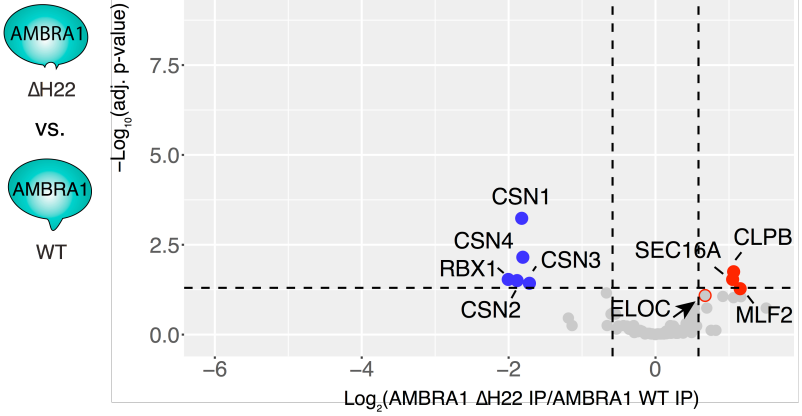
AMBRA1
ΔH22
vs.
AMBRA1
WT
DDA1
DDB1
Increase with mutation
Decrease with mutation
CSN1
CSN4
CSN3
RBX1
CSN2
SEC16A
CLPB
ELOC
MLF2
−Log10(adj. p-value)
Log2(AMBRA1 ΔH22 IP/AMBRA1 WT IP)

(D)

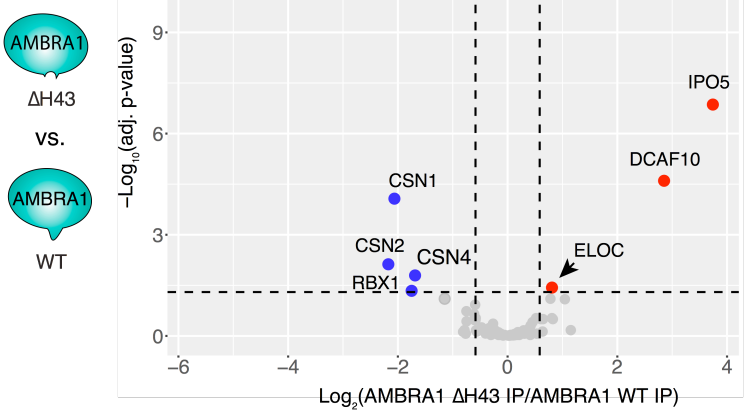
AMBRA1
ΔH43
vs.
AMBRA1
WT
DDA1
DDB1
Increase with mutation
Decrease with mutation
IPO5
DCAF10
CSN1
CSN2
CSN4
RBX1
ELOC
−Log10(adj. p-value)
Log2(AMBRA1 ΔH43 IP/AMBRA1 WT IP)

(E)

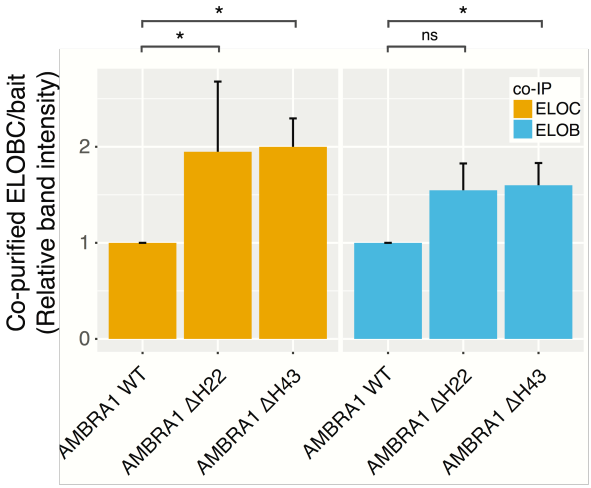

Figure 2.6 Comparative Proteomics in Identifying Proteolytic Substrates of CRL4^{AMBRA1}.

(A) The strategy taken to identify CRL4^{AMBRA1} substrates. Sequence alignment generated by T-coffee and visualized by ENDscript showing a short N-terminal sequence of AMBRA1 shares similar sequence and secondary structure with DDB2 as well as other DCAFs. The structure of DDB2 in complex with DDB1 was used as a template to represent the conserved motif (PDB ID: 3EI4). Depicted in cartoon, deletion of the predicted helical region is hypothesized to inhibit binding of AMBRA1 to DDB1 and the rest of the complex, stabilizing the substrate(s).

(B) Immunoblots showing loss of CUL4 and DDB1 interactions by removing the predicted helical region of AMBRA1 and confirming enhanced binding of identified substrates **(see Figure 2.6C and D)** by the mutants. Empty vector, FLAG-tagged DCAF1, AMBRA1 WT, ΔH22, and ΔH43 were affinity-purified with anti-FLAG beads from transfected 293T with or without VIF-Strep co-transfection. IP and input lysates were analyzed by immunoblot.

(C and D) Volcano plot showing gain (red) and loss (blue) of interactions by ΔH22 (C) and ΔH43 (D) mutants compared to WT AMBRA1 in three independent AP-MS experiments. This proteomic screen was performed on 293T co-expressing VIF-Strep and FLAG-tagged bait

proteins. X axis denoted Log_2 fold change of ΔH43-bound proteins to WT-bound proteins; vertical dash lines delineated > 1.5 and < 1.5 fold changes. Y axis denoted $-Log_{10}$ adjusted p-value to indicate statistical significance of each interactor; horizontal dash line delineated > 0.05 and < 0.05 adjusted p-values. Adjusted p-values were calculated based on Benjamini and Hochberg procedure that corrects raw p-values among all listed proteins in the specific comparison, in this case comparing either of the ΔH mutants with WT [51]. Please note that CUL4A and CUL4B were not detected in ΔH proteomic data at all, resulting in -infinity values and thus not shown on the plot. See also **Appendix Table 3**.

(E) Densitometric quantification of co-purified ELOC and ELOB band intensity relative to the purified FLAG bait intensity on immunoblot. WT, ΔH22, and ΔH43 AMBRA1 FLAG IPs were performed on 293T co-expressing the FLAG-tagged bait proteins with VIF-Strep. Statistical analysis of paired comparisons was carried out by Mann-Whitney-Wilcoxon Test. In the ELOC panel, p-value = 0.023 with WT and ΔH22; p-value = 0.023 with WT and ΔH43. In the ELOB panel, p-value = 0.243 with WT and ΔH22; p-value = 0.018 with WT and ΔH43. Bar graph represented mean + sem, n=3.

Figure 2.7

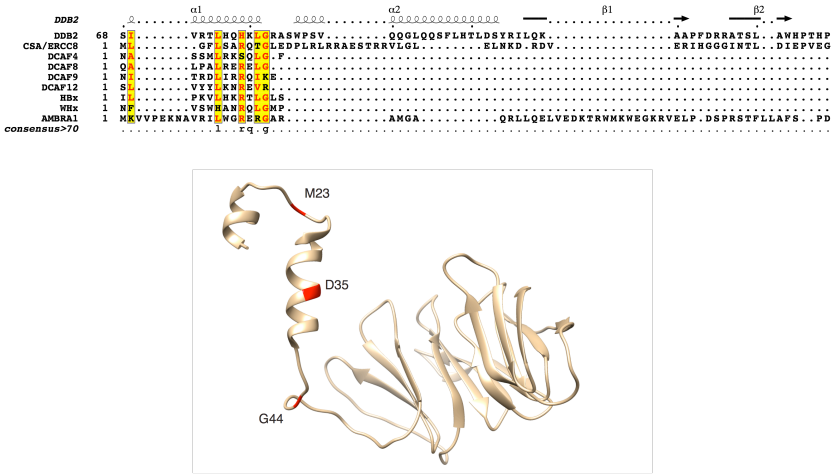

Figure 2.7 Predicted Secondary and Tertiary Structures of AMBRA1.

Upper panel depicts alignment of AMBRA1 N-terminal sequence with other DCAFs, an extension of **Figure 2.6A**. Lower panel represents a homology model of AMBRA1 N-terminal region encompassing a helical region important for DDB1 binding and a partial WD40 domain, generated by SWISS-MODEL using human CSA as a model [52]. Red colored residues denote breakpoints for generating ΔH22, ΔH34, and ΔH43 AMBRA1 mutants.

Chapter 3

$CRL4^{AMBRA1}$ Negatively Regulates CRL5 Complexes by Targeting ELOC for Polyubiquitination and Degradation

Biochemical Validation that $CRL4^{AMBRA1}$ Regulates ELOC

In addition, specificity of the AMBRA1 interaction with CUL4A/B, but not CUL5, suggests that AMBRA1 is a regulatory and not an integral component of CRL5 **(Figure 3.1)**. On the other hand, ELOC is not an integral component of CRL4, as neither of the CRL4 scaffold proteins (CUL4A and CUL4B) interact with ELOC.

Next, we determined whether ELOC is a proteasomal and $CRL4^{AMBRA1}$ substrate. We transfected myc-tagged ubiquitin or empty vector into 293T cells stably expressing FLAG-tagged ELOC, treated them with vehicle control or the proteasome inhibitor MG132, and performed denaturing IP on FLAG-tagged ELOC to examine the incorporation of myc-ubiquitin **(Figure 3.2)**. We found that both ELOC protein level and its polyubiquitination accumulated by proteasome inhibition. Strikingly, when AMBRA1 was knocked down with siRNA, ELOC polyubiquitination was nearly absent (**Figure 3.3A** in the presence of MG132; **Figure 3.3B** in the absence of MG132). In contrast, the CRL1 adapter SKP1 was not modified by polyubiquitination. SKP1 did not interact with AMBRA1, despite sharing 30% sequence identity with ELOC **(Figures 3.4)**. Moreover, we found that ELOC protein level accumulated when AMBRA1 was knocked down, with its accumulation strongly correlating with the degree of

AMBRA1 depletion by various AMBRA1 shRNAs **(Figure 3.5)**. Because of AMBRA1's known function in regulating autophagy initiation, we functionally validated AMBRA1 knockdown by examining p62/SQSTM1, which became stabilized when autophagy was inhibited [17, 53]. Additionally, despite ELOB accumulated by AMBRA1 depletion, ELOB did not demonstrate similar MG132-dependent polyubiquitination **(Figure 3.6)**. We reasoned that ELOB may be indirectly affected by AMBRA1 due to its interaction with ELOC, as ELOC and ELOB form a strong heterodimer (ELOBC) by hydrophobic interaction [54]. These data show that ELOC is polyubiquitinated and degraded in an AMBRA1 dependent manner.

To test whether the autophagy function of AMBRA1 possibly attributes to changes in ELOC level, we examined ELOC in autophagy defective background and found that neither ATG7 nor ATG12 depletion causes ELOC stabilization, indicating that ELOC accumulation following AMBRA1 knockdown is autophagy independent **(Figure 3.7)**. Interestingly, ELOC was previously identified in a systematic ubiquitin profiling study, in which ubiquitinated ELOC was found to accumulate after prolonged proteasomal inhibition [55]. Here, we report that ELOC is targeted by $CRL4^{AMBRA1}$.

AMBRA1 Regulates CRL5-Mediated Autocatalytic Degradation of SOCS3 and VIF

Because AMBRA1 associates with ELOC, we asked if AMBRA1 interacts with human SOCS proteins through ELOC and found that several human SOCS proteins co-purified with AMBRA1 **(Figure 3.8)**. Importantly, mutations of conserved BC-box motifs significantly decreased interactions with ELOC and AMBRA1, suggesting that the association between

AMBRA1 and the SOCS proteins was largely mediated by ELOC. Based on our findings, we speculate that $CRL4^{AMBRA1}$ may regulate CRL5/2 E3 ligase activity by targeting ELOC for polyubiquitination and degradation.

We hypothesized that ELOC accumulation following AMBRA1 knockdown may up-regulate CRL5/2 activity and therefore destabilize the SRs. Many SRs of CRL complexes have been reported to undergo autoubiquitination and autocatalytic degradation, especially in the absence of their substrates [7-9, 24, 56-58]. To test AMBRA1's effect on CRL5/2 autocatalysis, we assessed the stability of several CRL5/2 SRs in stable cell lines under control or AMBRA1 knockdown background using cycloheximide chase assays, in which protein translation was inhibited (**Figures 3.9** for CRL5 SRs; **Figure 3.10** for CRL2 SRs). As expected, both CRL5 and CRL2 SRs, including SOCS3, VIF, VHL, and PPIL5, were destabilized in AMBRA1 knockdown cells. To confirm that SR stability is regulated by autocatalysis, we examined VIF stability by knocking down ELOB, ELOC, or CUL5 (**Figure 3.11A**; quantification of immunoblot shown in **Figure 3.11B**). Indeed, VIF was stabilized in these CRL5-deficient conditions. Consistent with the idea, VIF was found more stable by the L145A mutation, which disrupts $CRL5^{VIF}$ assembly **(Figures 3.8 and 3.12)**[34]. Most importantly, decreased SOCS3 and VIF stability following AMBRA1 knockdown was reversed by concomitant ELOB, ELOC, or CUL5 depletion, confirming that CRL5-mediated autocatalysis destabilizes SRs and underscoring the complex dynamics underlying CRL regulation **(Figure 3.13)**.

$CRL4^{AMBRA1}$ E3 Ligase Activity is Required to Negatively Regulate the Assembly and Ubiquitin E3 Ligase Activity of CRL5 Complexes

To understand how SOCS3 and VIF autocatalysis is affected by AMBRA1, we evaluated if AMBRA1's E3 ligase activity regulates $CRL5^{SOCS3}$ and $CRL5^{VIF}$ complex assembly by targeting ELOC. $CRL5^{SOCS3}$ and $CRL5^{VIF}$ complex assembly was examined by affinity purification of FLAG-tagged SOCS3 and Strep-tagged VIF, respectively, followed by detection of co-purified endogenous ELOC, ELOB, and CUL5 with immunoblot. We found that SOCS3 binding to ELOC, ELOB, and CUL5 was dramatically decreased when WT AMBRA1 was over-expressed (**Figure 3.14A**, lane 2-3). By contrast, over-expression of ΔH mutant did not affect SOCS3 binding to ELOC and ELOB, albeit binding to CUL5 being slightly decreased (**Figure 3.14A**, lane 4-5). Similar results were observed for VIF; VIF binding to ELOC and ELOB was disrupted in the presence of WT AMBRA1 (**Figure 3.14B**, lane 1-2) and was unaffected by ΔH mutant nor DCAF11, another VIF-interacting DCAF identified in our HIV-1 proteomic study (**Figure 3.14B**, lane 3-4; **Figure 2.1**).

To further investigate whether disruption of CRL5 complexes by AMBRA1 compromises CRL5 E3 ligase activity, we examined SOCS3 and VIF autoubiquitination. Affinity tagged SOCS3 or VIF was purified under denaturing condition to assess their covalent modification with myc-ubiquitin in co-expression experiments. Consistent with the complex disruption results, we found that AMBRA1 over-expression reduced both SOCS3 and VIF autoubiquitination. SOCS3 autoubiquitination was reduced by over-expression of AMBRA1 and not by another SR of CRL4, DCAF1 **(Figure 3.14C)**. VIF autoubiquitination was similarly reduced by AMBRA1 albeit to a lesser extent when compared to the degree SOCS3 autoubiquitination was affected **(Figure 3.14D)**. As a side note, we showed that CBFβ over-expression reduced VIF

autoubiquitination (**Figure 3.14D**, lane 4), while CBFβ itself was polyubiquitinated, demonstrating that CBFβ-bound VIF was protected from autoubiquitination **(Figure 3.15)**. On the other hand, decreased VIF autoubiquitination by AMBRA1 was not a result of shielding effect, because ΔH mutant did not reduce VIF autoubiquitination despite showing slightly higher affinity for VIF (**Figure 3.14D**, lane 2-3; **Figure 3.14B**). Taken together, our results indicate that the ubiquitin E3 ligase function of AMBRA1 is important in down-regulating $CRL5^{SOCS3}$ and $CRL5^{VIF}$ complex formation and E3 ligase activity.

Figure 3.1

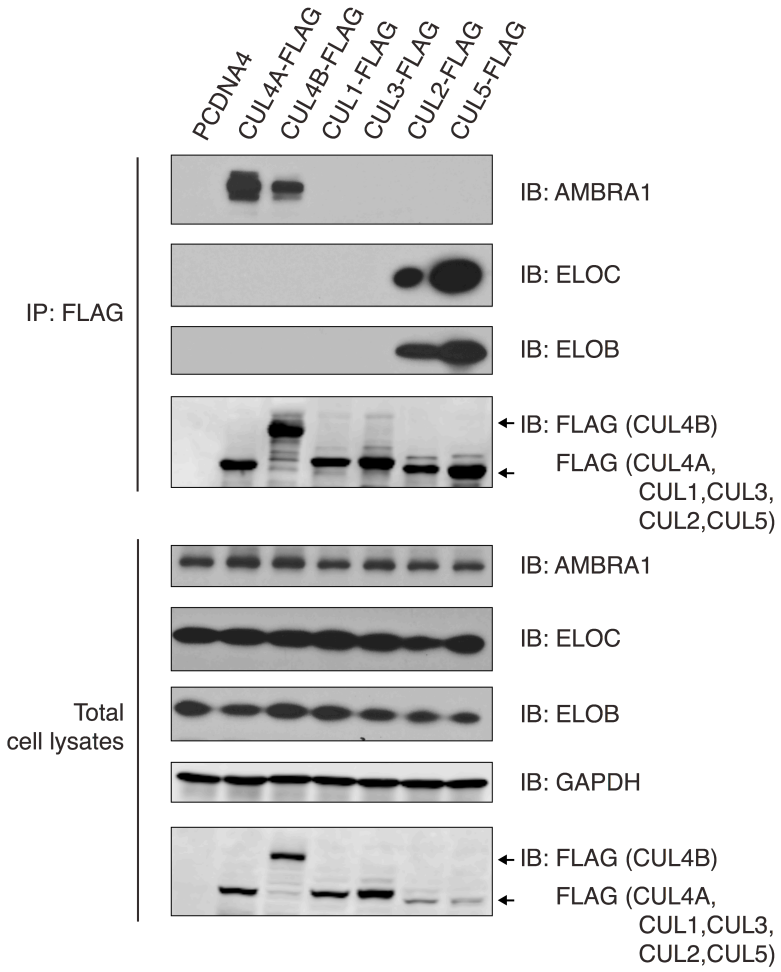

Figure 3.1 Cullin Specificity for AMBRA1 and ELOC.

FLAG-tagged cullins were expressed in 293T and affinity purified to examine co-purified AMBRA1, ELOC, and ELOB with immunoblot.

Figure 3.2

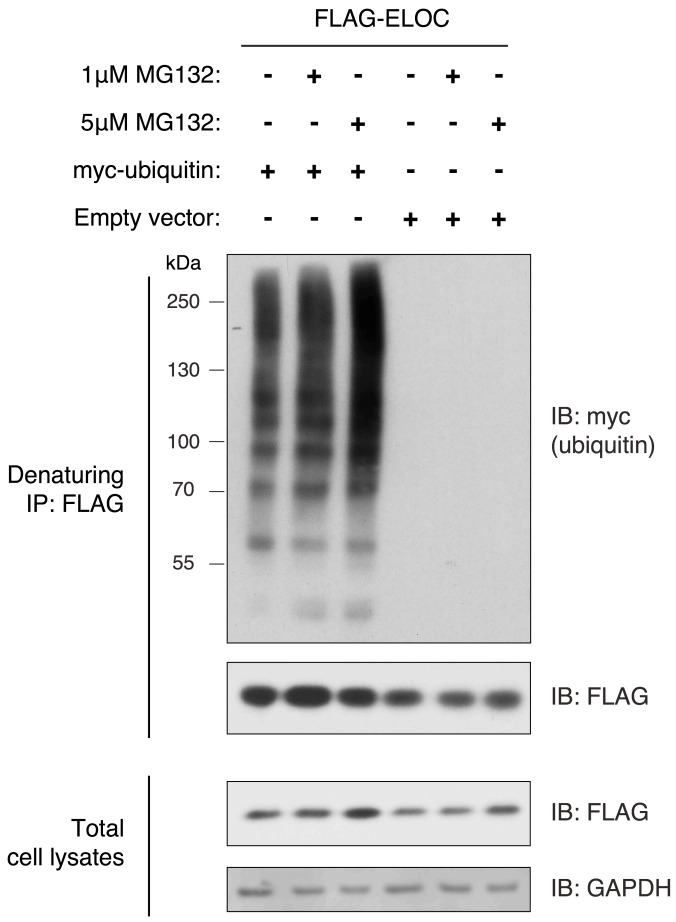

Figure 3.2 ELOC Polyubiquitination and It's Dependency on MG132 Treatment.

Denaturing IP of ELOC was performed on 293T stably expressing FLAG-ELOC transfected with myc-ubiquitin or Empty vector. Before harvested for IP, cells were treated with DMSO control, 1 μM or 5 μM MG132 for 6 hours. IP and input lysates were examined by immunoblot.

Figure 3.3

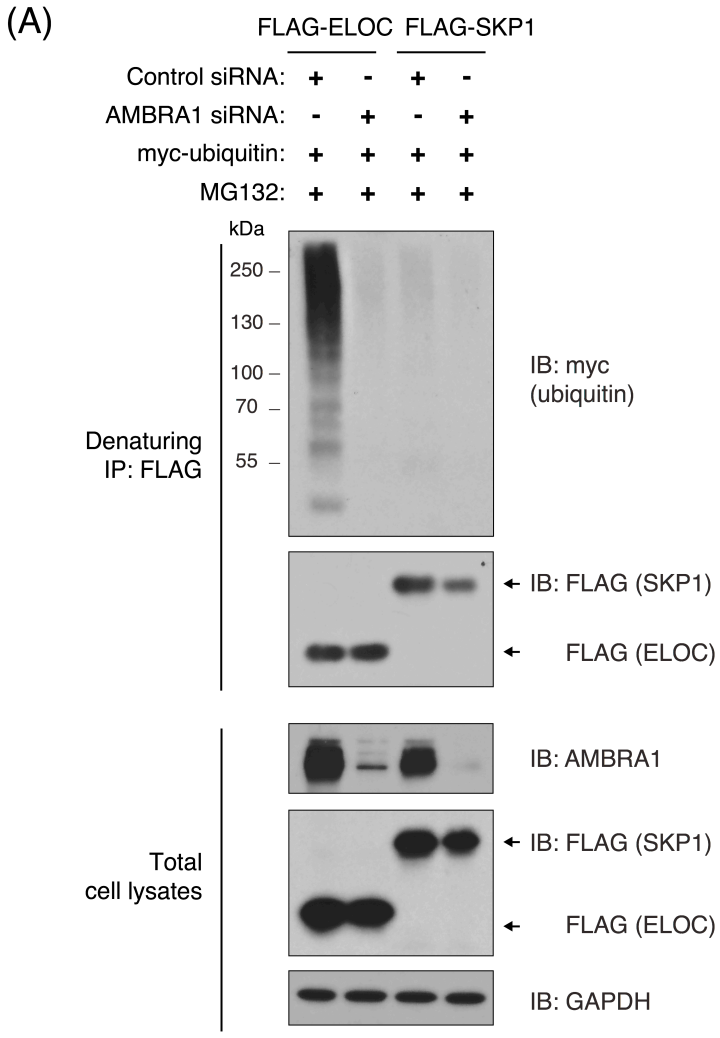
(A)
FLAG-ELOC
FLAG-SKP1
Control siRNA: + - + -
AMBRA1 siRNA: - + - +
myc-ubiquitin: + + + +
MG132: + + + +
kDa
250
130
100
70
55
Denaturing IP: FLAG
IB: myc (ubiquitin)
IB: FLAG (SKP1)
FLAG (ELOC)
Total cell lysates
IB: AMBRA1
IB: FLAG (SKP1)
FLAG (ELOC)
IB: GAPDH

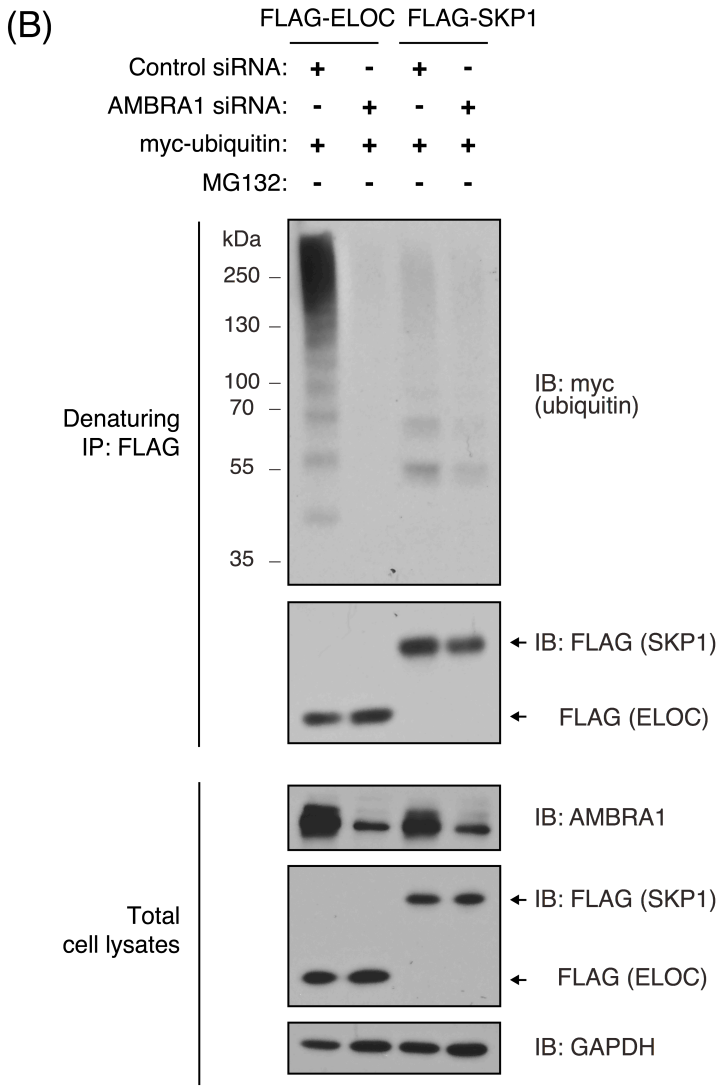

Figure 3.3 Elimination of ELOC Polyubiquitination in AMBRA1-Depleted Cells.

FLAG-ELOC or FLAG-SKP1 expressing 293T pre-treated with 10 nM of control or AMBRA1 siRNA was transfected with myc-ubiquitin. Before harvested for IP, cells were either treated with 5 μM MG132 **(A)** or vehicle DMSO control **(B)** for 6 hours. IP and input lysates were examined by immunoblot.

Figure 3.4

(A)

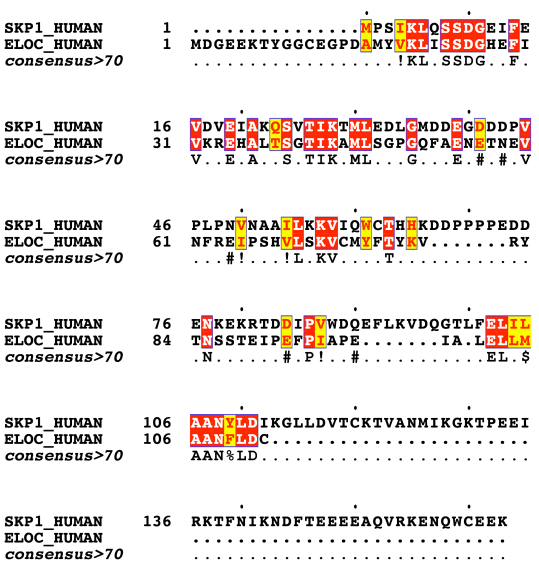
SKP1_HUMAN 1 ..............MPSIKLQSSDGEIFE
ELOC_HUMAN 1 MDGEEKTYGGCEGPDAMYVKLISSDGHEFI
consensus>70 ....!KL.SSDG..F.
SKP1_HUMAN 16 VDVEIAKQSVTIKTMLEDLGMDDFGDDDPV
ELOC_HUMAN 31 VKREHALTSGTIKAMLSGPGQFAENETNEV
consensus>70 V..E.A..S.TIK.ML...G...E.#.#.V
SKP1_HUMAN 46 PLPNVNAAILKKVIQWCLHHKDDPPPPEDD
ELOC_HUMAN 61 NFREIPSHVLSKVCMYFTYKV.......RY
consensus>70 ...#!...!L.KV....T............
SKP1_HUMAN 76 ENKEKRTDDIPVWDQEFLKVDQGTLFELIL
ELOC_HUMAN 84 TNSSTEIPEFPIAPE.......IA.LELLM
consensus>70 .N......#.P!..#..........EL.$
SKP1_HUMAN 106 AANYLDIKGLLDVTCKTVANMIKGKTPEEI
ELOC_HUMAN 106 AANFLDC.....................
consensus>70 AAN%LD.....................
SKP1_HUMAN 136 RKTFNIKNDFTEEEEAQVRKENQWCEEK
ELOC_HUMAN ....
consensus>70 ....

(B)

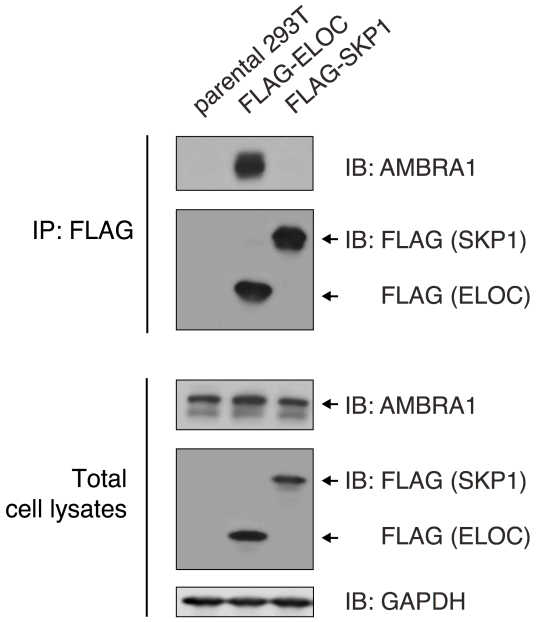
parental 293T
FLAG-ELOC
FLAG-SKP1
IP: FLAG
IB: AMBRA1
IB: FLAG (SKP1)
FLAG (ELOC)
Total
cell lysates
IB: AMBRA1
IB: FLAG (SKP1)
FLAG (ELOC)
IB: GAPDH

Figure 3.4 AMBRA1 Specifically Binds to ELOC and Not SKP1.

(A) Alignment of ELOC and SKP1 amino acid sequences.

(B) Specific binding of AMBRA1 to ELOC. Parental 293T or stable 293T expressing FLAG-ELOC or SKP1 were purified with anti-FLAG beads. IP and input lysates were examined by immunoblot.

Figure 3.5

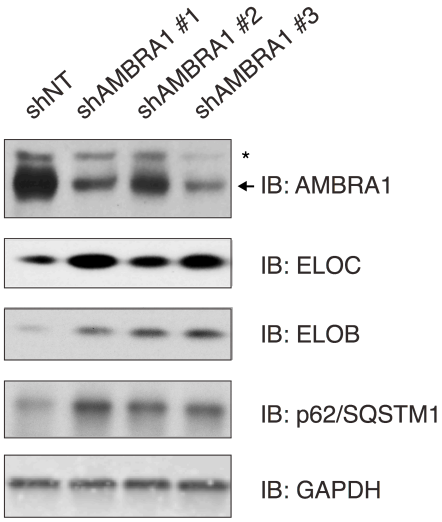

Figure 3.5 Accumulation of ELOC Protein in AMBRA1-Depleted 293T Cells.

Lysates harvested from 293T stably expressing non-targeting (NT) or AMBRA1 shRNAs was analyzed with immunoblot. This is representative of three experiments, in which stable lines were independently generated. Of note, the sequence of shAMBRA1 #1 corresponds to the sequence of siRNA used in **Figure 3.3**. Asterisk denotes nonspecific bands.

Figure 3.6

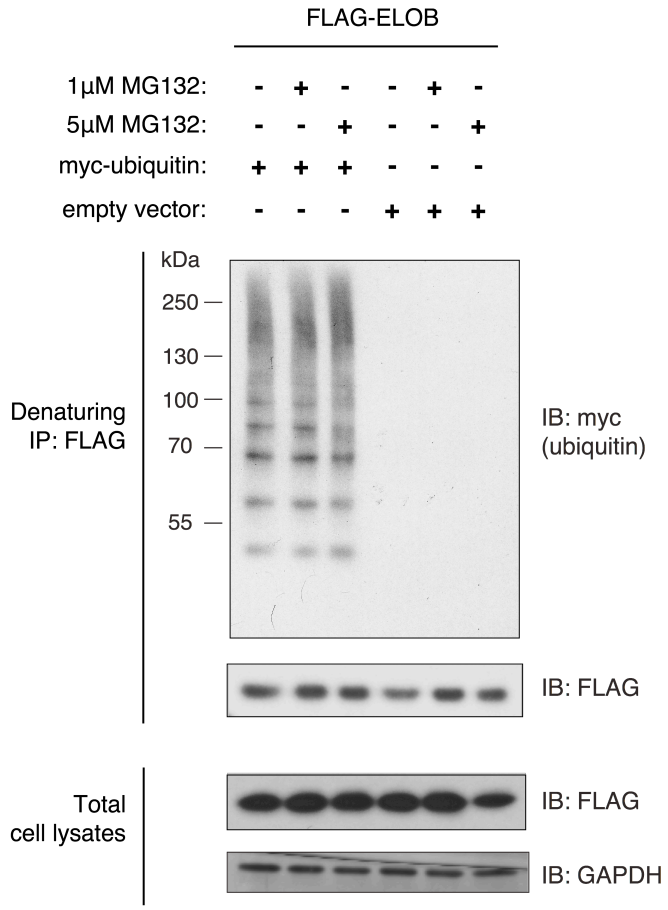

Figure 3.6 Proteasomal Inhibition Does Not Promote ELOB Polyubiquitination.

Similar to **Figure 3.2** but with FLAG-ELOB expressing 293T. 293T stably expressing FLAG-ELOB was transfected with myc-ubiquitin or Empty vector, followed by DMSO or MG132 treatment and denaturing IP. IP and input lysates were examined by immunoblot.

Figure 3.7

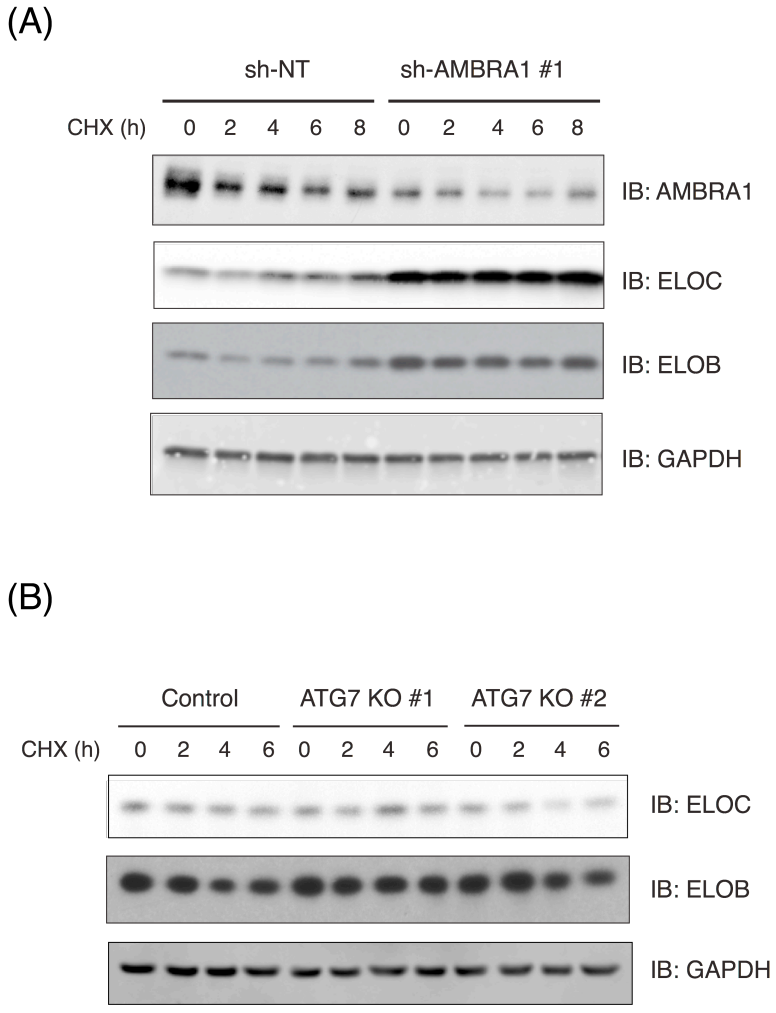
(A)
sh-NT
sh-AMBRA1 #1
CHX (h)
0 2 4 6 8 0 2 4 6 8
IB: AMBRA1
IB: ELOC
IB: ELOB
IB: GAPDH
(B)
Control
ATG7 KO #1
ATG7 KO #2
CHX (h)
0 2 4 6 0 2 4 6 0 2 4 6
IB: ELOC
IB: ELOB
IB: GAPDH

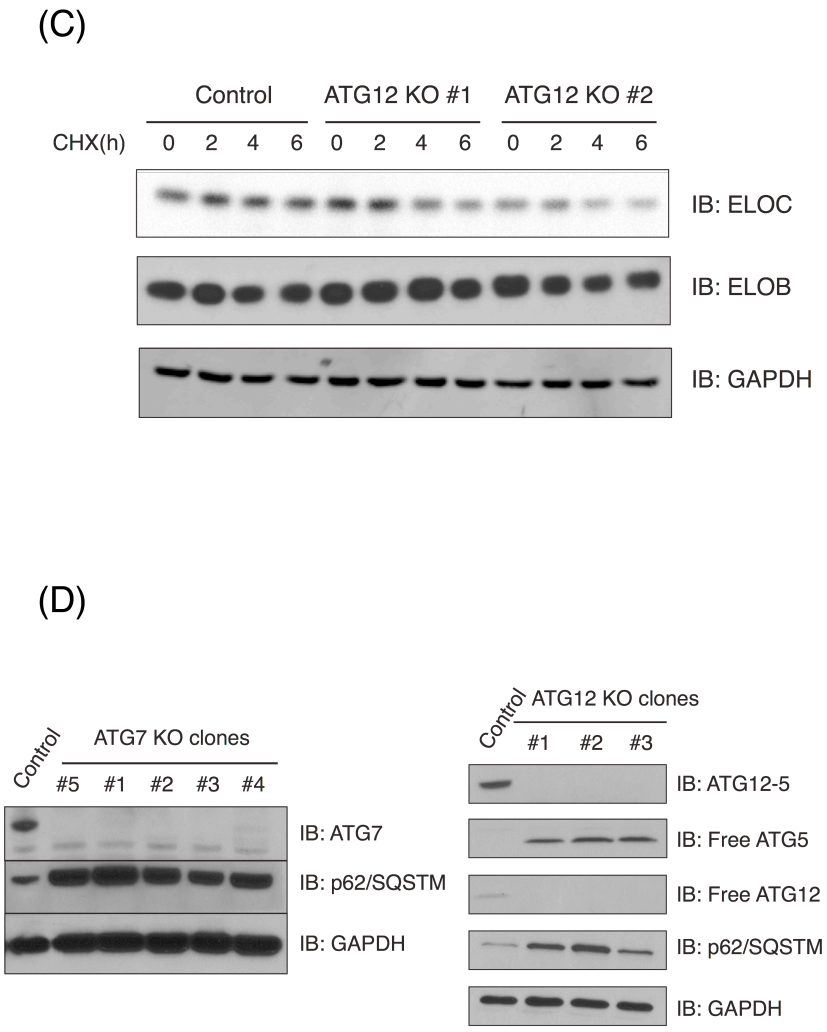

Figure 3.7. Autophagy Deficiency Does Not Promote ELOC Accumulation.

(A) 293T stably expressing non-targeting (NT) or AMBRA1 shRNA was treated with 100 μg/mL of cycloheximide (CHX) at different time points. Lysates were analyzed by immunoblot.

(B and C) ELOC and ELOB stability was monitored by CHX chase assay in control, ATG7, or ATG12 knockout 293T cells. 293T with scramble control, ATG7 (B), or ATG12 (C) sgRNA

mediated knockout was treated with 100 μg/mL of cycloheximide (CHX) at different time points. Lysates were analyzed by immunoblot.

(D) Functional validation of ATG7 and ATG12 knockout 293T. Lysates from control, ATG7 knockout, and ATG12 knockout clonal 293T were analyzed by immunoblot. ATG7 and ATG12 knockout were verified by the protein depletion and the accumulation of p62/SQSTM as a result of autophagy deficiency.

Figure 3.8

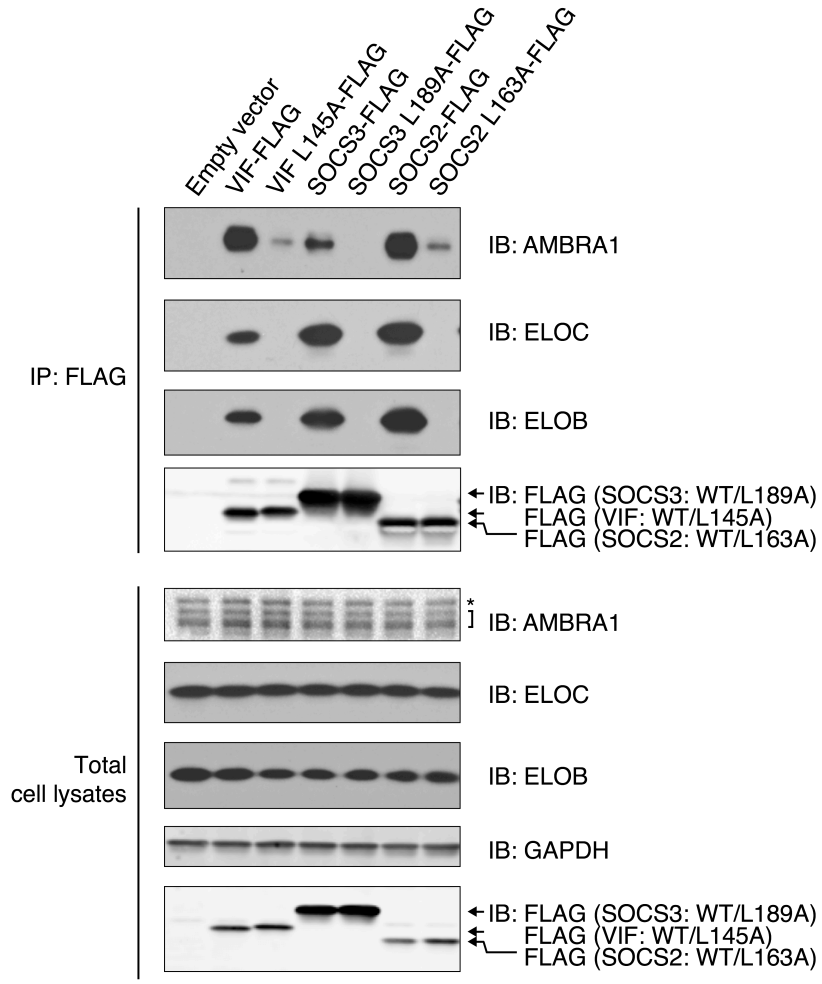

Figure 3.8 Mutation of BC-Box Disrupts Binding of SOCS Proteins and VIF to Both ELOC and AMBRA1.

293T transfected with FLAG-tagged VIF, SOCS2, SOCS3, and their respective BC-box point mutants was subjected to affinity purification. IP and input lysates were analyzed by immunoblot. Asterisk denotes nonspecific bands.

Figure 3.9

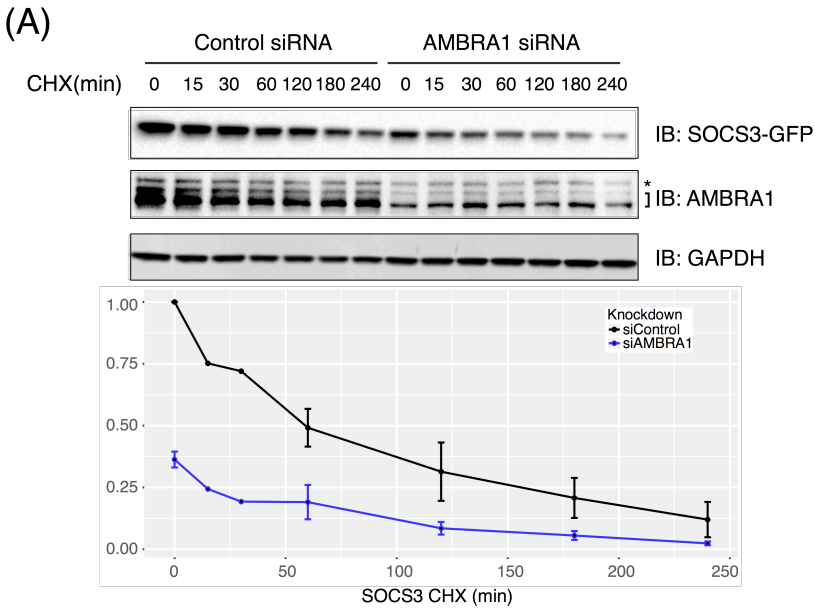
(A)
Control siRNA
AMBRA1 siRNA
CHX(min) 0 15 30 60 120 180 240 0 15 30 60 120 180 240
IB: SOCS3-GFP
IB: AMBRA1
IB: GAPDH
Knockdown
siControl
siAMBRA1
1.00
0.75
0.50
0.25
0.00
0 50 100 150 200 250
SOCS3 CHX (min)

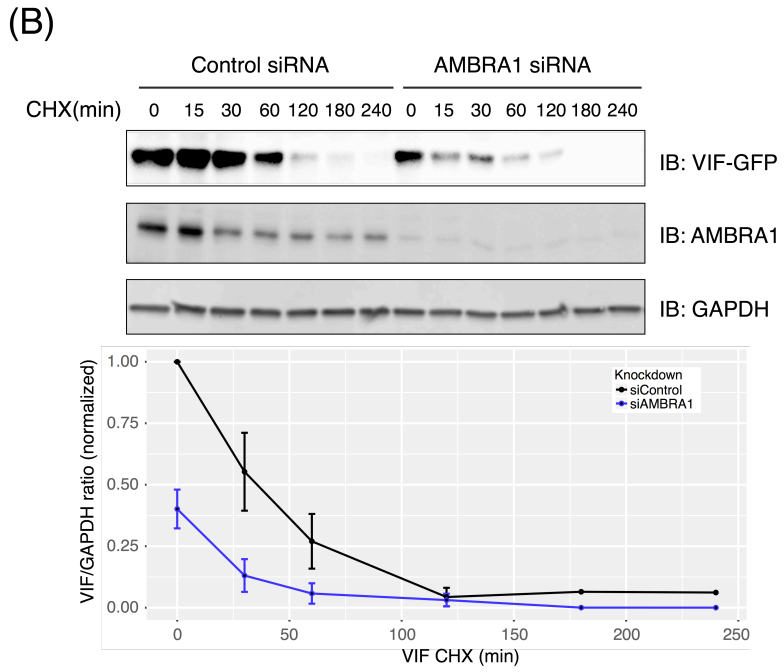
(B)
Control siRNA
AMBRA1 siRNA
CHX(min) 0 15 30 60 120 180 240 0 15 30 60 120 180 240
IB: VIF-GFP
IB: AMBRA1
IB: GAPDH
Knockdown
siControl
siAMBRA1
VIF/GAPDH ratio (normalized)
1.00
0.75
0.50
0.25
0.00
0 50 100 150 200 250
VIF CHX (min)

Figure 3.9 Destabilization of CRL5 Substrate Receptors by AMBRA1 Knockdown.

HEK293 stably expressing tet-on SOCS3-GFP **(A)** or VIF-GFP **(B)** was transfected with 10 nM of control or AMBRA1 siRNA for 72~96 hours. Protein expression was induced overnight with 1 μg/mL of doxycycline (dox), and followed by the addition of 100 μg/mL of cycloheximide (CHX) at different time points. Lysates were analyzed by immunoblot. Lower panels are densitometric quantification of relative SOCS3 and VIF band intensity (mean ± sem, n=3). Asterisk denotes nonspecific bands.

Figure 3.10

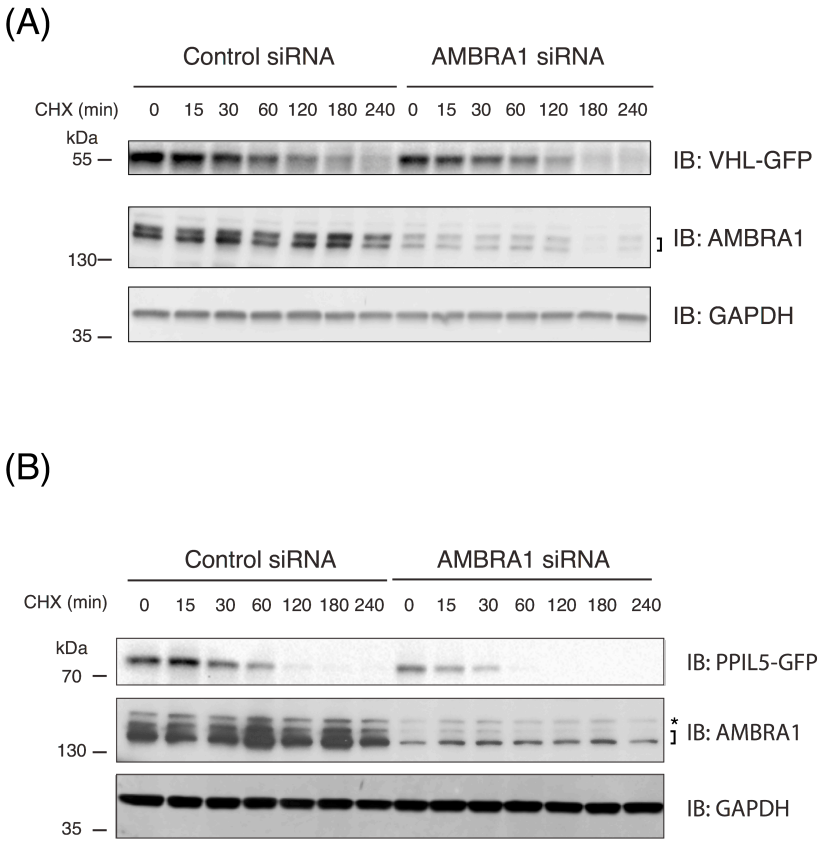

Figure 3.10. Destabilization of CRL2 Substrate Receptors by AMBRA1 Knockdown.

Similar to described in **Figures 3.9**, HEK293 stably expressing tet-on VHL-GFP **(A)** or PPIL5-GFP **(B)** was transfected with 10 nM of control or AMBRA1 siRNA for 72~96 hours. Protein expression was induced overnight with 1 μg/mL of doxycycline (dox), and followed by the addition of 100 μg/mL of cycloheximide (CHX) at different time points. Asterisk denotes nonspecific bands.

Figure 3.11

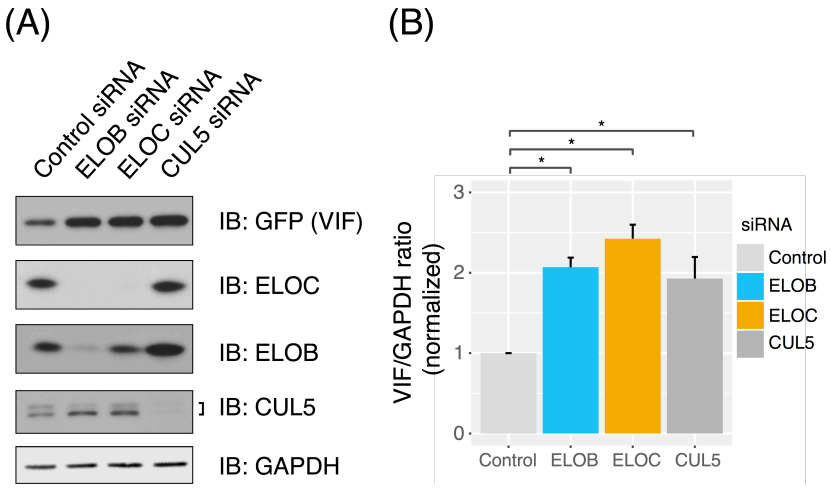

Figure 3.11 Stabilization of VIF by Inhibiting Autocatalysis.

(A) Similar to **Figure 3.9**, siRNA treated HEK293 tet-on VIF-GFP cells with dox-induced expression were analyzed by immunoblot for their steady state levels.

(B) Relative VIF band intensity on immunoblot was quantified and compared by Mann-Whitney-Wilcoxon Test (* p-value < 0.05). Bar graph represented mean + sem, n=3.

Figure 3.12

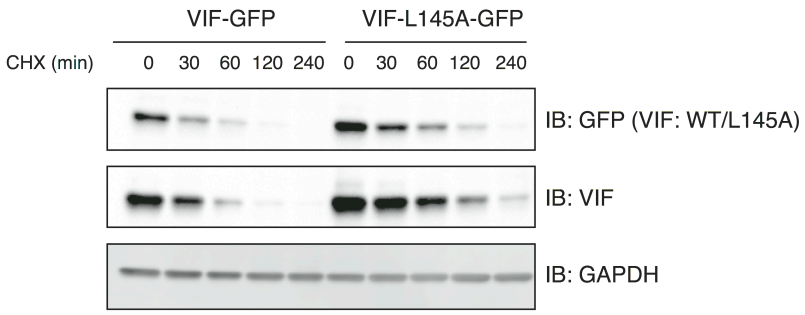

Figure 3.12 VIF is Stabilized by Blocking Its Autocatalysis.

HEK293 with tet-on VIF-GFP and VIF L145A-GFP expression was transfected with 10 nM of control or AMBRA1 siRNA for 72~96 hours. Protein expression was induced overnight with 1 μg/mL of doxycycline (dox), and followed by the addition of 100 μg/mL of cycloheximide (CHX) at different time points.

Figure 3.13

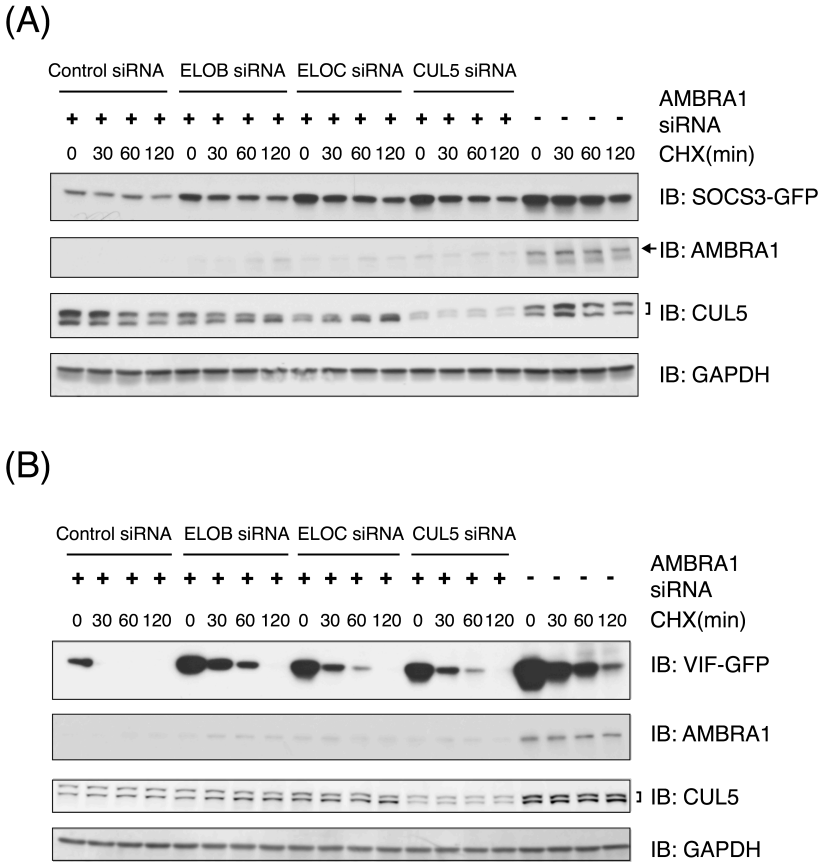

Figure 3.13 Rescue of SOCS3 and VIF Destabilization in AMBRA1-Depleted Background by Inhibiting Autocatalysis.

HEK293 with tet-on SOCS3-GFP **(A)** and VIF-GFP **(B)** were co-transfected with 5 nM of AMBRA1 siRNA in combination with 5 nM of control, ELOB, ELOC, or CUL5 siRNA. Cells were treated with dox and CHX as described in **Figure 3.9**.

Figure 3.14

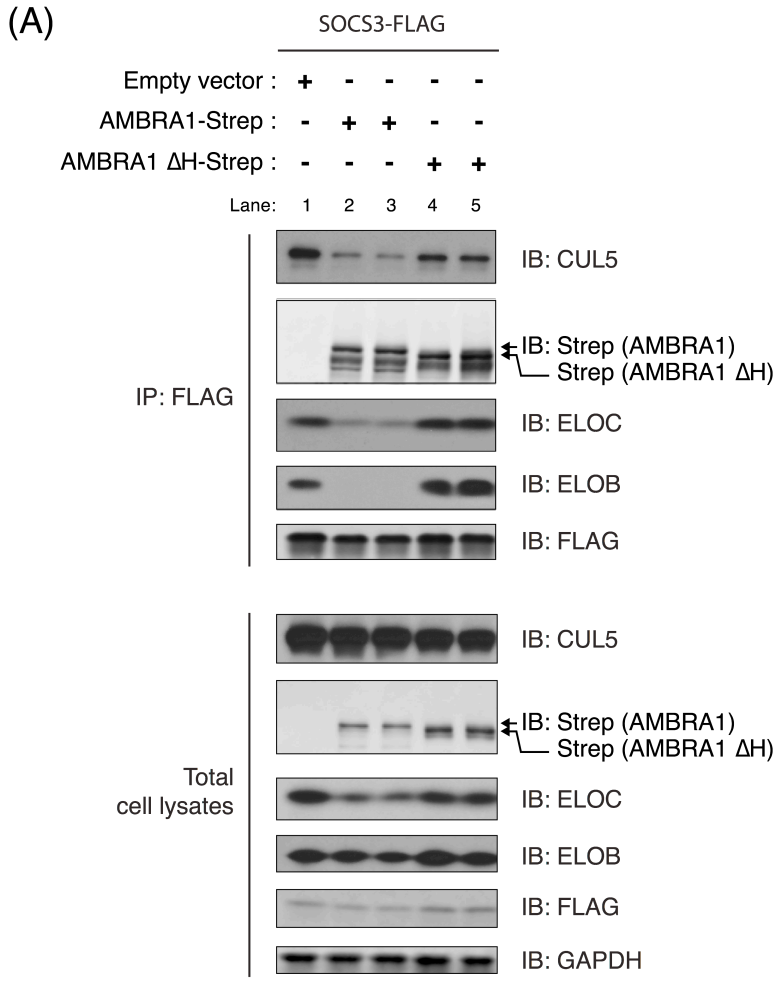
(A)
SOCS3-FLAG
Empty vector : + - - - -
AMBRA1-Strep : - + + - -
AMBRA1 ΔH-Strep : - - - + +
Lane: 1 2 3 4 5
IP: FLAG
IB: CUL5
IB: Strep (AMBRA1)
Strep (AMBRA1 ΔH)
IB: ELOC
IB: ELOB
IB: FLAG
Total
cell lysates
IB: CUL5
IB: Strep (AMBRA1)
Strep (AMBRA1 ΔH)
IB: ELOC
IB: ELOB
IB: FLAG
IB: GAPDH

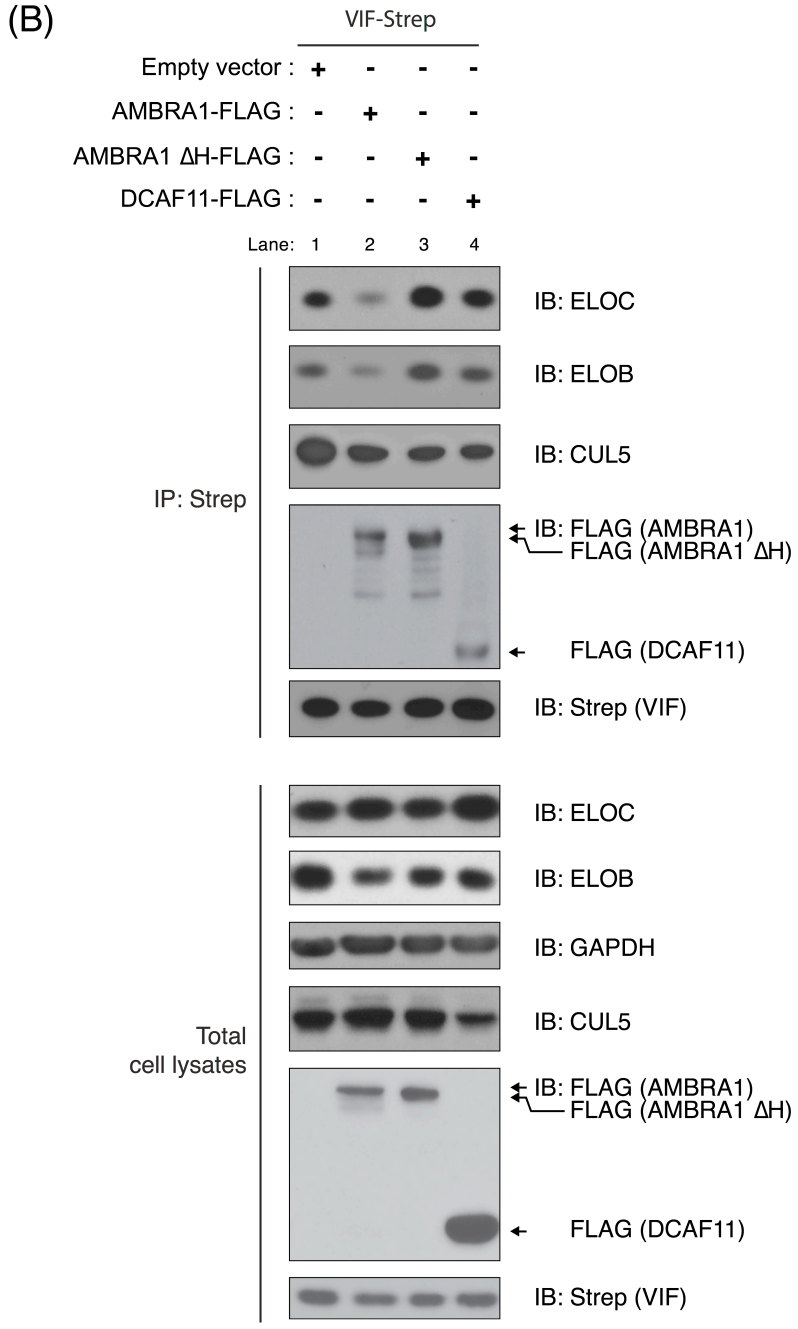
(B)
VIF-Strep
Empty vector : + - - -
AMBRA1-FLAG : - + - -
AMBRA1 ΔH-FLAG : - - + -
DCAF11-FLAG : - - - +
Lane: 1 2 3 4
IP: Strep
IB: ELOC
IB: ELOB
IB: CUL5
IB: FLAG (AMBRA1)
FLAG (AMBRA1 ΔH)
FLAG (DCAF11)
IB: Strep (VIF)
Total cell lysates
IB: ELOC
IB: ELOB
IB: GAPDH
IB: CUL5
IB: FLAG (AMBRA1)
FLAG (AMBRA1 ΔH)
FLAG (DCAF11)
IB: Strep (VIF)

(C)

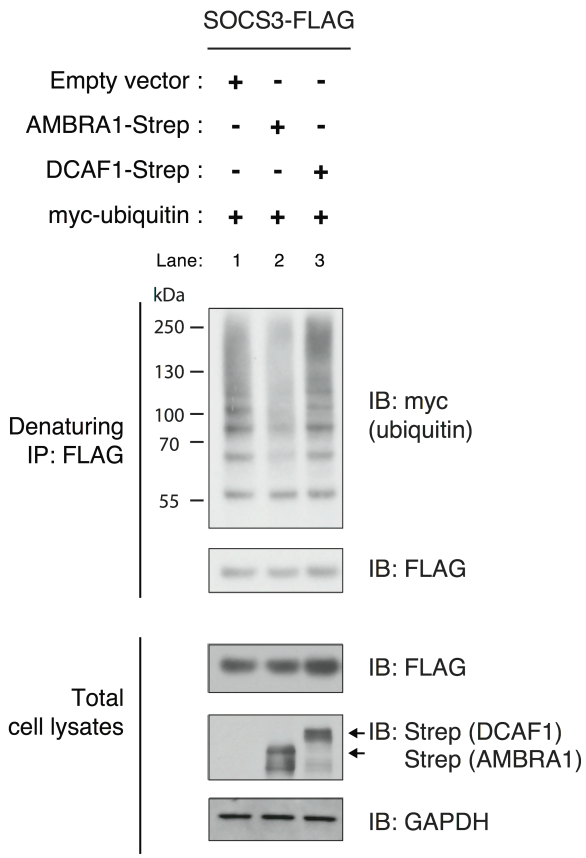
SOCS3-FLAG
Empty vector : + - -
AMBRA1-Strep : - + -
DCAF1-Strep : - - +
myc-ubiquitin : + + +
Lane: 1 2 3
kDa
250
130
100
70
55
Denaturing IP: FLAG
IB: myc (ubiquitin)
IB: FLAG
Total cell lysates
IB: FLAG
IB: Strep (DCAF1)
Strep (AMBRA1)
IB: GAPDH

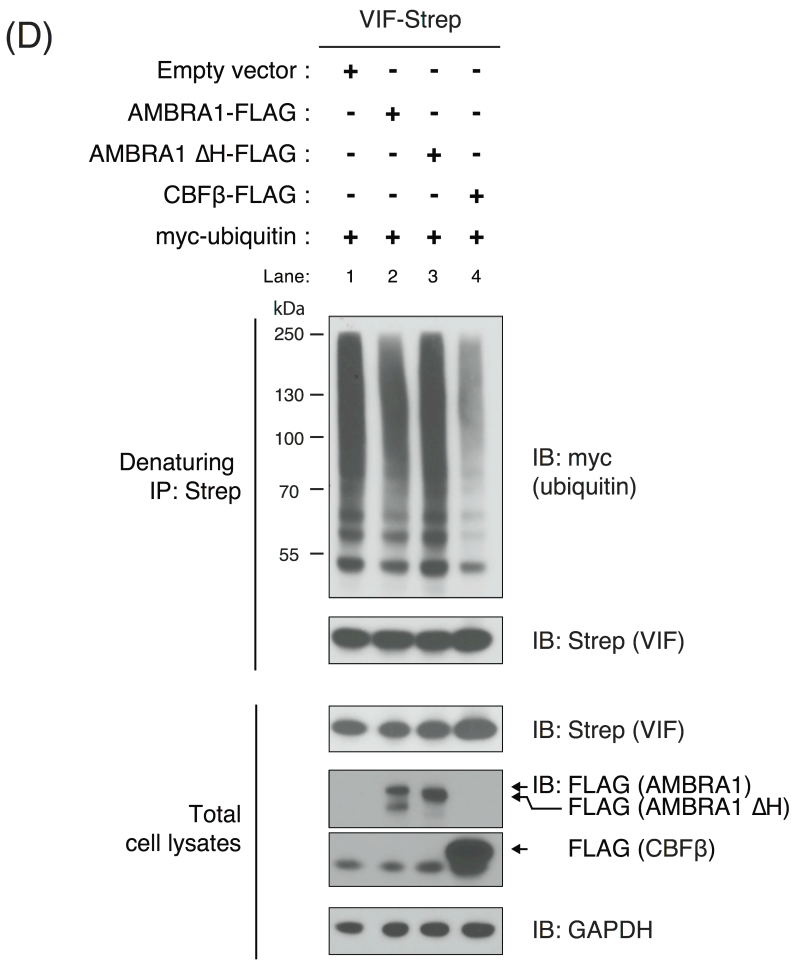

Figure 3.14 CRL4^{AMBRA1} Disrupts the Assembly and the E3 Ligase Activity of CRL5^{SOCS3} and CRL5^{VIF} Complexes.

(A) Disruption of CRL5^{SOCS3} assembly by WT AMBRA1 over-expression and not by ΔH mutant. 293T stably expressing SOCS3-FLAG was transfected with Empty vector, AMBRA1-Strep (2.5 and 5 μg), or ΔH-AMBRA1-Strep (2.5 and 5 μg). Lysates were affinity purified using

anti-FLAG beads to examine SOCS3 binding to CRL5 components. IP and input lysates were analyzed by immunoblot.

(B) Disruption of $CRL5^{VIF}$ assembly by WT AMBRA1 over-expression and not by ΔH mutant. 293T cells co-expressing Vif-Strep with Empty vector, AMBRA1-FLAG, ΔH-AMBRA1-FLAG, or DCAF11-FLAG. Lysates were purified with Strep-Tactin sepharose beads to examine VIF binding to CRL5 components. IP and input lysates were analyzed by immunoblot.

(C and D) Reduction in SOCS3 and VIF autoubiquitination by WT AMBRA1 over-expression and not by ΔH mutant. Similar to (A) and (B) but with the cells co-transfected with myc-ubiquitin and affinity purified under denaturing condition with anti-FLAG and Strep-Tactin beads, respectively. IP and input lysates were analyzed by immunoblot.

Figure 3.15

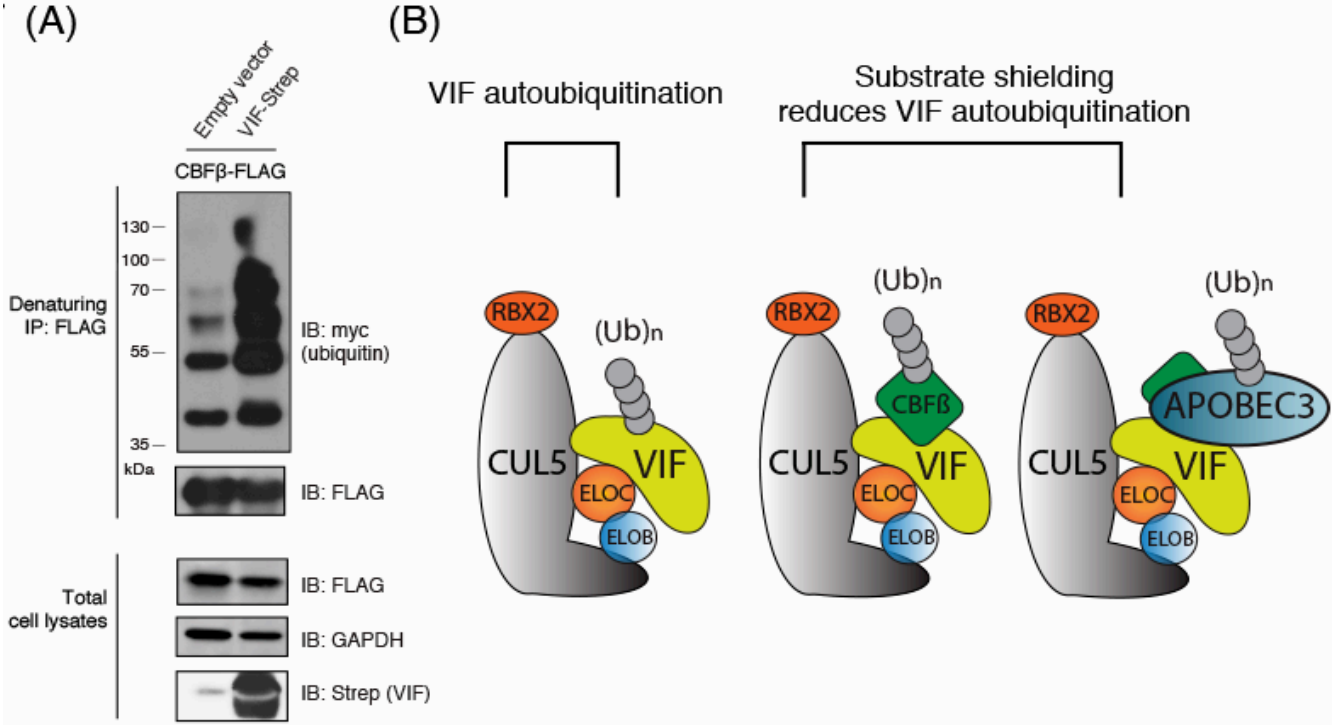

Figure 3.15 Substrate-Shielding Effect.

(A) Increased CBFβ polyubiquitination by VIF over-expression. 293T co-expressing FLAG-tagged CBFβ, myc-ubiquitin along with Empty vector or Strep-tagged VIF was affinity purified under denaturing condition with anti-FLAG to examine ubiquitin incorporation into CBFβ. IP and input lysates were analyzed by immunoblot.

(B) Model depicting substrate shielding effect. VIF is sensitive to autoubiquitination in the absence of its binding partner CBFβ and the VIF substrate APOBEC3.

Chapter 4

$CRL4^{AMBRA1}$ Modulates Pathways Regulated by $CRL5^{SOCS3}$ and $CRL5^{VIF}$

To evaluate the functional consequences of $CRL5^{SOCS3}$ and $CRL5^{VIF}$ down-regulation by $CRL4^{AMBRA1}$, we examined how AMBRA1 and its E3 ligase activity affects IL-6/STAT3 signaling and APOBEC3G (A3G) degradation, which are regulated by $CRL5^{SOCS3}$ and $CRL5^{VIF}$, respectively.

SOCS3 is a critical negative regulator of IL-6 induced STAT3 signaling pathway, and deletion of its BC-box leads to prolonged STAT3 phosphorylation (pTyr705 or pSTAT3) due to the lack of pSTAT3 suppression by $CRL5^{SOCS3}$ [59-61]. In IL-6 stimulation experiments, human hepatoma Hep3B stably expressing mCherry or AMBRA1 was treated with IL-6 at different time points and harvested for immunoblot. We found that AMBRA1 over-expression sensitized IL-6 induced STAT3 phosphorylation when compared to mCherry over-expression, suggestive of weakened pSTAT3 suppression from reduced $CRL5^{SOCS3}$ E3 ligase activity (**Figure 4.1A** and quantification of immunoblot in **Figure 4.1B**). In addition, SOCS3 knockdown phenocopied AMBRA1 over-expression in prolonged STAT3 phosphorylation **(Figure 4.2)**. Furthermore, Hep3B with AMBRA1 depletion showed blunted response to IL-6 induced STAT3 phosphorylation, consistent with the idea that up-regulated $CRL5^{SOCS3}$ activity enhanced pSTAT3 suppression (**Figure 4.3A** and quantification of immunoblot in **Figure 4.3B**). We showed that blunted IL-6/STAT3 response following AMBRA1 knockdown was reversed by concomitant SOCS3 knockdown or re-expression of WT AMBRA1, whereas re-expression of

ΔH mutant was insufficient to rescue pSTAT3 activation **(Figure 4.4)**. These results indicated that $CRL4^{AMBRA1}$ regulates IL-6/STAT3 pathway by modulating $CRL5^{SOCS3}$ activity.

We went on to examine AMBRA1's effect on $CRL5^{VIF}$ mediated A3G degradation. A3G belongs to the APOBEC3 family of cytidine deaminases, which are virus-induced restriction factors that can be encapsidated to virions and cause hypermutation in viral genomes [62, 63]. A3G is targeted by $CRL5^{VIF}$ for degradation during HIV-1 infection, and failure to neutralize A3G leads to unsuccessful infection. In co-transfection experiments, we found that VIF-mediated A3G degradation was enhanced in AMBRA1-depleted background generated with CRISPR/Cas9 system, whereas A3G was unaffected in the absence of VIF regardless of AMBRA1 levels, indicating that AMBRA1 regulates A3G degradation specifically by modulating VIF activity (**Figure 4.5** for AMBRA1-editing information; **Figures 4.6A and 4.6B**). Enhanced A3G degradation by VIF following AMBRA1 knockdown was reversed by re-expression of AMBRA1 (**Figure 4.6C**). Additionally, we showed that over-expression of both ELOC and ELOB phenocopied AMBRA1 knockdown, supporting that $CRL5^{VIF}$ function and thereby A3G levels can be regulated through ELOBC **(Figure 4.6D)**. These data indicated that regulation of $CRL5^{VIF}$ activity by $CRL4^{AMBRA1}$ correlates with perturbations in A3G degradation.

Taken together, we identified the key adapter protein ELOC of CRL5 and CRL2 complexes being targeted by $CRL4^{AMBRA1}$ for polyubiquitination and degradation (**Figure 4.7**, i). We further showed that $CRL4^{AMBRA1}$ negatively regulates the assembly and activity of CRL5 complexes by targeting ELOC. Using $CRL5^{SOCS3}$ and $CRL5^{VIF}$ as examples, we showed that

AMBRA1 level affects the magnitude and kinetic profile of their responsible pathways. SOCS3 constitutes an important negative feedback loop for IL-6/STAT3 signaling, in which STAT3 phosphorylation induced by IL-6 drives the expression of SOCS3 as well as proliferative and inflammatory factors (**Figure 4.7**, ii) [64]. $CRL5^{SOCS3}$ dysfunction sensitizes IL6-STAT3 signaling, as what we observed in AMBRA1 over-expressing cells, whereas overly active $CRL5^{SOCS3}$ in AMBRA1-depleted cells blunts IL-6-induced STAT3 activation. Similarly, AMBRA1 knockdown leads to overly active $CRL5^{VIF}$ that degrades A3G more efficiently, and enhanced A3G degradation can be reversed by re-expression of AMBRA1 (**Figure 4.7**, iii).

Figure 4.1

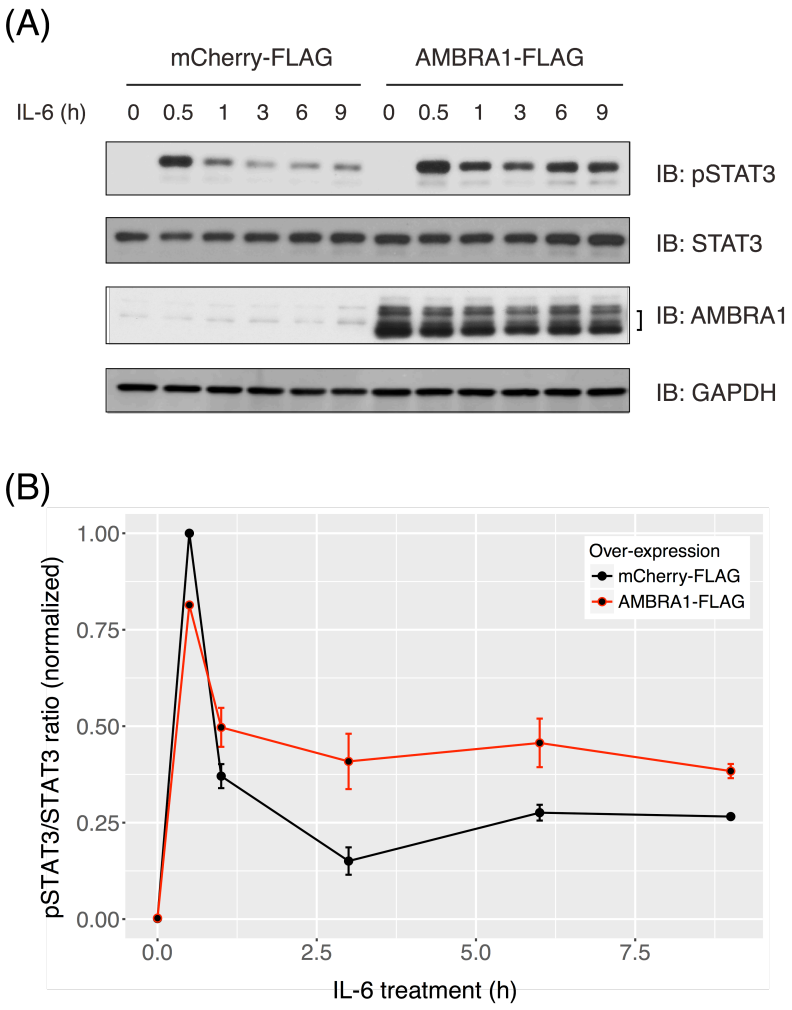

Figure 4.1 AMBRA1 Overexpression Sensitizes IL-6/STAT3 Signaling.

(A) Hep3B cells stably expressing mCherry-FLAG or AMBRA1-FLAG was starved for 12 hours and treated with 20 ng/mL of IL-6 at different time points. Lysates were analyzed with immunoblot.

(B) Quantification of pSTAT3/total STAT3 ratios from three independent experiments described in **(A)** (mean ± sem, n=3).

Figure 4.2

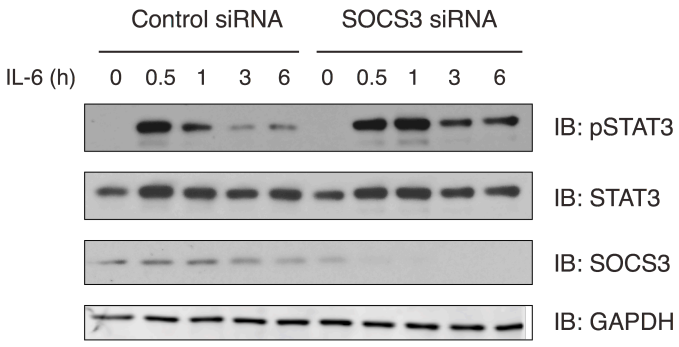

Figure 4.2 SOCS3 Knockdown Sensitizes IL-6/STAT3 Signaling.

Hep3B pre-treated with control or SOCS3 siRNA was stimulated with IL-6 and analyzed as described in **Figure 4.1**.

Figure 4.3

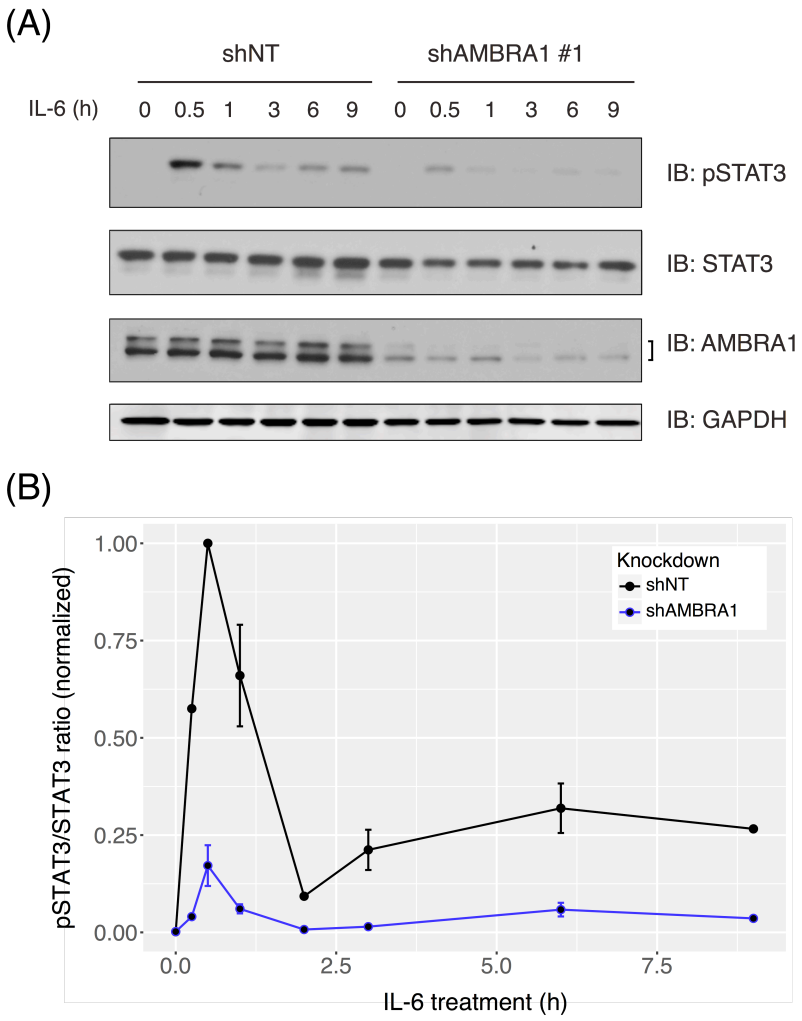

Figure 4.3 AMBRA1 Knockdown Blunts IL-6/STAT3 Signaling.

(A) Hep3B stably expressing non-targeting (NT) or AMBRA1 shRNA was stimulated with IL-6 and analyzed as described in **Figure 4.1**.

(B) Quantification of pSTAT3/total STAT3 ratios from three independent experiments described in **(A)** (mean ± sem, n=3).

Figure 4.4

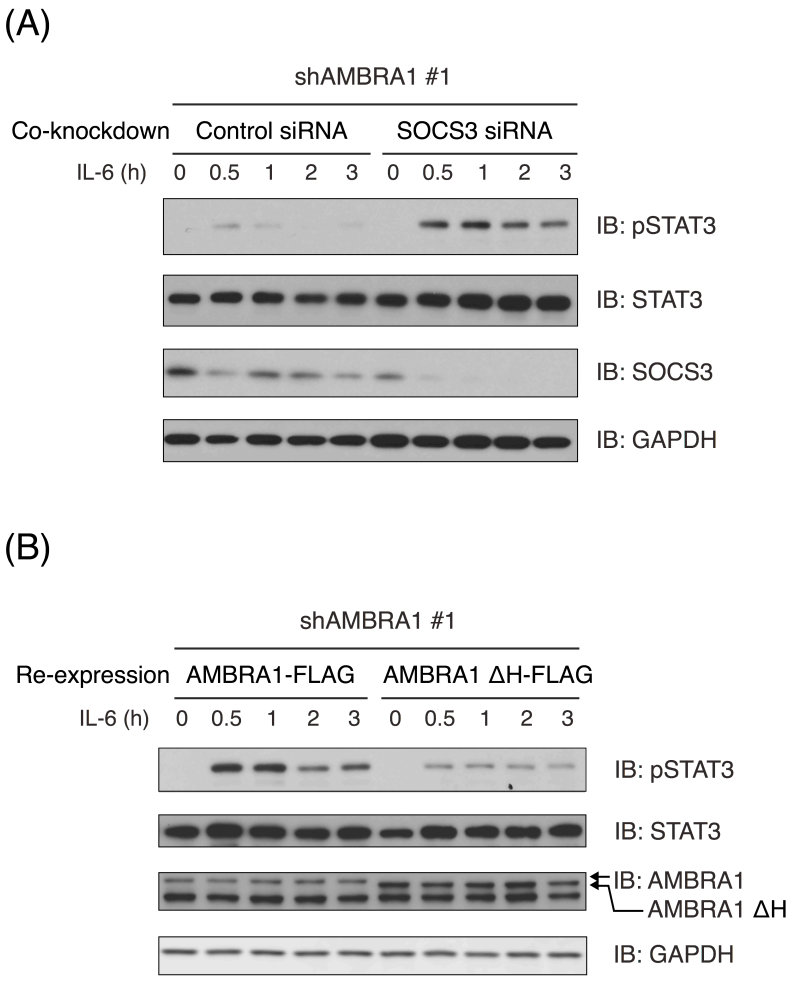

Figure 4.4 Rescue of Blunted IL-6 /STAT3 Response in AMBRA1-Knockdown Background by SOCS3 Knockdown and Re-Expression of WT AMBRA1.

(A) Knocking down SOCS3 rescued blunted IL-6 /STAT3 response in AMBRA1 knockdown background. Hep3B stably expressing shAMBRA1 #1 was transfected with control or SOCS3 siRNA, followed by IL-6 treatment.

(B) Re-expression of WT AMBRA1 and not ΔH mutant rescued blunted IL-6 /STAT3 response in AMBRA1 knockdown background. Hep3B stably expressing shAMBRA1 #1 was transduced and selected for WT AMBRA1 or ΔH mutant expression; the established re-expression cell lines were then treated with IL-6 and analyzed by immunoblot.

Figure 4.5

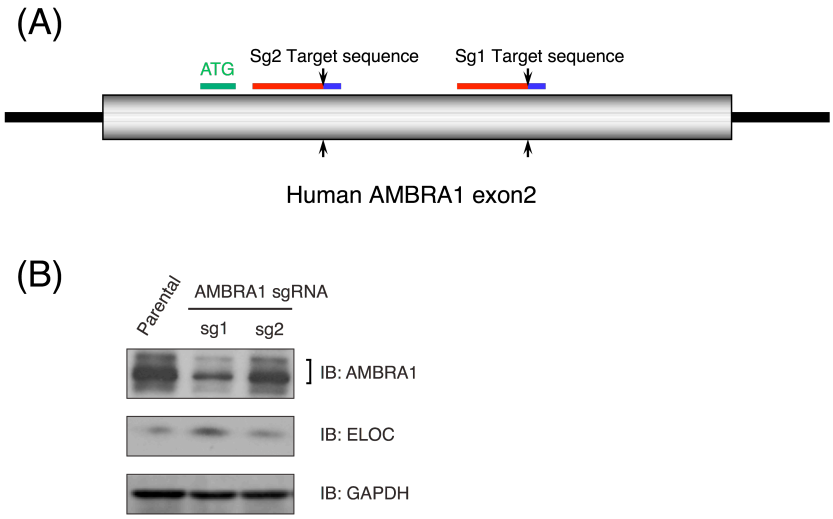

Figure 4.5 AMBRA1-Knockout 293T Cells Generated with the CRISPR/Cas9 System.

(A) Cartoon depicts the CRISPR/Cas9-targeted regions with two different AMBRA1 single chimeric guide RNAs (sg1 and sg2), with the guide RNA sequences colored in red and the photospacer-associated motifs (PAMs) colored in blue.

(B) 293T transfected with AMBRA1 guide RNA encoding plasmids (sg1 and sg2 cloned to SpCas9-P2A-GFP, Addgene #48138) for 48~72 hours was FACS-sorted into tubes based on GFP expression. Expanded polyclonal AMBRA1 knockout cells were analyzed along with parental 293T using immunoblot.

(C) Alignment of the sequence reads from parental 293T and AMBRA1 KO #4 cells (clonally selected from sg1-transfected 293T) encompassing human AMBRA1 exon2. "-" denotes deletion of nucleotides. Please note that AMBRA1 KO #2 cells (also edited with sg1) may contain a large insertion/deletion that was unable to be amplified with the same set of PCR primers.

Figure 4.6

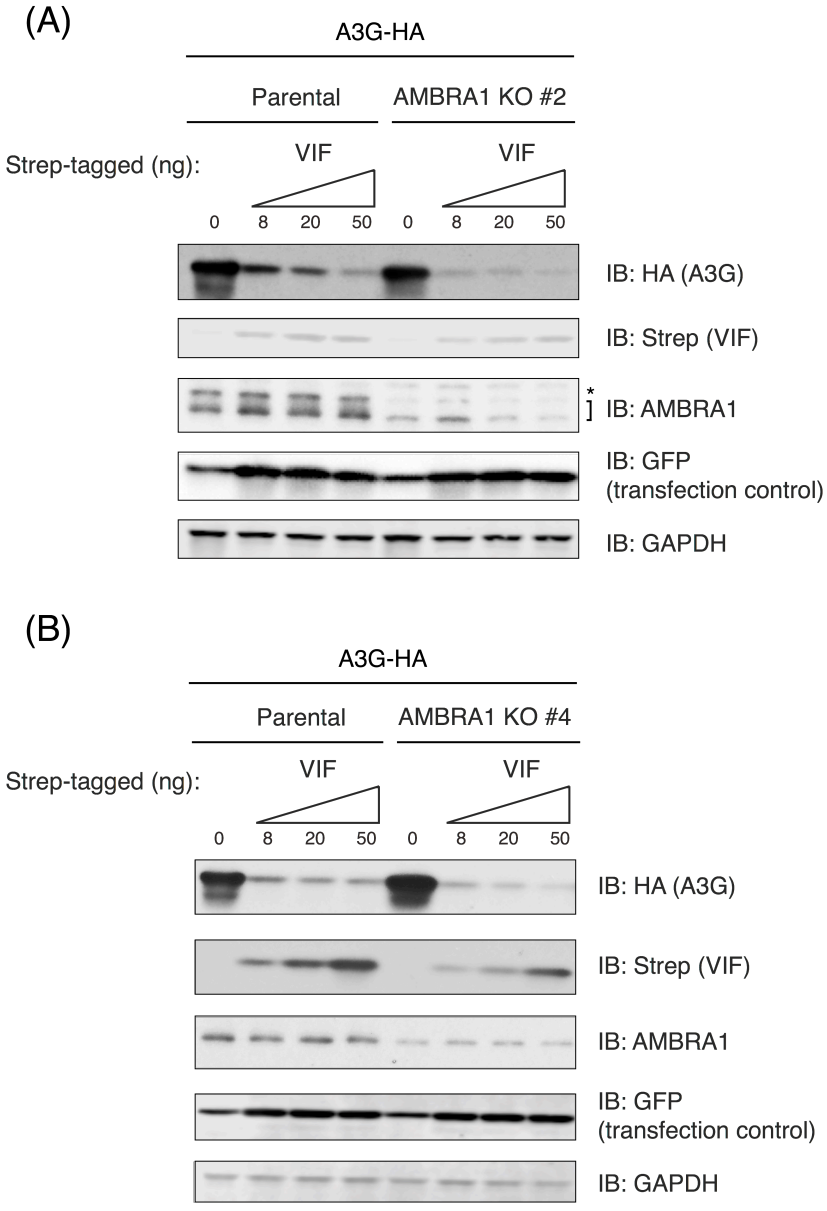
(A)
A3G-HA
Parental
AMBRA1 KO #2
Strep-tagged (ng):
VIF
VIF
0 8 20 50 0 8 20 50
IB: HA (A3G)
IB: Strep (VIF)
*
IB: AMBRA1
IB: GFP
(transfection control)
IB: GAPDH
(B)
A3G-HA
Parental
AMBRA1 KO #4
Strep-tagged (ng):
VIF
VIF
0 8 20 50 0 8 20 50
IB: HA (A3G)
IB: Strep (VIF)
IB: AMBRA1
IB: GFP
(transfection control)
IB: GAPDH

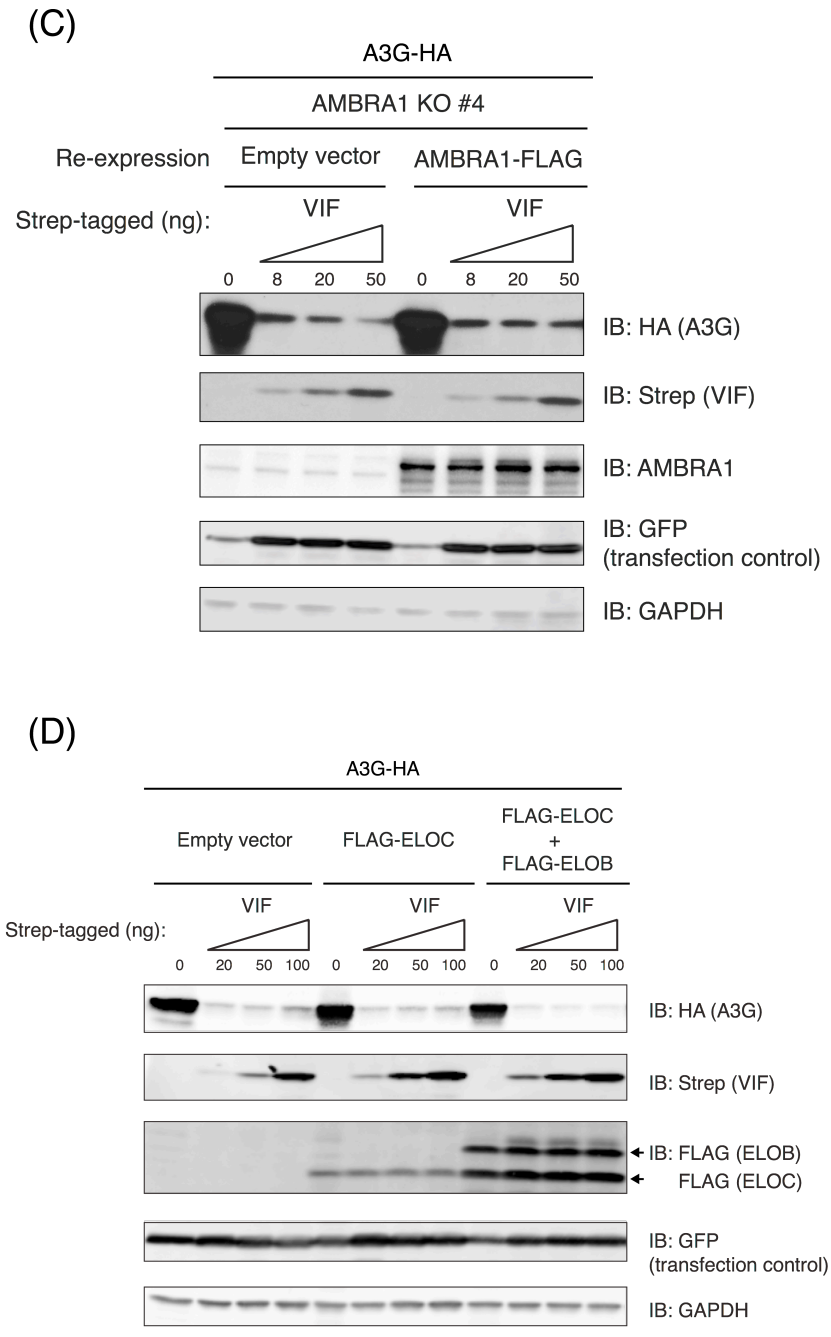

Figure 4.6 APOBEC3G Degradation by CRL5^{VIF} Is Upregulated in AMBRA1-Depleted Background.

(A and B) Co-expression of HA-tagged APOBEC3G (A3G), increasing amounts of Strep-tagged VIF, and transfection control GFP in parental 293T, AMBRA1 knockout cells KO #2 **(A)** or KO #4 **(B)**. The total amount of DNA transfected was kept constant adding Empty vector. Lysates were analyzed by immunoblots. Asterisk denotes nonspecific bands.

(C) Similar to described in **(B)** but included Empty vector control or re-expression of AMBRA1 in AMBRA1 KO #4.

(D) Similar co-transfection experiment was carried out along with Empty vector control, FLAG-ELOC, or co-expression of FLAG-ELOC and FLAG-ELOB.

Figure 4.7

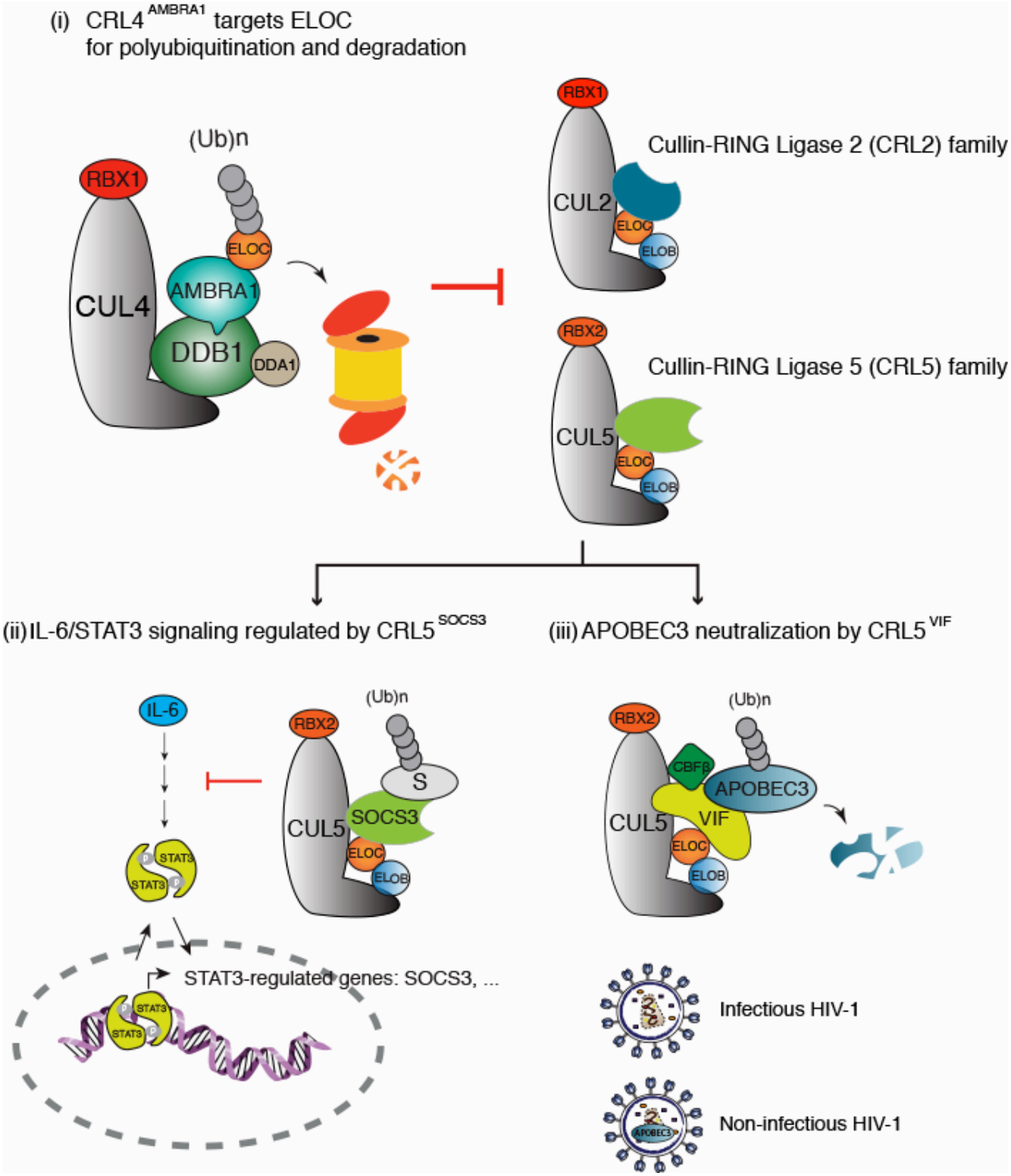
(i) CRL4 AMBRA1 targets ELOC
for polyubiquitination and degradation
(Ub)n
RBX1
ELOC
AMBRA1
CUL4
DDB1
DDA1
RBX1
Cullin-RING Ligase 2 (CRL2) family
CUL2
ELOC
ELOB
RBX2
Cullin-RING Ligase 5 (CRL5) family
CUL5
ELOC
ELOB
(ii) IL-6/STAT3 signaling regulated by CRL5 SOCS3
(iii) APOBEC3 neutralization by CRL5 VIF
IL-6
STAT3
STAT3
(Ub)n
RBX2
S
CUL5
SOCS3
ELOC
ELOB
STAT3-regulated genes: SOCS3, ...
STAT3
STAT3
(Ub)n
RBX2
CBFβ
APOBEC3
CUL5
VIF
ELOC
ELOB
Infectious HIV-1
Non-infectious HIV-1

Figure 4.7 Proposed Model Depicting How $CRL4^{AMBRA1}$ Regulates CRL5/2 Complexes and Thereby Modulates CRL5/2-Regulated Pathways.

$CRL4^{AMBRA1}$ targets ELOC for polyubiquitination and degradation (i), and thereby negatively regulates the assembly and ubiquitin E3 ligase activity of CRL5 and potentially CRL2 complexes. In this study, we examined how AMBRA1 and its E3 ligase function (as demonstrated by ΔH mutant in loss of function) modulate the responses of IL-6/STAT3 signaling (ii) and APOBEC3 degradation (iii), which are regulated by $CRL5^{SOCS3}$ and $CRL5^{VIF}$ complexes. S denotes unknown substrates.

Chapter 5

Discussion and Conclusions

Here we demonstrated that a shared module among by a subfamily of CRLs can be ubiquitinated by another CRL E3 ligase to achieve heterologous regulation of the CRL subfamily. We discovered that $CRL4^{AMBRA1}$ targets ELOC, the essential adaptor protein that mediates the assembly of CRL5/2 complexes for polyubiquitination and proteasomal degradation. This mechanism underlies the crosstalk between $CRL4^{AMBRA1}$ and CRL5 complexes suggested by previous studies [31, 36] and is now further defined in our work. The requirement of AMBRA1's E3 ligase function in $CRL5^{SOCS3}$ and $CRL5^{VIF}$ complex regulation and their respective downstream pathways epitomizes that $CRL4^{AMBRA1}$ regulates a broad range of CRL5 and potentially CRL2 complexes.

CRLs and other ubiquitin E3 ligases undergo complex regulatory processes, including autocatalysis, heterologous ubiquitination by another E3 ligase, and other mechanisms targeting different moieties of the E3 complex [41, 65]. SRs of CRL1, CRL3, and CRL4 are prone to autocatalytic degradation when the ligases are overly active [7, 8, 24, 58]. Conversely, CRL2 and CRL5 SRs, except for VHL and VIF, have not been well-studied for their autocatalytic activities [34, 66]. Here, we showed that CRL5 SRs SOCS3 and VIF are auto-ubiquitinated and their protein levels are regulated by autocatalysis. To examine the effect of a CRL regulator on the target CRLs, researchers have commonly assessed SR stability. For example, many CRL1 SRs are destabilized in a COP9 signalosome (CSN)-defective background as a result of CRL1

hyperactivation [10]. Additionally, depleting Glomulin, a RBX1-binding protein that negatively regulates RBX1-containing CRL complexes, causes hyperactivation of the complexes, destabilizing the CRL1 SR FBW7, RBX1, and RBX1-bound cullins [11, 12]. Hyperactivation of $CRL1^{FBW7}$ is associated with accumulation of its substrates Cyclin E and c-Myc due to premature destruction of FBW7 and the rest of the complex. Here, we discovered that AMBRA1 depletion similarly destabilizes SOCS3 and VIF as a result of CRL5 hyperactivation **(Figure 3.9)**. Surprisingly, elevated $CRL5^{SOCS3}$ and $CRL5^{VIF}$ activities positively correlated with pSTAT3 suppression and increased substrate clearance, respectively **(Figures 4.3 and 4.6)**. We reasoned that $CRL5^{SOCS3}$ and $CRL5^{VIF}$ complexes may predominantly contain SR-substrate heterodimers instead of monomers, whereas $CRL1^{FBW7}$ assembly and autocatalysis likely precede substrate recruitment [67-69]. Consistent with this idea, suppressing SR autocatalytic degradation in the presence of its substrate, also known as the substrate-shielding effect, occurs in CRL complexes [57, 70, 71].

CRL master regulators including CSN, CAND1, and Glomulin control the assembly and disassembly of CRL complexes on a global level, whereas heterologous CRL regulation can target a specific CRL complex such as $CRL4^{CDT2}$ disruption by $CRL1^{FBXO11}$ via CDT2 degradation [15, 16]. Interestingly, regulation of CRL5 subfamily by $CRL4^{AMBRA1}$ falls in the middle of CRL regulatory spectrum. Dynamic assembly of needed CRL complexes ensures timely substrate degradation in response to environmental cues. CAND1 as an exchange factor promotes the dissociation between cullins and SR-adapter dimers once the cullins are deneddylated by CSN, followed by the assembly of adapter-free cullins and new SR-adapter dimers, thus shaping the repertoire of CRL complexes [72, 73]. In contrast to CAND1,

$CRL4^{AMBRA1}$ is an ubiquitin E3 ligase and requires the ligase activity to promote disassembly of target CRLs. In theory, $CRL4^{AMBRA1}$ can act on both cullin-bound and cullin-free ELOC. We showed that $CRL4^{AMBRA1}$ attenuates CRL5 activity by targeting the cullin-bound ELOC. It remains unclear whether $CRL4^{AMBRA1}$ also operates on a pool of cullin-free SR-adapter dimers. Of note, SRs and the associated adapters form strong subcomplexes before encountering the cullins [74-76]. It is tempting to suggest that $CRL4^{AMBRA1}$ may remodel SR-adapter dimers via ELOC degradation and thus affect the landscape of CRL5 complexes.

AMBRA1 was previously shown to inhibit CRL5-mediated DEPTOR degradation by sequestering ELOB. However, how $CRL4^{AMBRA1}$ regulates CRL5 was not studied beyond the change in AMBRA1 levels via CRL4-mediated autocatalysis. Antonioli et al. showed that the AMBRA1-ELOB interaction was transiently up-regulated shortly after serum starvation, and it concomitantly interfered with CRL5 function to stabilize DEPTOR [36]. In contrast to the sequestration model, we found that $CRL4^{AMBRA1}$ mediates ELOC polyubiquitination and degradation, which is required for AMBRA1's effect on CRL5 disassembly. In addition, we showed that ELOBC were co-purified with AMBRA1, DDB1, and VIF **(Figure 2.5)**, arguing against AMBRA1-DDB1 and AMBRA1-ELOBC being mutually exclusive complexes as previously suggested [36]. It remains unknown how $CRL4^{AMBRA1}$ coordinates with other ubiquitin E3 ligases to regulate the autophagy response and their sequence of action [29, 36, 77]. Despite the established connection between AMBRA1 and autophagy, our study focuses on the role of $CRL4^{AMBRA1}$ in regulating human SOCS proteins and HIV-1 VIF.

We showed that $CRL4^{AMBRA1}$ modulates the amplitude and duration of IL-6 induced STAT3 activation by regulating $CRL5^{SOCS3}$. Similarly, $CRL4^{AMBRA1}$ regulates $CRL5^{VIF}$-mediated A3G degradation. Blocking inhibitory events may help to fine-tune substrate stability and to precisely control signaling kinetics and intensity that control time-sensitive cellular processes. Our prior knowledge of such regulation is limited to cell cycle progression [15, 16]. Here, we reason that a similar mechanism for CRL5 regulation by $CRL4^{AMBRA1}$ is important for cytokine signaling and viral infection with respect to modulating the output of STAT3 phosphorylation and the level of the antiviral DNA-editing enzyme A3G. SOCS3 requires its E3 ligase function to fully suppress STAT3 signaling [61]. Although the identity of $CRL5^{SOCS3}$ substrates *in vivo* remains poorly defined (reviewed by [78, 79]), reconstituted $CRL5^{SOCS3}$ complex was found to ubiquitinate the IL-6/STAT3 signaling transducers JAK2 and gp130 *in vitro* [80]. IL-6/STAT3 signaling strongly interacts with pro-inflammatory pathways to govern diverse immune responses, and SOCS3 controls timely termination of STAT3 activation. Prolonged activation of STAT3 or SOCS3 dysfunction has been linked to aberrant T cell development, tumorigenesis and other malignancies (reviewed by [64, 81]). Further studies are needed to understand the functional effects of $CRL4^{AMBRA1}$ targeting ELOC to downregulate $CRL5^{SOCS3}$.

In summary, our study reveals a new paradigm of CRL regulation. $CRL4^{AMBRA1}$ is the first case reported to target a shared adapter of a CRL subfamily. We suggest that $CRL4^{AMBRA1}$ may play an important role in regulating a network of cytokine suppressors that require their CRL5 ligase function to counteract overshooting cytokine responses [61, 82]. It requires further work to understand whether and how $CRL4^{AMBRA1}$ controls $CRL5^{VIF}$ activity along with human CRL5 complexes to affect HIV-1 replication kinetics.

Chapter 6

Materials and Methods

Cell Culture and Generation of Stable Cell Lines with cDNA or shRNA Expression

293T and HEK293 were obtained from UCSF Cell Culture Facility. 293T was maintained in high glucose DMEM media supplemented with 10% fetal bovine serum (FBS)(Gibco), 1mM sodium pyruvate (Na-Py), and 1% penicillin/streptomycin (Pen/Strep). HEK293 was cultured in MEM with Earle's salts containing 10% FBS, 1mM Na-Py, 2mM L-Glutamine, and 1% Pen/Strep. Hep3B was obtained from Dr. Rik Derynck's laboratory (UCSF). Stable cell lines with cDNA or shRNA expression were generated by lentivirus transduction followed by antibiotics selection at an optimal concentration as determined by kill curve, or alternatively followed by FACS (fluorescence activated cell sorting) based on fluorescent protein expression with the lentiviral vectors used. Lentiviruses were prepared according to the manufacturers' protocols, and were concentrated with 8.5% of PEG-6000 and 0.3M of NaCl and resuspended in culture media or PBS. Lentiviral vector for cDNA expression used include: pCDH-EF1-MCS-IRES-GFP (SBI; for FLAG-ELOC, FLAG-SKP1), Tet-On 3G inducible expression system (Clontech; for SOCS3-GFP, VIF-GFP, VHL-GFP, PPIL5-GFP; for AMBRA1-FLAG and AMBRA1 ΔH-FLAG in rescue experiments), pCDH-EF1-MCS-T2A-HygroR (SBI; for mCherry-FLAG and AMBRA1-FLAG overexpression in IL-6 experiments); Lentiviral vectors for shRNA expression were in pLKO.1 (Sigma-Aldrich).

Recombinant DNA Constructs and Sequences of shRNA/siRNA

DNA expression constructs were prepared by standard molecular cloning and were sequence verified. Mutants of VIF/SOCS expression constructs and shRNA-resistant AMBRA1 constructs were generated by site-directed mutagenesis in PCDNA4/TO vector using Pfu Turbo DNA polymerase (Agilent) and were subcloned to lentiviral vectors when necessary. All HIV-1 recombinant DNA (rDNA) constructs used in this study were described previously [31]. The sequence information of human rDNAs include the following: AMBRA1 (NM_017749.3), DCAF1 (NM_014703.2), ELOC (NM_005648.3), ELOB (NM_007108.3), SKP1 (NM_170679.2), SOCS3 (NM_003955.4), SOCS2 (NM_003877.4), VHL (NM_000551.3), PPIL5/LRR1 (NM_152329.3), and CBFβ (NM_001755.2). The siRNA and shRNA (Sigma-Aldrich) sequences used include the following: Control sh-NT (SHC002), sh-AMBRA1 #1 (TRCN0000417120; target GGCTTGGCCTATGGTACTAAC), sh-AMBRA1 #2 (TRCN0000441636; target GGCCACTGGGAAAGAATTTAC), sh-AMBRA1 #3 (TRCN0000167886; target CCCACTTTCTCCTAGTAACAT), si-AMBRA1 (pre-designed Stealth#3156, Thermo, UUUGUUAGUACCAUAGGCCAAGCCA), si-ELOB (GCUGUACAAGGAUGACCAAtt), si-ELOC (CGAACUUCUUAGAUUGUUAtt), si-CUL5 (AGCUGAUUCAGUUAAUAUAtt), si-SOCS3 (pre-designed SASI_Hs01_00179195, Sigma-Aldrich), si-Control (Stealth siRNA negative control medium GC, Cat#12935300, Thermo).

Transfection of DNA Plasmids and siRNAs

DNA plasmids used in mammalian cell transfection were prepared with NucleoBond Xtra Midi EF (Macherey-Nagel) and quantified with NanoDrop One UV-Vis spectrophotometer

(Thermo Scientific). Plasmids were transfected in 293T using Polyjet (SignaGen), and cells were harvested 24~48 hour post-transfection. Dried siRNAs were resuspended in 1X siRNA buffer (Dharmacon), aliquoted and stored at -80ºC. For 293T and HEK293, cells were seeded at 4~5×10^5 per well in 6-well format (Corning Costar), and transfected with 10 nM siRNA ~6 hour post-seeding using RNAiMAX (Thermo Scientific); cells were split to 12-well plates 3~4 day post-transfection for downstream experiments. For Hep3B, cells were seeded at 3×10^5 per 6mm dishes and transfected with 5-10nM siRNA using DharmaFECT 4 (Dharmacon) shortly after seeding; culture media were replaced with fresh media ~4 hour post-transfection. Hep3B may be treated with siRNA again after 3 days and split on the 5th day for downstream experiments.

Generation of AMBRA1-Knockout and ATG-Knockout Cell Lines

293T cells with AMBRA1 knockout were generated by transient transfection of all-in-one SpCas9-P2A-GFP (Addgene #48138) encoding U6 driven expression of AMBRA1 sgRNAs (#1 TGGTAGAAGATAAAACCCGG; #2 AGAATGCTGTCCGGATACTC); cells were sorted 48~72 hour post-transfection based on GFP expression. 293T cells with ATG7 and ATG12 knockout were generated by transient transfection of SpCas9-P2A-puro (Addgene #48139) encoding U6 driven expression of sgRNA targeting ATG7 (ATAGCTGGGCAGCAACGGGC) and ATG12 (GAAACTGCAGCGGAAGACGG); cells were selected 48~72 hour post-transfection using 1 μg/ml puromycin (Sigma-Aldrich) for 48 hours. For DNA analysis, genomic DNA samples were prepared using QuickExtract (Epicentre) supplemented with RNase and Proteinase K. Polyclonal knockout populations were collected for Surveyor (IDT), TIDE [83], and immunoblotting. Single-sorted knockout cells were expanded/banked and confirmed by

genotyping as well as immunoblotting. The following primers were used to PCR amplify the edited regions, followed by standard molecular cloning procedure and Sanger sequencing to confirm indel: AMBRA1 — forward primer tagaactagtggatccCTTCTCGTTGCAGAAGTCGT and reverse primer gcttgatatcgaattcCAGATATGTCAACTCTCCCACACA; ATG7 — forward primer caccg TGGGGGACAGTAGAACAGCA and reverse primer aaac CCTGGATGTCCTCTCCCTGA; ATG12 — forward primer caccgAGCCGGGAACACCAAGTTT and reverse primer aaacGTGGCAGCCAAGTATCAGGC.

Cell Lysis, Western Blotting, and Antibodies

For IP-WB, CHX and other standard assays, cells were lysed in 1X RIPA buffer containing 50 mM Tris-HCl, pH 7.5, 150 mM NaCl, 1 % NP-40, 0.5 % sodium deoxycholate, 0.1 % SDS, 1X protease inhibitor cocktail (Roche), and 1X phosphatase inhibitor cocktail (Roche). Lysates were quantified with BCA assay (Bio-Rad); samples were prepared in 1X LDS sample buffer supplemented with 1X TCEP solution (Thermo), boiled for 5 minutes, and separated by SDS-PAGE (NuPAGE gels with MES/SDS buffer, Thermo; Criterion Tris-HCl gels with Tris/Glycine/SDS buffer, Bio-Rad). Gels were stacked with 0.22 μm activated PVDF membrane and filter papers following standard wet blotting procedure using Mini Trans-Blot Cell or Criterion Blotter (Bio-Rad). Endogenous proteins and epitope tags were detected by Western blotting using the following antibodies: rabbit polyclonal anti-AMBRA1 (ABC131, EMD-Millipore and A302, Bethyl), mouse monoclonal anti-ELOC (#610761, BD Biosciences), rabbit monoclonal anti-ELOB (ab154854, Abcam), rabbit monoclonal anti-CUL4A (ab92554, Abcam),

mouse monoclonal anti-DDB1 (#39-9901, Thermo Fisher), mouse monoclonal anti-STAT3 (#9139, Cell Signaling Technology/CST), rabbit monoclonal anti-Phospho-STAT3 (Tyr705) (#9145, CST), rabbit polyclonal anti-SOCS3 (#2932, CST), anti-GAPDH (rabbit polyclonal #2118, CST and mouse monoclonal MA5-15738, Thermo Fisher), anti-GFP (rabbit polyclonal ab6556, Abcam and mouse monoclonal sc9996, Santa Cruz), mouse monoclonal anti-HA (#2367, CST), rabbit polyclonal anti-Myc (ab9106, Abcam), anti-p62/SQSTM (guinea pig polyclonal GP62-C, Progen and mouse monoclonal #2C11, Novus). Additional antibodies used in the supplementary data include the following: LC3 (ABC232, EMD-Millipore), ATG7 (sc8668, Santa Cruz), ATG12 (CST). Chemicals used for autophagy flux assays include: DMSO (Sigma-Aldrich), HBSS (UCSF Cell Culture Facility), Bafilomycin A1 (Calbiochem). Other chemicals used include: doxycycline, puromycin, and cycloheximide (Sigma-Aldrich), Zeocin (Thermo Fisher)

IL-6 Stimulation and Cell Lysate Preparation

For IL-6 stimulation assays, Hep3B was serum-starved for 12 hours, and treated with 20 ng/mL IL-6 (EMD-Millipore; freshly diluted in serum-free media) for the indicated times. Cells were washed once with DPBS, snap frozen on dry ice, and lysed in modified RIPA buffer containing 50mM HEPES, pH 7.4, 150mM NaCl, 10% glycerol, 1% TritonX-100, 1% sodium deoxycholate, 0.1 % SDS, 1.5 mM $MgCl_2$, 1 mM EGTA, 100 mM NaF, 1 mM PMSF, 10 µg/mL leupeptin, 1 mM Na_3VO_4, and 10 mM $Na_4P_2O_7$. Lysates were quantified and analyzed by immunoblotting as described.

Affinity Purification, Mass Spectrometry, and Data analysis

Affinity purification was performed as previously described with some modifications [31]. Purified samples were further processed and analyzed by Orbitrap-based mass spectrometry (Thermo Scientific) and/or western blotting. For label-free quantification in mass spectrometry, raw data for peptide identification and intensity was analyzed by MaxQuant [84]. The resulting files containing peptide information were further scored by CompPASS for Vif-AMBRA1 interaction network, and by SAINT in combination with MSstats for ΔH43/WT and ΔH22/WT AMBRA1 comparative proteomics, respectively [85-87]. Data visualization was implemented in Cytoscape and R [88, 89].

Tandem Affinity Purification

293T co-expressing Strep-tagged and FLAG-tagged bait proteins were purified in two steps. Cells were lysed in 50 mM Tris-HCl pH 7.5, 150 mM NaCl, and 1 mM EDTA (IP buffer without the detergents) containing 0.5 % NP-40 and 0.25 % CHAPS (same buffer was used in single purification) on a tube rotator at 4°C for 30 minutes. The cleared lysates were collected after centrifugation and were purified with Strep-Tactin beads for at least two hours at 4°C. The beads were washed three times with the IP buffer containing 0.05 % NP-40 (wash buffer), and eluted with 1X D-Desthiobiotin buffer (IBA). The eluates were immunoprecipitated with anti-FLAG M2 beads (Sigma-Aldrich) for at least two hours at 4°C. The beads were then washed three times with wash buffer and followed by an additional wash with IP buffer to remove detergents. The

immunoprecipitates were eluted in IP buffer containing 100 μg/mL of 3X FLAG peptides (MS-grade, Elimbio) and 0.05 % RapiGest SF surfactant (Waters).

Cell-Based Ubiquitination Assay

293T cells were pelleted and heat-denatured in 50mM Tris-HCl pH 7.5, 1% SDS, and 5mM DTT containing 5 μg/mL DUB inhibitor PR-619 (Lifesensors). The cell lysates were diluted 10-fold to reduce the concentration of SDS, pre-cleared using sepharose beads, and the supernatants were collected for immunoprecipitation. After overnight incubation with anti-FLAG M2 (Sigma-Aldrich) or Strep-Tactin beads (IBA), the beads were washed three times with high-salt buffer containing 50 mM Tris-HCl pH 7.5, 500 mM NaCl, 1 mM EDTA, 0.5 % NP-40, 10 % glycerol, 1 mM 2-Mercaptolethanol, and a cocktail of protease inhibitors (Roche). The affinity-tagged proteins were eluted with 250 μg/mL of 3X FLAG peptides (Sigma-Aldrich) or 1X D-Desthiobiotin buffer (IBA).

Quantification of WB-Band Intensity and Statistical Analysis

Densitometric quantification of band intensity on immunoblots was carried out by Image Studio Lite software (LI-COR). Mann-Whitney-Wilcoxon Test was implemented in R using plyr package with the wilcox.test() function. Volcano plots for visualizing comparative proteomics were generated by R, plotting statistical significance ($-\text{Log}_{10}$ transformed) versus fold change (Log_2 transformed).

Chapter 7

Future Directions

7.1 The Implication of AMBRA1 in HIV-1 Infection

$CRL4^{AMBRA1}$ is a negative regulator of CRL5 complexes including $CRL5^{VIF}$. Thus, we hypothesized that the enhanced VIF-dependent A3G degradation by AMBRA1 knockdown would promote HIV-1 infectivity and/or enhance its replication kinetics. However, we found that AMBRA1 is required independent of its ubiquitin E3 ligase function during the early stage of HIV-1 life cycle, which complicates the interpretation of HIV-1 spreading infection, a standard assay for VIF functions. Furthermore, HIV-1 infection induces the autocatalytic degradation of AMBRA1 via CRL4. These findings are consistent with $CRL4^{AMBRA1}$ serving to negatively regulate $CRL5^{VIF}$ activity and is somehow antagonized by the virus. Nevertheless, it requires further investigation to clarify how AMBRA1 affects the early stage of HIV-1 infection and mechanistically how $CRL4^{AMBRA1}$ function is perturbed by HIV-1.

Introduction of HIV-1 Infection and Reporter Assays

HIV-1 life cycle includes entry, reverse transcription, integration, production of viral proteins, assembly, and release of viral particles. HIV-1 employs multiple alternative splicing mechanisms to generate viral mRNAs. During the early phase of HIV-1 infection, viral gene expression is limited to small and multiply spliced mRNAs that do not require nuclear export

machineries, including *rev, tat, and nef*. During the late stage of HIV-1 infection, one of the early proteins, REV, binds unspliced *gag* and *pol* transcripts and incompletely spliced *env, vif, vpr and vpu* transcripts at their intronic rev response elements (RRE), facilitating export to the cytoplasm via the CRM1 nuclear export pathway. Two types of reporter viruses are commonly used to analyze the early and the late stages of HIV-1 infection — *nef*:GFP and GAG-GFP viruses, respectively. The early-gene reporter *nef*:GFP contains the fluorescent marker in replacement for *nef*, which enhances viral infectivity *in vivo* but is dispensable *in vitro*. The late-gene reporter has the fluorescent maker inserted near the C-terminus of p17 (matrix protein, p17) and before p24 (capsid protein, p24) within the *gag* reading frame, and displays wild-type (WT) morphology and infectivity; the insertion of GFP does not interfere with processing of the GAG precursor into p17 and p24 [90]. Dual reporter virus with two spectrally nonoverlapping fluorescent makers can also be used to analyze single-cycle HIV-1 replication kinetics [91].

To assess the dynamic ranges of fluorescent reporter viruses and p24 immunostaining, we infected SupT11-A3G cells with Vsvg-pseudotyped *nef*:GFP or GAG-GFP virus, and stained with PE-conjugated p24 antibody. In both cases, the fluorescent signals plateaued at high concentrations of viruses, whereas immunostained signals displayed relatively higher dynamic ranges **(Figure 7.1.1)**. Thus, it is important to keep in mind that infection with these HIV-1 fluorescent reporter viruses particularly at a high multiplicity of infection (MOI) may lead to underestimation of infectivity.

To confirm whether the observed immunostained signals reflect HIV-1 infectivity, we treated Vsvg-HIV-1-infected SupT11-A3G with various concentrations of Zidovudine (AZT), a reverse

transcriptase inhibitor. We found that cells infected with a low MOI (~30% infected cells) were sensitive to AZT treatment, which reduced infectivity by more than 70% at 1 μM **(Figure 7.1.2A)**. Cell infected with a high MOI (~100% infected cells) were relatively tolerant to AZT, which only reduced infectivity by 30% at 1 μM **(Figure 7.1.2B)**.

VIF is nearly absent in viral particles [92] and it predominantly functions in virus-producing cells during virus assembly to block the incorporation of the antiviral APOBEC3 (A3) proteins. When A3-expressing cells (also called non-permissive cells) are infected with VIF-deficient HIV-1, newly assembled virions can encapsidate A3 proteins that thwart the next round of infection. In single-cycle infection assays with Vsvg-pseudotyped HIV-1, non-permissive cells infected with the WT and VIF-deleted viruses at the same expected MOIs showed comparable intracellular p24 staining **(Figure 7.1.3)**. This finding confirms that VIF has negligible effects on the single-cycle infection, in which next round of infection cannot be initiated without a virally encoded envelop protein.

AMBRA1 Has an Ambiguous Phenotype in HIV-1 Spreading Infection

To investigate whether AMBRA1 affects HIV-1 replication kinetics by modulating $CRL5^{VIF}$ activity, we infected control and AMBRA1-depleted SupT11-A3G cells with WT or VIF-deficient NL4-3 HIV-1 at a MOI that results in ~1% infection in CEM-GFP cells **(Figure 7.1.4)**. AMBRA1 knockdown resulted in ELOC accumulation in SupT11-A3G cells and another human T cell line H9 **(Figure 7.1.5)**, confirming that $CRL4^{AMBRA1}$ targets ELOC for degradation in these cells as we reported in 293T cells. We found that the peak infectivity in control SupT11-

A3G cells infected with WT HIV-1 occurred on day 9 after exposure to the virus, whereas infection of the AMBRA1-depleted cells peaked on day 7 and its infectivity dramatically decreased on day 9 **(Figure 7.1.6A)**. Immunoblotting analysis of the infected cells on day 7 showed that the infected AMBRA1-depleted cells had a lower amount of loaded protein based on HSP90, suggesting of massive cell death due to peak HIV-1 infection **(Figure 7.1.6B)**. These findings suggest two possibilities — (1) there might be a competing mechanism that complicates the observed infectivity; (2) the effect of $CRL5^{VIF}$ regulation by $CRL4^{AMBRA1}$ may be too subtle to be captured by spreading infection. Spreading infection is an intrinsically noisy assay because of the asynchronous nature of HIV-1 infection [93]. The reduced infectivity under AMBRA1 knockdown background thus requires confirmation with single-cycle infection assays.

AMBRA1 is Required During the Early Stage of HIV-1 Infection

We generated AMBRA1-depleted background in SupT11-A3G and HeLa cells for subsequent single-cycle infection assays either with stable shRNA expression or using the CRISPR/Cas9 system. Similar to described in Figure 4.5, SupT11-A3G cells transiently expressed Cas9 and AMBRA1 guide RNA sg1 were clonally selected; the *ambra1* genomic editing and protein depletion were confirmed by immunoblotting and sequencing **(Figure 7.1.7A)**. In both the AMBRA1 KO#20 and KO#21, an indel was generated after the start codon. However, lower molecular-weight AMBRA1 isoforms were still present, which were potentially translated from the downstream alternative start codon Met40. It requires further experiments to confirm this.

Single-cycle infection assays in parental SupT11-A3G, AMBRA1 KO#20, and KO#21 cells revealed that AMBRA1 is required for HIV-1 infection and it affects both early and late HIV-1 reporters **(Figure 7.1.7B)**. This result indicates that knocking down AMBRA1 undermines the viral early-gene replication through a yet unclear mechanism, which also causes collateral damage in the subsequent events of the viral life cycle. To confirm the infectivity defect under AMBRA1 knockdown background, we performed the same assay in SupT11-A3G cells with stable shRNA expression using both the reporter viruses (not shown) and the plain virus **(Figure 7.1.7C)**. AMBRA1-depleted SupT11-A3G showed dramatic reductions in infectivity at both low and high MOIs as detected by p24 immunostaining **(Figure 7.1.7C)**.

Next, to understand whether AMBRA1's ubiquitin E3 function plays a role in the single-cycle infection, we examined if DDB1 knockdown phenocopies the reduced infectivity and if such reduction can be rescued by re-expression of the ΔH mutant. Here, we used HeLa cells for easy transfection and rescue experiments. We found that DDB1 depletion had no effect on single-cycle infection with the GAG-GFP reporter virus, whereas AMBRA1 knockdown consistently reduced infectivity **(Figure 7.1.8A-B)**. In addition, re-expression of WT AMBRA1 and the ΔH mutant recovered similar degrees of infectivity, indicating that AMBRA1's ubiquitin E3 ligase activity does not account for the infectivity defect followed by AMBRA1 depletion **(Figure 7.1.8C)**. Importantly, we showed that the reduced infectivity caused by AMBRA1 knockdown compromised VIF protein level. These findings indicate that the early viral replication defect hinders the interpretation of VIF phenotype in spreading infection assays, which occurs at the late stage of HIV-1 life cycle and the subsequent rounds of infection **(Figure 7.1.9)**. In spite of decreased infectivity, AMBRA1 knockdown facilitated A3G degradation in

SupT11-A3G when infected with Vsvg-pseudotyped HIV-1 **(Figure 7.1.10)**. Of note, AMBRA1 knockdown does not significantly affect cell proliferation within 48 hours, the time frame of HIV-1 single-cycle infection assays, excluding the possibility that changes of cell growth may slow infectivity **(Figure 7.1.11)**.

AMBRA1 is Degraded via $CRL4^{AMBRA1}$ Autocatalysis During HIV-1 Infection

Because of the seemingly conflicting roles of AMBRA1 being required during the early stage of HIV-1 infection and acting as a negative regulator of $CRL5^{VIF}$ later, we sought to understand if AMBRA1 and/or its ubiquitin E3 ligase function are perturbed during the course of infection. Immunoblotting of SupT11-A3G cells at different time points after HIV-1 exposure showed that AMBRA1 protein level gradually decreased during viral infection **(Figure 7.1.12)**. Increasing amounts of WT and VIF-deficient HIV-1 similarly resulted in AMBRA1 downregulation, indicating that VIF was not responsible for AMBRA1 reduction **(Figure 7.1.13)**. Notably, the ΔH mutant-expressing SupT11-A3G cells were resistant to the virus-induced AMBRA1 downregulation when compared to the WT AMBRA1-expressing cells, suggesting that AMBRA1 downregulation was a result of enhanced $CRL4^{AMBRA1}$ autocatalysis **(Figure 7.1.14)**. It requires further work to understand why overexpressing the ΔH mutant stabilized A3G in the context of infection, whereas the overexpressed WT AMBRA1 and A3G were degraded at nearly the same time frame. Taken together, AMBRA1 is required during the early stage of HIV-1 infection, and its protein level is downregulated during the course of viral infection as a result of enhanced autocatalysis. These findings explained the reduced infectivity and little kinetic difference in the spread-infected AMBRA1-knockdown cells. As AMBRA1 is degraded during

HIV-1 infection, it provides very little window to discern any kinetic differences in viral replication.

Discussion and Conclusions — AMBRA1 and HIV-1 Infection

We found that early HIV-1 replication is compromised in the infected AMBRA1-depleted cells, and showed that such replication defect is not due to AMBRA1's ubiquitin E3 ligase function. It has been previously reported that autophagy deficiency compromised HIV-1 early replication [94]. Thus, it is tempting to suggest that AMBRA1's role in autophagy regulation may account for its requirement during the early stage of HIV-1 life cycle.

Our finding of AMBRA1 downregulation during HIV-1 infection presents an interesting yet complex question of how AMBRA1's ubiquitin E3 ligase activity is regulated. Antonioli et al. showed that prolonged starvation leads to AMBRA1 degradation as a result of enhanced $CRL4^{AMBRA1}$ activity [36]. It is possible that viral infection may induce a similar stress response that results in AMBRA1 degradation. Alternatively, HIV-1 protein(s) might account for AMBRA1 degradation through a more direct mechanism. The deletion of VIF does not interfere with the virus-induced AMBRA1 degradation, indicating that other viral factors may be responsible for this action.

These findings show the intricate connection between AMBRA1 and HIV-1 infection. Although initial spreading infection results showed no apparent difference between control and AMBRA1 knockdown cells, a series of single-cycle assays indicated that AMBRA1 may have

dual roles in HIV-1 infection. First, it is required for HIV-1 early-gene replication. Although it needs further experiments to clarify how AMBRA1 is mechanistically involved in this step, depletion of several autophagy genes shows similar HIV-1 replication defect, suggesting that AMBRA1's autophagy function may be responsible for the observation. Second, AMBRA1 is degraded via autocatalysis during HIV-1 infection. Although this seems to be consistent with AMBRA1's role as a *bona fide* negative regulator of $CRL5^{VIF}$ and is thereby antagonized by HIV-1, it requires further work to understand the mechanism. Due to AMBRA1's multiple roles in HIV-1 infection, we have not conclusively determined whether the enhanced $CRL5^{VIF}$ activity and A3G degradation followed by AMBRA1 depletion promotes viral replication and infectivity. Based on our current findings, I propose to take on the substrate ELOC instead of AMBRA1 itself in the future to address the role of $CRL4^{AMBRA1}$ in HIV-1 replication kinetics.

7.2 ELOC Ubiquitination Site

We sought to identify ELOC ubiquitination site(s), which would be valuable information in future functional experiments, as we hypothesized that replacing endogenous ELOC with an ubiquitination-resistant mutant may enhance CRL5 activity. The ubiquitin remnant profiling study from Kim et al. identified K32 and K43-containing ELOC peptides, and showed that proteasome inhibition promoted the accumulation of the K32 and not the K43 peptides, suggesting that the K32 ubiquitination may signal for ELOC proteasomal degradation [55]. Interestingly, although both ELOC K32 and K43 residues are conserved among different species, K32 is unique to ELOC and does not exist in its paralogue SKP1 **(Figure 3.4A)**. Therefore, we test whether the K32R mutation abolishes ELOC polyubiquitination. Ubiquitin chain extension

was examined as previously described with denaturing IP and immunoblotting. We found that the K32R mutant displayed very little polyubiquitination when compared to the WT ELOC in the presence of MG132 **(Figure 7.2.1A)**. In addition, the K32R mutant was nearly unresponsive to MG132-induced accumulation of the protein level and polyubiquitination, which has been reproducibly shown in the WT ELOC **(Figure 7.2.1B; Figure 3.2)**. These data showed that the K32 residue is the ELOC main ubiquitination site and signals for proteasomal degradation.

7.3 Supplementary Materials and Methods

HIV-1 Infection Assays

HIV-1 spreading infection was performed as previously described [95]. HIV-1 particles were harvested from 293T transfected with WT or VIF-deficient NL4-3 HIV-1 proviral plasmids. Their titers were determined by infecting CEM-GFP reporter cell line. The virus titers resulting in 1% of CEM-GFP infection after 48 hours were used to initiate spreading infection in SupT11-A3G cells. For infectivity measurements, an aliquot of supernatants from the infected cells was taken every two days (replenished with the equal volume of fresh media) and the titer was determined by infecting CEM-GFP cells. A separate set of infected cells was prepared for immunoblotting analysis. For HIV-1 single-cycle experiments, Vsvg-pseudotyped HIV-1 particles were prepared from 293T expressing Vsvg and Env-deleted NL4-3 HIV-1. SupT11-A3G or HeLa cells were incubated with the indicated amount of viral particles for one hour, and followed by virus removal and replacing with fresh media. The infected cells were fixed

(trypsinization was required for HeLa cells) and analyzed by flow cytometry after 48 hours. The remaining cells may be lysed and analyzed by immunoblotting.

Figure 7.1.1

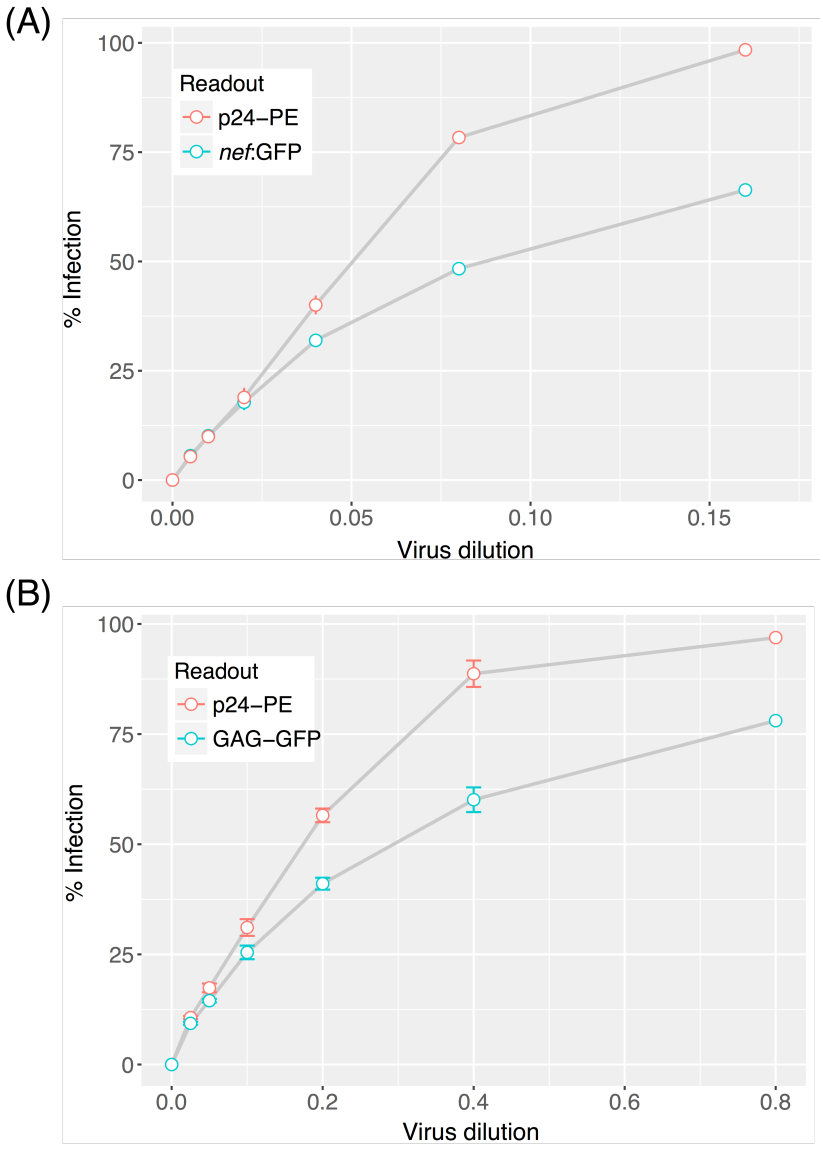

Figure 7.1.1 p24 Immunostaining Displays A Higher Dynamic Range Than the Fluorescent Reporters.

SupT11 cells with stable expression of HA-tagged A3G (SupT11-A3G) was infected with Vsvg-pseudotyped *nef*:GFP **(A)** or GAG-GFP **(B)** NL4-3 HIV-1 strain at the indicated dilutions. After incubating with the virus for an hour, the cells were span to remove the virus and resuspended in fresh culture media. The cells were then fixed, p24-immunostained, and analyzed by flow cytometry after 48 hours. Scattered plot represented mean + sem, n=2.

Figure 7.1.2

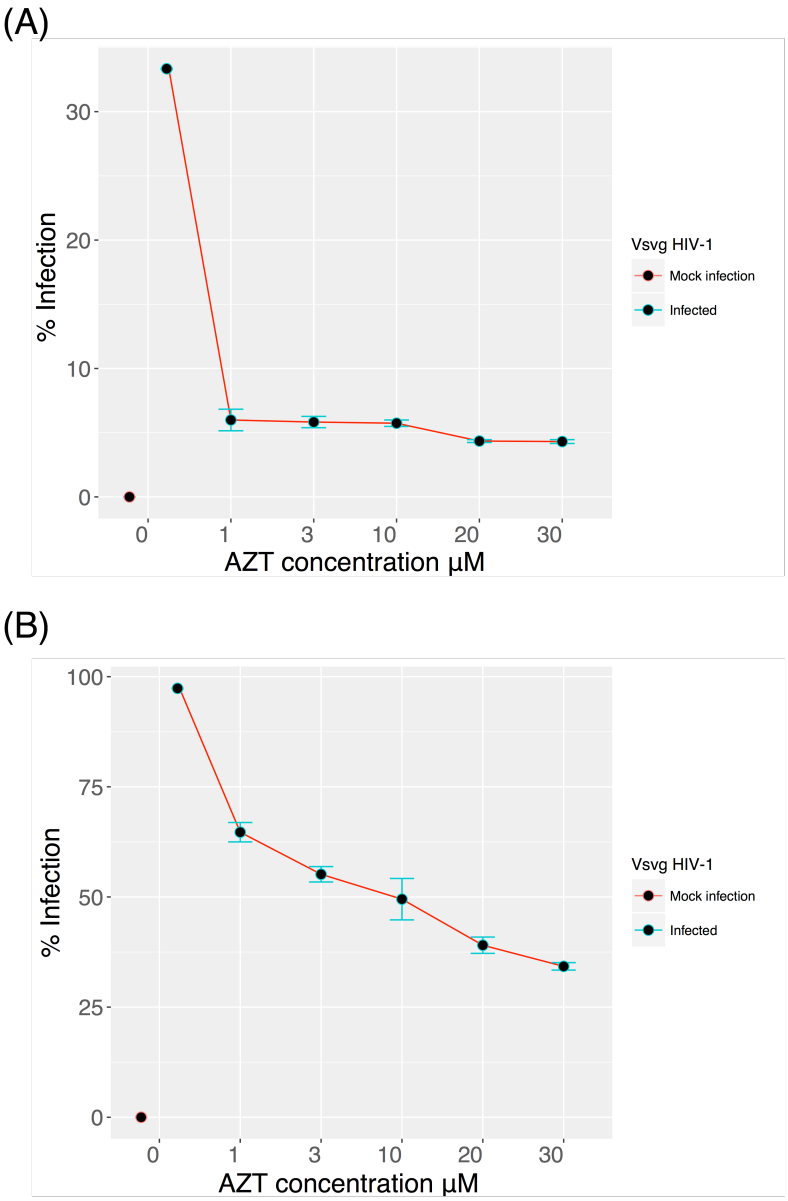

Figure 7.1.2 Sensitivity of HIV-1 Infected Cells to the RT Inhibitor Zidovudine (AZT).

SupT11-A3G cells were infected with Vsvg-pseudotyped NL4-3 HIV-1 at two different MOIs that resulted in 33% **(A)** and nearly 100% infection **(B)**. Similar to described in Figure 7.7.1, after incubation with the virus, the cells were resuspended in fresh culture media containing AZT at the indicated concentrations. The cells were then fixed, p24-immunostained and analyzed by flow cytometry 48 hours after virus exposure. Scattered plot represented mean + sem, n=2.

Figure 7.1.3

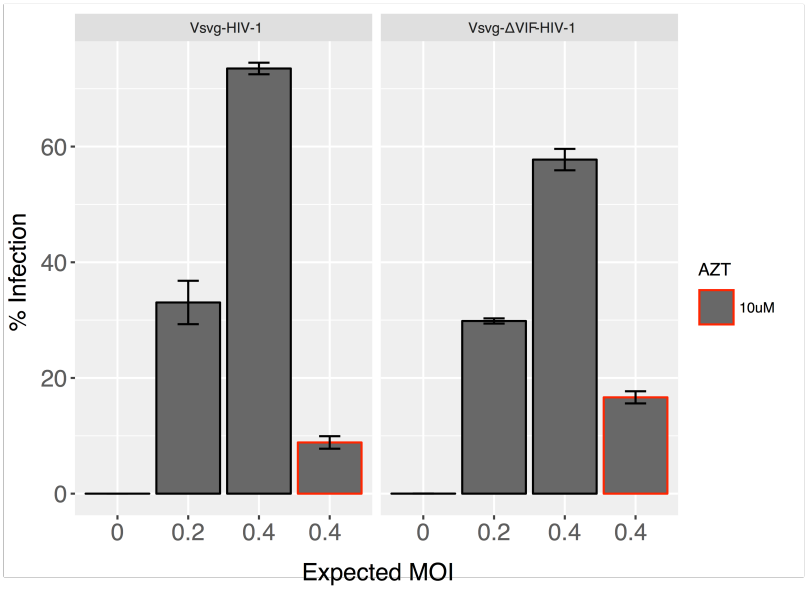

Figure 7.1.3 Vsvg-Pseudotyped WT and VIF-Deleted HIV-1 Result In Comparable Infectivity In Single-Cycle Infection Assays.

SupT11-A3G cells were infected with the previously tittered Vsvg-pseudotyped WT or VIF-deleted HIV-1 at the indicated MOIs (calculated based on the viral titers). The cells were then fixed, p24-immunostained, and analyzed by flow cytometry after 48 hours. Bar graph represented mean + sem, n=3.

Figure 7.1.4

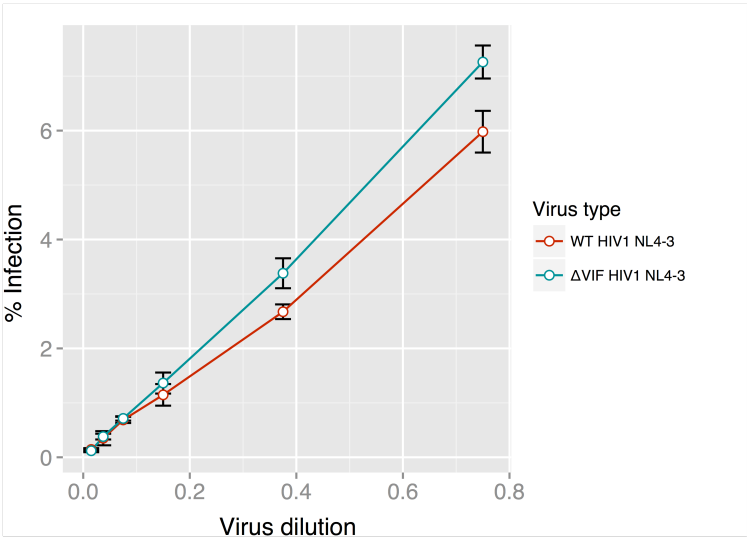

Figure 7.1.4 Virus titers of WT and VIF-Deficient HIV-1 in CEM-GFP Reporter T Cell Line.

Batch-prepared WT and VIF-deficient NL4-3 viruses were tittered in CEM-GFP reporter cell line which expresses GFP upon HIV-1 infection driven by the stably integrated NL4-3 LTR. Infected CEM-GFP cells were then fixed and analyzed by flow cytometry after 48 hours. Scattered plot represented mean + sem, n=3.

Figure 7.1.5

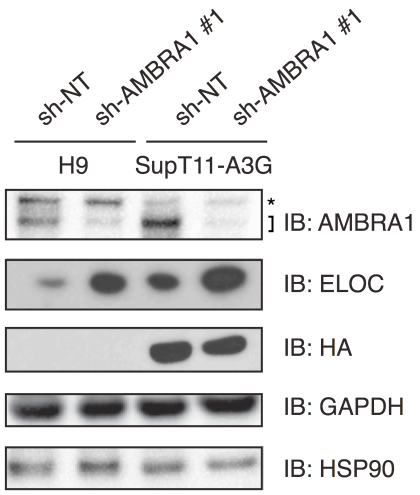

Figure 7.1.5 ELOC Accumulation in AMBRA1-Depleted T Cell Lines.

H9 and SupT11-A3G cells with stable shRNA expression were lysed and analyzed by immunoblotting to examine the steady state levels of ELOC and other proteins of interest. Both GAPDH and HSP90 served as loading controls.

Figure 7.1.6

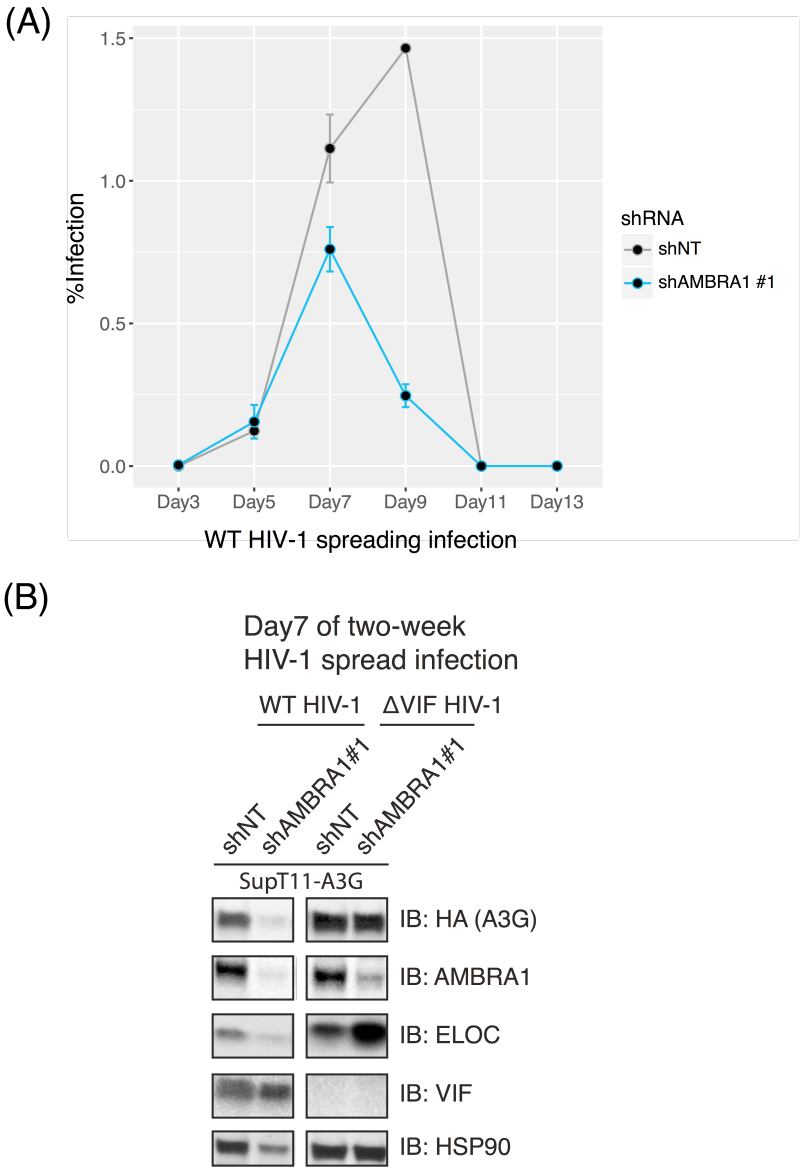

Figure 7.1.6 AMBRA1 Depletion Has a Subtle Phenotype in HIV-1 Spreading Infection.

SupT11-A3G cells with stable shRNA expression were infected with replication competent WT NL4-3 HIV-1. An aliquot of supernatant containing newly released virions from the infected SupT11-A3G cells was taken every two days and tittered in CEM-GFP reporter cell line. Infected CEM-GFP cells were then fixed and analyzed by flow cytometry after 48 hours. **(A)** The infectivity was plotted at different time points. The same experiment was performed with VIF-deficient NL4-3 HIV-1 in parallel and showed zero infectivity throughout the course of infection (not shown). Scattered plot represented mean + sem, n=3. **(B)** Aliquots of infected cells on day 7 were lysed and analyzed by immunoblotting.

Figure 7.1.7

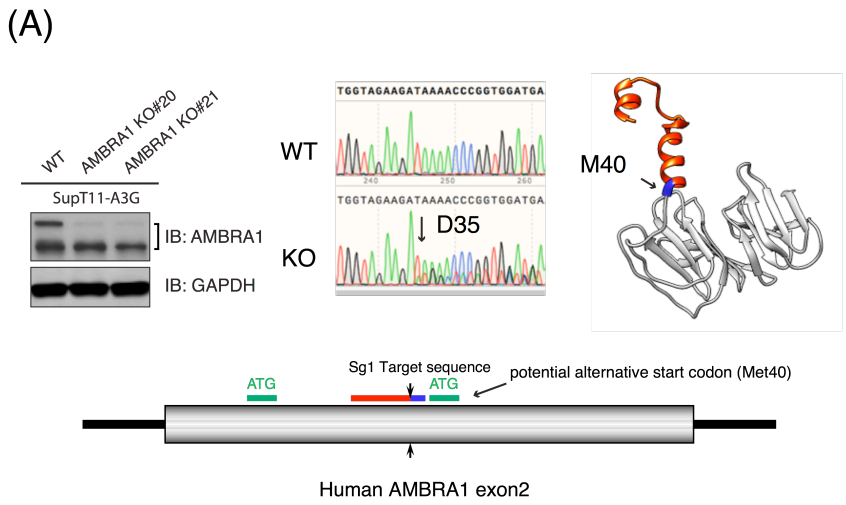
(A)
WT
AMBRA1 KO#20
AMBRA1 KO#21
SupT11-A3G
IB: AMBRA1
IB: GAPDH
WT
KO
TGGTAGAAGATAAAACCCGGTGGATGA
TGGTAGAAGATAAAACCCGGTGGATGA
D35
M40
ATG
Sg1 Target sequence
ATG
potential alternative start codon (Met40)
Human AMBRA1 exon2

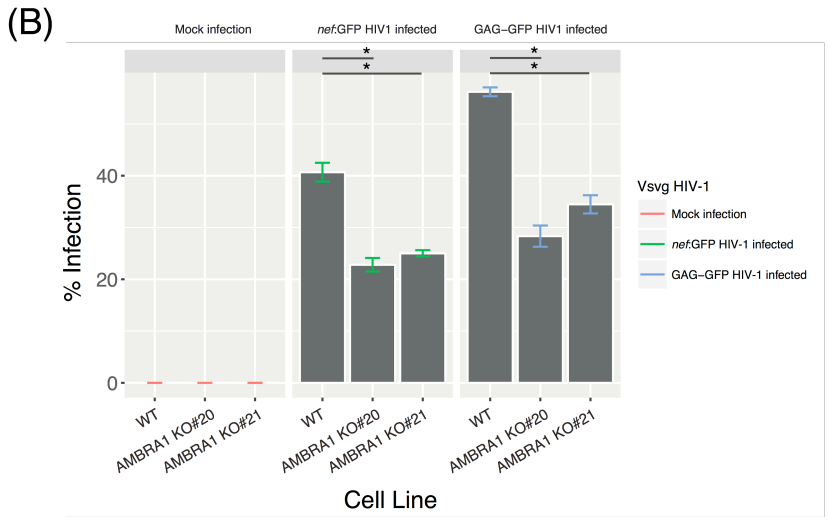
(B)
Mock infection
nef:GFP HIV1 infected
GAG–GFP HIV1 infected
% Infection
40
20
0
WT
AMBRA1 KO#20
AMBRA1 KO#21
Cell Line
Vsvg HIV-1
Mock infection
nef:GFP HIV-1 infected
GAG–GFP HIV-1 infected

(C)

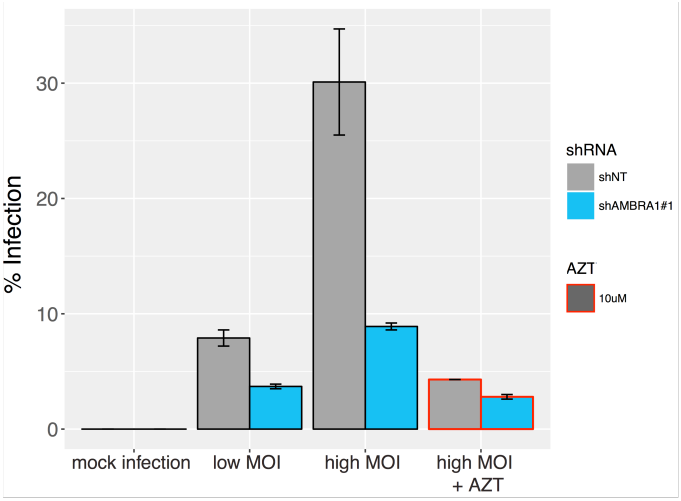

Figure 7.1.7 AMBRA1 Depletion in SupT11-A3G Cells Reduces Infectivity in Single-Cycle Assays with Both Early-Gene and Late-Gene Reporters.

(A) AMBRA1-knockout SupT11-A3G cells were clonally selected and examined by immunoblotting and sequencing. The identified indel site precedes AMBRA1 M40, a potential downstream start codon.

(B) SupT11-A3G parental and AMBRA1 KO cells were infected with Vsvg-pseudotyped *nef*:GFP or GAG-GFP reporter HIV-1 and analyzed by flow cytometry. Bar graph represented mean + sem, n=3, *p-value ≤ 0.05.

(C) SupT11-A3G with control and AMBRA1 shRNA expression were infected with plain Vsvg-pseudotyped HIV-1. The cells were then fixed, p24-immunostained, and analyzed by flow cytometry after 48 hours. Bar graph represented mean + sem, n=3.

Figure 7.1.8

(A)

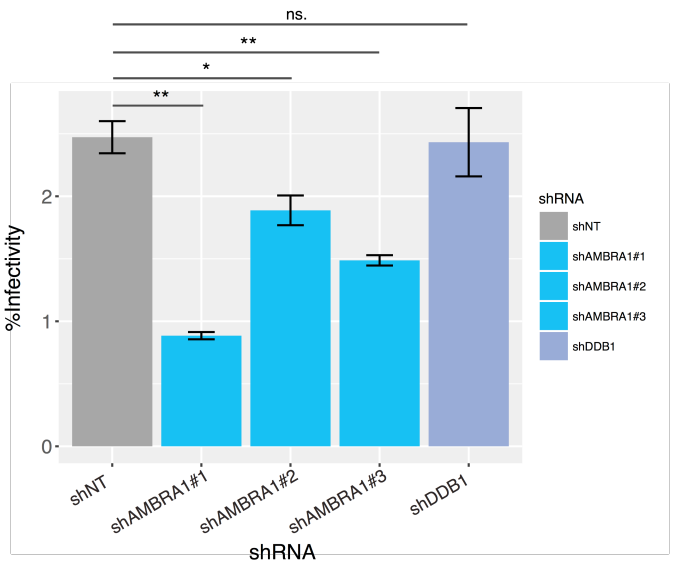

(B)

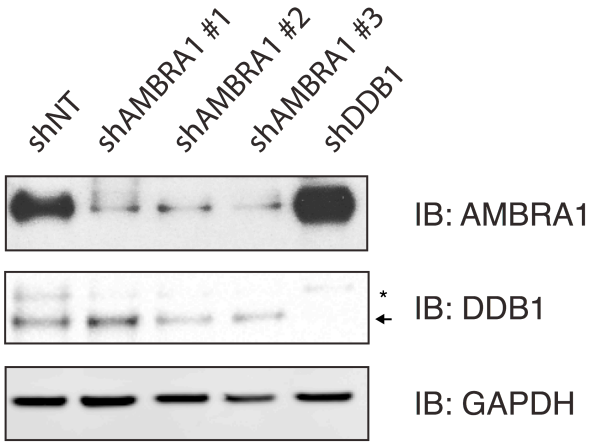

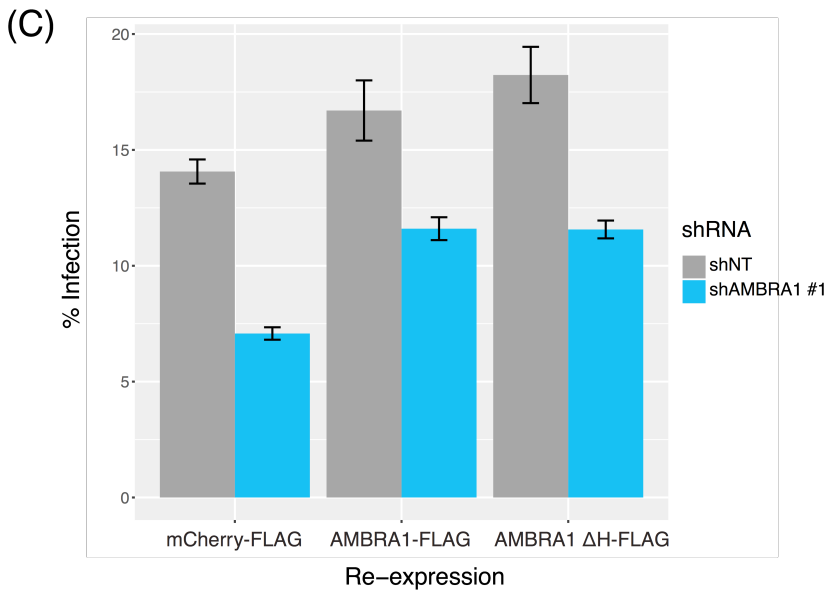

Figure 7.1.8 AMBRA1 Knockdown Reduces Infectivity in Single-Cycle Assays Independent of AMBRA1's Ubiquitin E3 Ligase Function.

(A) HeLa cells with stable shRNA expression were infected with Vsvg-pseudotyped GAG-GFP reporter HIV-1. The cells were then trypsinized, fixed, and analyzed by flow cytometry after 48 hours. Bar graph represented mean + sem, n=3.

(B) Aliquots of uninfected HeLa cells with stable shRNA expression were lysed and analyzed by immunoblotting.

(C) Similar to (A), shRNA-expressing HeLa cells were transfected with FLAG-tagged mCherry control, WT AMBRA1, or the ΔH mutant prior to infection. Bar graph represented mean + sem, n=3.

Figure 7.1.9

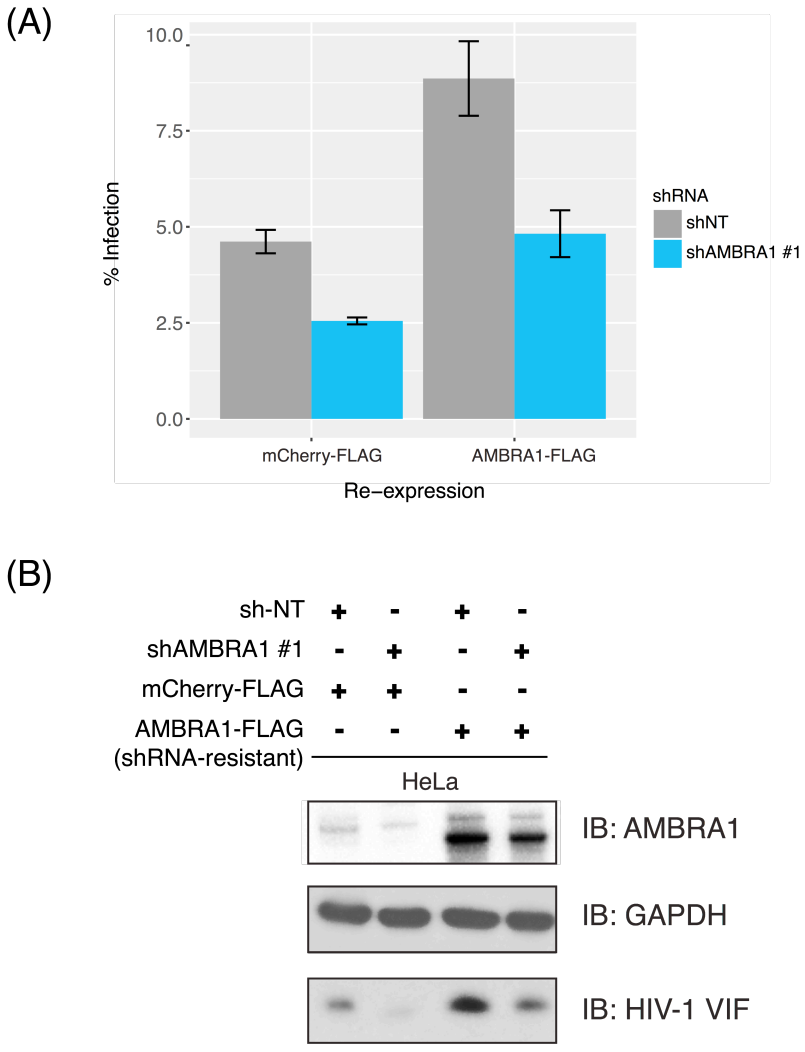

Figure 7.1.9 Reduction of Infectivity by AMBRA1 Knockdown in Single-Cycle Assays Compromises VIF Synthesis.

(A) Similar to described in **Figure 7.1.8C**, shRNA-expressing HeLa cells were transiently transfected with control or shRNA-resistant AMBRA1 plasmid, followed by infection with Vsvg-pseudotyped GAG-GFP reporter HIV-1. Bar graph represented mean + sem, n=3.

(B) Aliquots of the infected cells were lysed and analyzed by immunoblotting.

Figure 7.1.10

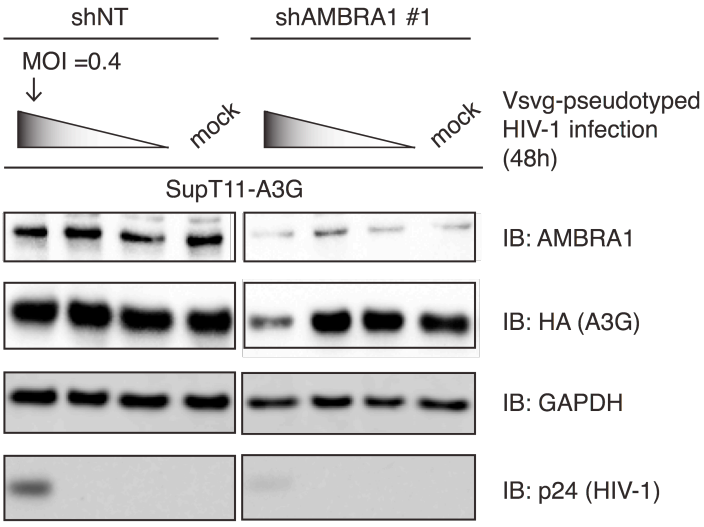

Figure 7.1.10 AMBRA1 Knockdown Facilitates VIF-mediated A3G Degradation in the Context of HIV-1 Infection in Spite of Reduced Infectivity.

SupT11-A3G cells with control or AMBRA1 shRNA expression were titrated with serial dilutions of Vsvg-pseudotyped HIV-1. The infected cells were lysed and analyzed by immunoblotting.

Figure 7.1.11

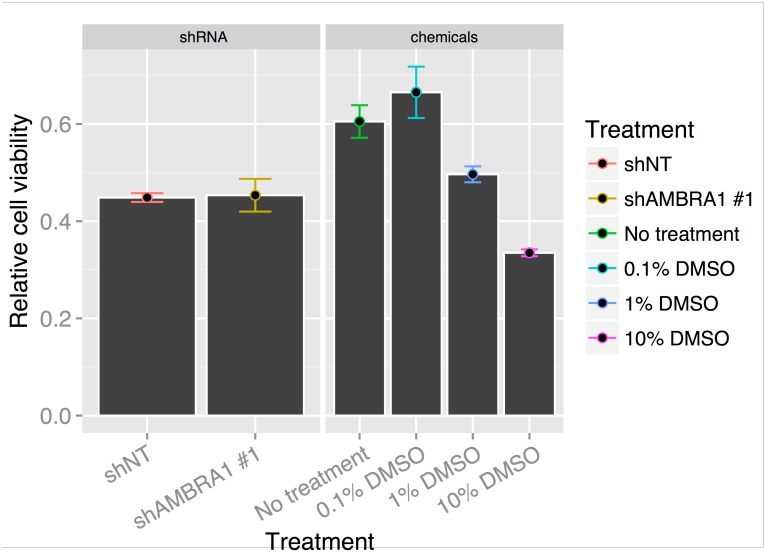

Figure 7.1.11 AMBRA1 Knockdown Does Not Significantly Affect Cell Proliferation Within 48 Hours.

The same number of HeLa cells with control or AMBRA1 shRNA expression was seeded in a 96-well plate. Forty-eight hours after seeding, the cells were treated with XTT reagent, which reacted with live cells and the absorbance was measured at 450 nm.

Figure 7.1.12

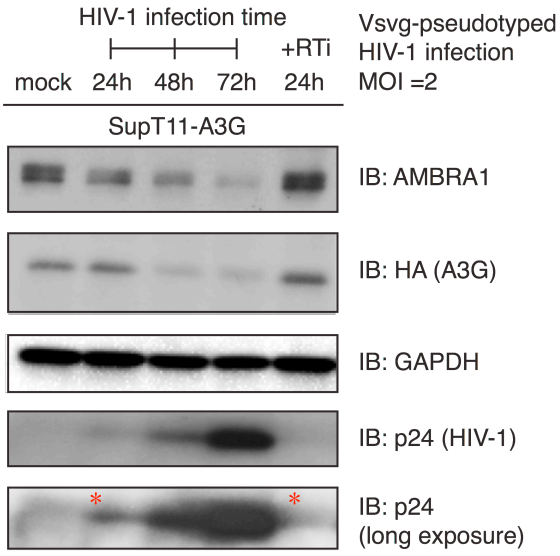

Figure 7.1.12 AMBRA1 Protein Level is Downregulated During HIV-1 Infection.

SupT11-A3G cells infected with the same amount of Vsvg-pseudotyped HIV-1 were lysed at different time points and analyzed by immunoblotting.

Figure 7.1.13

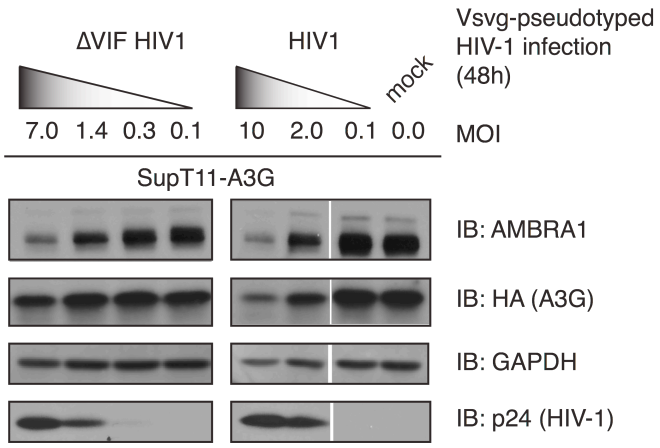

Figure 7.1.13 Downregulation of AMBRA1 by HIV-1 is Independent of VIF Expression.

SupT11-A3G cells were infected with increasing amounts of Vsvg-pseudotyped WT or VIF-deleted HIV-1. The cells were lysed 48-hour post-infection and analyzed by immunoblotting.

Figure 7.1.14

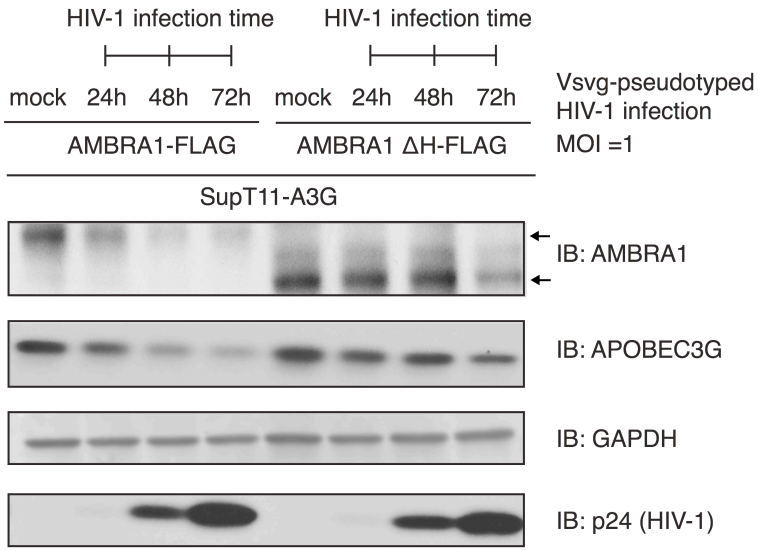

Figure 7.1.14 The ΔH AMBRA1 Mutant Is Resistant to Virus-Induced Downregulation.

Similar to described in **Figure 7.1.12**, SupT11-A3G cells with stable expression of WT AMBRA1 or the ΔH mutant were infected with the same amount of virus. The infected cells were lysed at different time points and analyzed by immunoblotting.

Figure 7.2.1

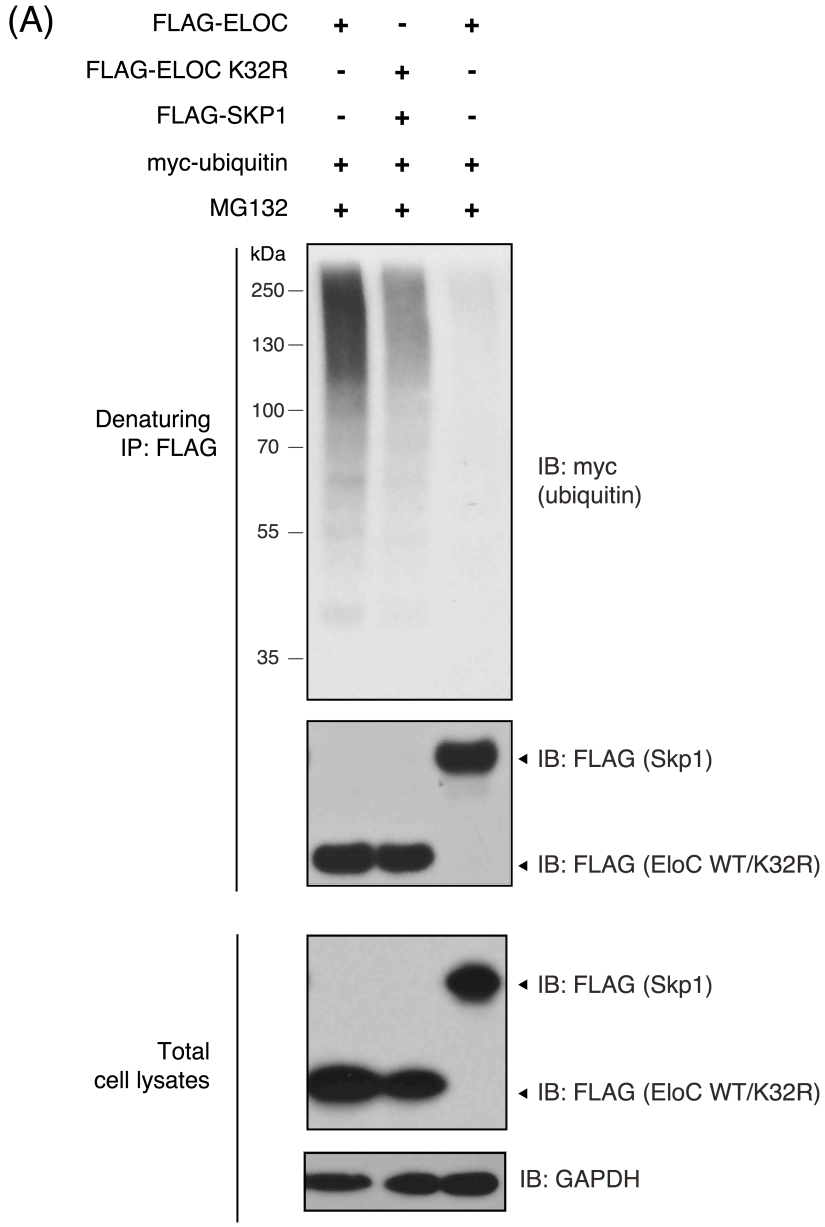
(A)
FLAG-ELOC + - +
FLAG-ELOC K32R - + -
FLAG-SKP1 - + -
myc-ubiquitin + + +
MG132 + + +
kDa
250
130
100
70
55
35
Denaturing
IP: FLAG
IB: myc
(ubiquitin)
IB: FLAG (Skp1)
IB: FLAG (EloC WT/K32R)
Total
cell lysates
IB: FLAG (Skp1)
IB: FLAG (EloC WT/K32R)
IB: GAPDH

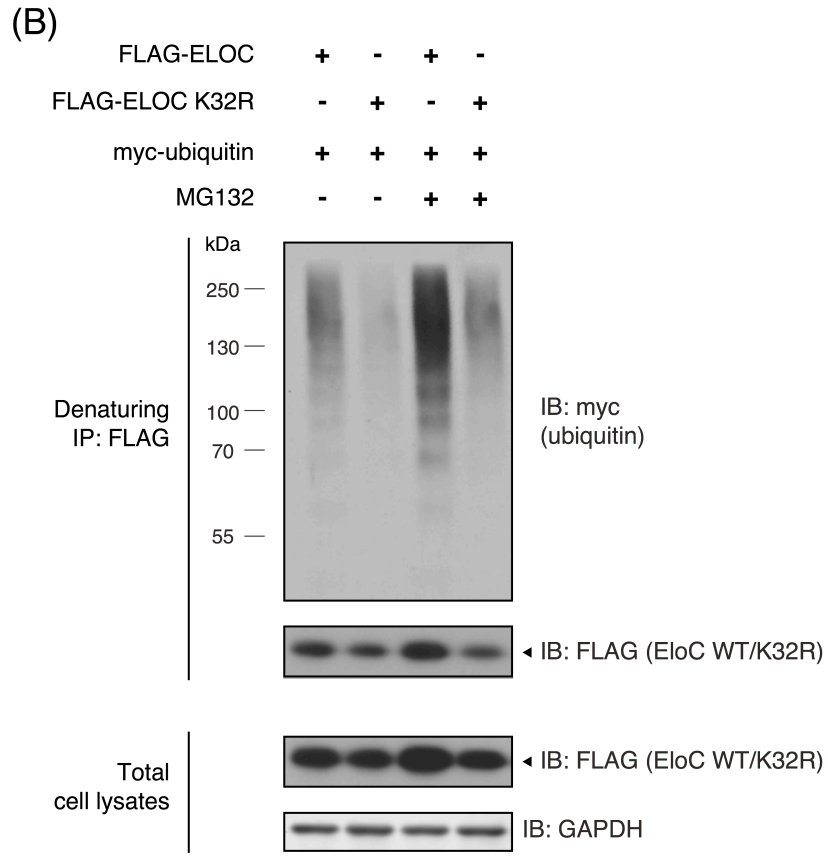

Figure 7.2.1 ELOC K32R Mutation Reduces ELOC Polyubiquitination.

(A) Similar to described in **Figure 3.3**, 293T cells with stable expression of FLAG-ELOC, FLAG-ELOC K32R mutant, or FLAG-SKP1 were transfected with myc-ubiquitin, treated with 5 μM of MG132 for 6 hours, and followed by denaturing IP. IP and input lysates were examined by immunoblot.

(B) Ubiquitin chain extension in ELOC and the K32R mutant in the absence and in the presence of MG132.

Appendix

Table 1. List of CompPASS-scored human AMBRA1 interacting proteins

bait_name	prey_uniprot	gene_entrez_id	comppass_D	prey_description
AMBRA1	Q9C0C7	AMRA1_HUMAN	600072.4268	Activating molecule in BECN1-regulated autophagy protein 1
AMBRA1	Q9BW61	DDA1_HUMAN	92925.48823	DET1- and DDB1-associated protein 1 (Placenta cross-immune reaction antigen 1) (PCIA-1)
AMBRA1	Q9H3G5	CPVL_HUMAN	2216.501026	Probable serine carboxypeptidase CPVL (EC 3.4.16.-) (Carboxypeptidase, vitellogenic-like) (Vitellogenic carboxypeptidase-like protein) (VCP-like protein) (hVLP)
AMBRA1	Q15369	ELOC_HUMAN	352.6194045	Transcription elongation factor B polypeptide 1 (Elongin 15 kDa subunit) (Elongin-C) (EloC) (RNA polymerase II transcription factor SIII subunit C) (SIII p15)
AMBRA1	Q8TD19	NEK9_HUMAN	265.1899673	Serine/threonine-protein kinase Nek9 (EC 2.7.11.1) (Nercc1 kinase) (Never in mitosis A-related kinase 9) (NimA-related protein kinase 9) (NimA-related kinase 8) (Nek8)
AMBRA1	Q9UNE7	CHIP_HUMAN	237.1265542	E3 ubiquitin-protein ligase CHIP (EC 6.3.2.-) (Antigen NY-CO-7) (CLL-associated antigen KW-8) (Carboxy terminus of Hsp70-interacting protein) (STIP1 homology and U box-containing protein 1)
AMBRA1	O95816	BAG2_HUMAN	80.81202986	BAG family molecular chaperone regulator 2 (BAG-2) (Bcl-2-associated athanogene 2)

bait_name	prey_uniprot	gene_entrez_id	comppass_D	prey_description
AMBRA1	Q16531	DDB1_HUMAN	72.83953072	DNA damage-binding protein 1 (DDB p127 subunit) (DNA damage-binding protein a) (DDBa) (Damage-specific DNA-binding protein 1) (HBV X-associated protein 1) (XAP-1) (UV-damaged DNA-binding factor) (UV-damaged DNA-binding protein 1) (UV-DDB 1) (XPE-binding factor) (XPE-BF) (Xeroderma pigmentosum group E-complementing protein) (XPCe)
AMBRA1	P63167	DYL1_HUMAN	70.28424297	Dynein light chain 1, cytoplasmic (8 kDa dynein light chain) (DLC8) (Dynein light chain LC8-type 1) (Protein inhibitor of neuronal nitric oxide synthase) (PIN)
AMBRA1	P04792	HSPB1_HUMAN	43.1722819	Heat shock protein beta-1 (HspB1) (28 kDa heat shock protein) (Estrogen-regulated 24 kDa protein) (Heat shock 27 kDa protein) (HSP 27) (Stress-responsive protein 27) (SRP27)
AMBRA1	Q13620	CUL4B_HUMAN	37.05935124	Cullin-4B (CUL-4B)
AMBRA1	Q13619	CUL4A_HUMAN	35.71173847	Cullin-4A (CUL-4A)
AMBRA1	P61962	DCAF7_HUMAN	28.35	DDB1- and CUL4-associated factor 7 (WD repeat-containing protein 68) (WD repeat-containing protein An11 homolog)
AMBRA1	A3KMH1	VWA8_HUMAN	18	von Willebrand factor A domain-containing protein 8
AMBRA1	Q15370	ELOB_HUMAN	15.86735782	Transcription elongation factor B polypeptide 2 (Elongin 18 kDa subunit) (Elongin-B) (EloB) (RNA polymerase II transcription factor SIII subunit B) (SIII p18)

bait_name	prey_uniprot	gene_entrez_id	comppass_D	prey_description
AMBRA1	Q9NZL4	HPBP1_HUMAN	12.19735669	Hsp70-binding protein 1 (HspBP1) (Heat shock protein-binding protein 1) (Hsp70-binding protein 2) (HspBP2) (Hsp70-interacting protein 1) (Hsp70-interacting protein 2)
AMBRA1	P10809	CH60_HUMAN	11.73436901	60 kDa heat shock protein, mitochondrial (60 kDa chaperonin) (Chaperonin 60) (CPN60) (Heat shock protein 60) (HSP-60) (Hsp60) (HuCHA60) (Mitochondrial matrix protein P1) (P60 lymphocyte protein)
AMBRA1	Q14257	RCN2_HUMAN	11.42539066	Reticulocalbin-2 (Calcium-binding protein ERC-55) (E6-binding protein) (E6BP)
AMBRA1	P49411	EFTU_HUMAN	11.05344572	Elongation factor Tu, mitochondrial (EF-Tu) (P43)
AMBRA1	P28331	NDUS1_HUMAN	10.27075324	NADH-ubiquinone oxidoreductase 75 kDa subunit, mitochondrial (EC 1.6.5.3) (EC 1.6.99.3) (Complex I-75kD) (CI-75kD)
AMBRA1	Q9Y5V3	MAGD1_HUMAN	9.675594166	Melanoma-associated antigen D1 (MAGE tumor antigen CCF) (MAGE-D1 antigen) (Neurotrophin receptor-interacting MAGE homolog)
AMBRA1	Q13098	CSN1_HUMAN	8.599797773	COP9 signalosome complex subunit 1 (SGN1) (Signalosome subunit 1) (G protein pathway suppressor 1) (GPS-1) (JAB1-containing signalosome subunit 1) (Protein MFH)
AMBRA1	O95831	AIFM1_HUMAN	8.260145682	Apoptosis-inducing factor 1, mitochondrial (EC 1.-.-.-) (Programmed cell death protein 8)
AMBRA1	P50402	EMD_HUMAN	7.156767611	Emerin

bait_name	prey_uniprot	gene_entrez_id	comppass_D	prey_description
AMBRA1	P36776	LONM_HUMAN	6.873863542	Lon protease homolog, mitochondrial (EC 3.4.21.-) (LONHs) (Lon protease-like protein) (LONP) (Mitochondrial ATP-dependent protease Lon) (Serine protease 15)
AMBRA1	Q13509	TBB3_HUMAN	6.712819129	Tubulin beta-3 chain (Tubulin beta-4 chain) (Tubulin beta-III)
AMBRA1	Q15293	RCN1_HUMAN	6.593023256	Reticulocalbin-1
AMBRA1	Q93008	USP9X_HUMAN	6.189572749	Probable ubiquitin carboxyl-terminal hydrolase FAF-X (EC 3.4.19.12) (Deubiquitinating enzyme FAF-X) (Fat facets in mammals) (hFAM) (Fat facets protein-related, X-linked) (Ubiquitin thioesterase FAF-X) (Ubiquitin-specific protease 9, X chromosome) (Ubiquitin-specific-processing protease FAF-X)
AMBRA1	P04350	TBB4A_HUMAN	6.073140602	Tubulin beta-4A chain (Tubulin 5 beta) (Tubulin beta-4 chain)
AMBRA1	Q96EY1	DNJA3_HUMAN	6.048	DnaJ homolog subfamily A member 3, mitochondrial (DnaJ protein Tid-1) (hTid-1) (Hepatocellular carcinoma-associated antigen 57) (Tumorous imaginal discs protein Tid56 homolog)
AMBRA1	O14654	IRS4_HUMAN	5.909144688	Insulin receptor substrate 4 (IRS-4) (160 kDa phosphotyrosine protein) (py160) (Phosphoprotein of 160 kDa) (pp160)
AMBRA1	O60220	TIM8A_HUMAN	5.462792808	Mitochondrial import inner membrane translocase subunit Tim8 A (X-linked deafness dystonia protein)

bait_name	prey_uniprot	gene_entrez_id	comppass_D	prey_description
AMBRA1	Q9UJS0	CMC2_HUMAN	5.362916144	Calcium-binding mitochondrial carrier protein Aralar2 (Citrin) (Mitochondrial aspartate glutamate carrier 2) (Solute carrier family 25 member 13)
AMBRA1	Q9BUF5	TBB6_HUMAN	5.103192011	Tubulin beta-6 chain
AMBRA1	P38606	VATA_HUMAN	5.076684673	V-type proton ATPase catalytic subunit A (V-ATPase subunit A) (EC 3.6.3.14) (V-ATPase 69 kDa subunit) (Vacuolar ATPase isoform VA68) (Vacuolar proton pump subunit alpha)
AMBRA1	Q9H078	CLPB_HUMAN	4.155602908	Caseinolytic peptidase B protein homolog (Suppressor of potassium transport defect 3)
AMBRA1	O14545	TRAD1_HUMAN	3.78872411	TRAF-type zinc finger domain-containing protein 1 (Protein FLN29)
AMBRA1	Q9BW92	SYTM_HUMAN	3.78872411	Threonine--tRNA ligase, mitochondrial (EC 6.1.1.3) (Threonyl-tRNA synthetase) (ThrRS) (Threonyl-tRNA synthetase-like 1)
AMBRA1	P12236	ADT3_HUMAN	3.454973532	ADP/ATP translocase 3 (ADP,ATP carrier protein 3) (ADP,ATP carrier protein, isoform T2) (ANT 2) (Adenine nucleotide translocator 3) (ANT 3) (Solute carrier family 25 member 6)
AMBRA1	P62877	RBX1_HUMAN	3.334313581	E3 ubiquitin-protein ligase RBX1 (EC 6.3.2.-) (Protein ZYP) (RING finger protein 75) (RING-box protein 1) (Rbx1) (Regulator of cullins 1)
AMBRA1	Q04837	SSBP_HUMAN	3.286335345	Single-stranded DNA-binding protein, mitochondrial (PWP1-interacting protein 17)

bait_name	prey_uniprot	gene_entrez_id	comppass_D	prey_description
AMBRA1	Q3ZCQ8	TIM50_HUMAN	3.100027337	Mitochondrial import inner membrane translocase subunit TIM50
AMBRA1	Q13501	SQSTM_HUMAN	3.036364964	Sequestosome-1 (EBI3-associated protein of 60 kDa) (EBIAP) (p60) (Phosphotyrosine-independent ligand for the Lck SH2 domain of 62 kDa) (Ubiquitin-binding protein p62)
AMBRA1	Q99615	DNJC7_HUMAN	2.91998558	DnaJ homolog subfamily C member 7 (Tetratricopeptide repeat protein 2) (TPR repeat protein 2)
AMBRA1	Q9Y5L4	TIM13_HUMAN	2.791740395	Mitochondrial import inner membrane translocase subunit Tim13
AMBRA1	Q9NXW2	DJB12_HUMAN	2.67903251	DnaJ homolog subfamily B member 12
AMBRA1	O00410	IPO5_HUMAN	2.455995703	Importin-5 (Imp5) (Importin subunit beta-3) (Karyopherin beta-3) (Ran-binding protein 5) (RanBP5)
AMBRA1	P30837	AL1B1_HUMAN	2.112952183	Aldehyde dehydrogenase X, mitochondrial (EC 1.2.1.3) (Aldehyde dehydrogenase 5) (Aldehyde dehydrogenase family 1 member B1)
AMBRA1	O60762	DPM1_HUMAN	1.970675428	Dolichol-phosphate mannosyltransferase (EC 2.4.1.83) (Dolichol-phosphate mannose synthase) (DPM synthase) (Dolichyl-phosphate beta-D-mannosyltransferase) (Mannose-P-dolichol synthase) (MPD synthase)
AMBRA1	Q9HCN8	SDF2L_HUMAN	1.845374056	Stromal cell-derived factor 2-like protein 1 (SDF2-like protein 1)

Table 2. List of identified proteins in VIF-AMBRA1 tandem IPs from three independent AP-MS experiments

Acc #	Num Unique	% Cov	Protein Name	Experiment
Q9C0C7	81	68	AMBRA1	Vif-strep and AMBRA1-FLAG tandem IP replicate 1
Q16531	27	29.9	DDB1	
Q15369	8	58	EloC	
Q15370	11	87.3	EloB	
P61962	2	8.2	DCAF7	
Q13951	2	19.8	CBFβ	
P69723	2	14.1	VIF	
Acc #	**Num Unique**	**% Cov**	**Protein Name**	**Experiment**
Q9C0C7	81	66.4	AMBRA1	Vif-strep and AMBRA1-FLAG tandem IP replicate 2
Q16531	19	23.6	DDB1	
Q15369	4	39.3	EloC	
Q15370	12	84.7	EloB	
P61962	4	17.8	DCAF7	
Q13951	2	15.9	CBFβ	
P69723	1	7.3	VIF	
Acc #	**Num Unique**	**% Cov**	**Protein Name**	**Experiment**
Q9C0C7	81	68	AMBRA1	Vif-strep and AMBRA1-FLAG tandem IP replicate 3
Q16531	27	29.9	DDB1	
Q15369	8	58	EloC	
Q15370	11	80.5	EloB	
P61962	2	8.2	DCAF7	
Q13951	2	19.8	CBFβ	
P69723	1	6.8	VIF	

Table 3.1. Label-free quantitative proteomic data comparing the WT and ΔH43 AMBRA1 mutant in the presence of VIF

Protein	log2FC	adj.pvalue	issue	Protein_name	Protein_desc
O14641	Inf	0	oneConditionMissing	DVL2_HUMAN	Segment polarity protein dishevelled homolog DVL-2 (Dishevelled-2) (DSH homolog 2)
Q13619	-Inf	0	oneConditionMissing	CUL4A_HUMAN	Cullin-4A (CUL-4A)
Q13620	-Inf	0	oneConditionMissing	CUL4B_HUMAN	Cullin-4B (CUL-4B)
Q5TA31	Inf	0	oneConditionMissing	RN187_HUMAN	E3 ubiquitin-protein ligase RNF187 (EC 6.3.2.-) (RING domain AP1 coactivator 1) (RACO-1) (RING finger protein 187)
Q9BW61	-5.72563519	3.08E-12	NA	DDA1_HUMAN	DET1- and DDB1-associated protein 1 (Placenta cross-immune reaction antigen 1) (PCIA-1)
Q16531	-5.318165312	5.03E-11	NA	DDB1_HUMAN	DNA damage-binding protein 1 (DDB p127 subunit) (DNA damage-binding protein a) (DDBa) (Damage-specific DNA-binding protein 1) (HBV X-associated protein 1) (XAP-1) (UV-damaged DNA-binding factor) (UV-damaged DNA-binding protein 1) (UV-DDB 1) (XPE-binding factor) (XPE-BF) (Xeroderma pigmentosum group E-complementing protein) (XPCe)
O00410	3.741242917	1.38E-07	NA	IPO5_HUMAN	Importin-5 (Imp5) (Importin subunit beta-3) (Karyopherin beta-3) (Ran-binding protein 5) (RanBP5)
Q5QP82	2.852117381	2.51E-05	NA	DCA10_HUMAN	DDB1- and CUL4-associated factor 10 (WD repeat-containing protein 32)
Q13098	-2.063027937	8.51E-05	NA	CSN1_HUMAN	COP9 signalosome complex subunit 1 (SGN1) (Signalosome subunit 1) (G protein pathway suppressor 1) (GPS-1) (JAB1-containing signalosome subunit 1) (Protein MFH)
P61201	-2.173976764	0.007509376	NA	CSN2_HUMAN	COP9 signalosome complex subunit 2 (SGN2) (Signalosome subunit 2) (Alien homolog) (Thyroid receptor-interacting protein 15) (TR-interacting protein 15) (TRIP-15)

Protein	log2FC	adj.pvalue	issue	Protein_name	Protein_desc
Q9BT78	-1.686384619	0.016071288	NA	CSN4_HUMAN	COP9 signalosome complex subunit 4 (SGN4) (Signalosome subunit 4) (JAB1-containing signalosome subunit 4)
Q15369	0.809210256	0.036835454	NA	ELOC_HUMAN	Transcription elongation factor B polypeptide 1 (Elongin 15 kDa subunit) (Elongin-C) (EloC) (RNA polymerase II transcription factor SIII subunit C) (SIII p15)
P62877	-1.749531703	0.045973595	NA	RBX1_HUMAN	E3 ubiquitin-protein ligase RBX1 (EC 6.3.2.-) (Protein ZYP) (RING finger protein 75) (RING-box protein 1) (Rbx1) (Regulator of cullins 1)
Q9H078	0.780556929	0.078999046	NA	CLPB_HUMAN	Caseinolytic peptidase B protein homolog (Suppressor of potassium transport defect 3)
Q9UNS2	-1.147036412	0.078999046	NA	CSN3_HUMAN	COP9 signalosome complex subunit 3 (SGN3) (Signalosome subunit 3) (JAB1-containing signalosome subunit 3)
Q15773	1.043462261	0.081638986	NA	MLF2_HUMAN	Myeloid leukemia factor 2 (Myelodysplasia-myeloid leukemia factor 2)
Q9H3G5	-0.590888106	0.118705995	NA	CPVL_HUMAN	Probable serine carboxypeptidase CPVL (EC 3.4.16.-) (Carboxypeptidase, vitellogenic-like) (Vitellogenic carboxypeptidase-like protein) (VCP-like protein) (hVLP)
Q14257	-0.750785227	0.184533963	NA	RCN2_HUMAN	Reticulocalbin-2 (Calcium-binding protein ERC-55) (E6-binding protein) (E6BP)
O75306	-0.609767633	0.223089265	NA	NDUS2_HUMAN	NADH dehydrogenase [ubiquinone] iron-sulfur protein 2, mitochondrial (EC 1.6.5.3) (EC 1.6.99.3) (Complex I-49kD) (CI-49kD) (NADH-ubiquinone oxidoreductase 49 kDa subunit)
Q5TAQ9	0.808335552	0.296038223	NA	DCAF8_HUMAN	DDB1- and CUL4-associated factor 8 (WD repeat-containing protein 42A)
Q8TD19	0.51980401	0.296038223	NA	NEK9_HUMAN	Serine/threonine-protein kinase Nek9 (EC 2.7.11.1) (Nercc1 kinase) (NimA-related protein kinase 9) (NimA-related kinase 8)

Protein	log2FC	adj.pvalue	issue	Protein_name	Protein_desc
Q9H936	-0.580904652	0.296038223	NA	GHC1_HUMAN	Mitochondrial glutamate carrier 1 (GC-1) (Glutamate/H(+) symporter 1) (Solute carrier family 25 member 22)
O15294	0.824417756	0.316899448	NA	OGT1_HUMAN	UDP-N-acetylglucosamine--peptide N-acetylglucosaminyltransferase 110 kDa subunit (EC 2.4.1.255) (O-GlcNAc transferase subunit p110) (O-linked N-acetylglucosamine transferase 110 kDa subunit) (OGT)
O43164	0.607815038	0.316899448	NA	PJA2_HUMAN	E3 ubiquitin-protein ligase Praja-2 (Praja2) (EC 6.3.2.-) (RING finger protein 131)
Q8NB90	0.645301489	0.316899448	NA	SPAT5_HUMAN	Spermatogenesis-associated protein 5 (ATPase family protein 2 homolog) (Spermatogenesis-associated factor protein)
A3KMH1	-0.584514212	0.336927927	NA	VWA8_HUMAN	von Willebrand factor A domain-containing protein 8
P38606	-0.602365887	0.336927927	NA	VATA_HUMAN	V-type proton ATPase catalytic subunit A (V-ATPase subunit A) (EC 3.6.3.14) (V-ATPase 69 kDa subunit) (Vacuolar ATPase isoform VA68) (Vacuolar proton pump subunit alpha)
Q9UL15	-0.748504295	0.369101376	NA	BAG5_HUMAN	BAG family molecular chaperone regulator 5 (BAG-5) (Bcl-2-associated athanogene 5)
O60762	0.454318458	0.389940129	NA	DPM1_HUMAN	Dolichol-phosphate mannosyltransferase (EC 2.4.1.83) (Dolichol-phosphate mannose synthase) (DPM synthase) (Dolichyl-phosphate beta-D-mannosyltransferase) (Mannose-P-dolichol synthase) (MPD synthase)
P50402	-0.265051719	0.433705427	NA	EMD_HUMAN	Emerin
O60220	0.420681803	0.487736896	NA	TIM8A_HUMAN	Mitochondrial import inner membrane translocase subunit Tim8 A (Deafness dystonia protein 1) (X-linked deafness dystonia protein)
P55786	-0.47385532	0.55875091	NA	PSA_HUMAN	Puromycin-sensitive aminopeptidase (PSA) (EC 3.4.11.14)

Protein	log2FC	adj.pvalue	issue	Protein_name	Protein_desc
vifprotein	0.404223406	0.55875091	NA	NA	NA
O00165	-0.334569042	0.583744738	NA	HAX1_HUMAN	HCLS1-associated protein X-1 (HS1-associating protein X-1) (HAX-1) (HS1-binding protein 1) (HSP1BP-1)
O15269	-0.414035265	0.67250219	NA	SPTC1_HUMAN	Serine palmitoyltransferase 1 (EC 2.3.1.50) (Long chain base biosynthesis protein 1) (LCB 1) (Serine-palmitoyl-CoA transferase 1) (SPT 1) (SPT1)
O95816	-0.233564613	0.67250219	NA	BAG2_HUMAN	BAG family molecular chaperone regulator 2 (BAG-2) (Bcl-2-associated athanogene 2)
P51570	-0.453971527	0.67250219	NA	GALK1_HUMAN	Galactokinase (EC 2.7.1.6) (Galactose kinase)
P51784	-0.785669627	0.67250219	NA	UBP11_HUMAN	Ubiquitin carboxyl-terminal hydrolase 11 (EC 3.4.19.12) (Deubiquitinating enzyme 11) (Ubiquitin thioesterase 11) (Ubiquitin-specific-processing protease 11)
Q15293	-0.421462662	0.67250219	NA	RCN1_HUMAN	Reticulocalbin-1
Q15370	1.151737919	0.67250219	NA	ELOB_HUMAN	Transcription elongation factor B polypeptide 2 (Elongin 18 kDa subunit) (Elongin-B) (EloB) (RNA polymerase II transcription factor SIII subunit B) (SIII p18)
Q8IWZ3	-0.474571153	0.67250219	NA	ANKH1_HUMAN	Ankyrin repeat and KH domain-containing protein 1 (HIV-1 Vpr-binding ankyrin repeat protein) (Multiple ankyrin repeats single KH domain) (hMASK)
Q9BUF5	-0.283917408	0.67250219	NA	TBB6_HUMAN	Tubulin beta-6 chain
O15027	0.293264133	0.68146097	NA	SC16A_HUMAN	Protein transport protein Sec16A (SEC16 homolog A)
P21953	-0.452192823	0.68146097	NA	ODBB_HUMAN	2-oxoisovalerate dehydrogenase subunit beta, mitochondrial (EC 1.2.4.4) (Branched-chain alpha-keto acid dehydrogenase E1 component beta chain) (BCKDE1B) (BCKDH E1-beta)
Q13501	-0.576283851	0.68146097	NA	SQSTM_HUMAN	Sequestosome-1 (EBI3-associated protein of 60 kDa) (EBIAP) (p60) (Ubiquitin-binding protein p62)

Protein	log2FC	adj.pvalue	issue	Protein_name	Protein_desc
P51617	-0.561619377	0.741006243	NA	IRAK1_HUMAN	Interleukin-1 receptor-associated kinase 1 (IRAK-1) (EC 2.7.11.1)
Q9UJC3	0.637654573	0.741006243	NA	HOOK1_HUMAN	Protein Hook homolog 1 (h-hook1) (hHK1)
P10809	-0.811249517	0.754550521	NA	CH60_HUMAN	60 kDa heat shock protein, mitochondrial (60 kDa chaperonin) (Chaperonin 60) (CPN60) (Heat shock protein 60) (HSP-60) (Hsp60) (HuCHA60) (Mitochondrial matrix protein P1) (P60 lymphocyte protein)
Q96EY1	-0.224975023	0.754550521	NA	DNJA3_HUMAN	DnaJ homolog subfamily A member 3, mitochondrial (DnaJ protein Tid-1) (hTid-1) (Hepatocellular carcinoma-associated antigen 57) (Tumorous imaginal discs protein Tid56 homolog)
Q9UJS0	-0.233831408	0.772877232	NA	CMC2_HUMAN	Calcium-binding mitochondrial carrier protein Aralar2 (Citrin) (Mitochondrial aspartate glutamate carrier 2) (Solute carrier family 25 member 13)
Q9Y5L4	0.186796304	0.772877232	NA	TIM13_HUMAN	Mitochondrial import inner membrane translocase subunit Tim13
P00367	0.213841211	0.780747065	NA	DHE3_HUMAN	Glutamate dehydrogenase 1, mitochondrial (GDH 1) (EC 1.4.1.3)
P36776	-0.408406122	0.780747065	NA	LONM_HUMAN	Lon protease homolog, mitochondrial (EC 3.4.21.-) (LONHs) (Lon protease-like protein) (LONP) (Mitochondrial ATP-dependent protease Lon) (Serine protease 15)
Q04837	0.346070124	0.780747065	NA	SSBP_HUMAN	Single-stranded DNA-binding protein, mitochondrial (Mt-SSB) (MtSSB) (PWP1-interacting protein 17)
O14654	0.189028153	0.78145947	NA	IRS4_HUMAN	Insulin receptor substrate 4 (IRS-4) (160 kDa phosphotyrosine protein) (py160) (Phosphoprotein of 160 kDa) (pp160)
Q99615	-0.16662015	0.78145947	NA	DNJC7_HUMAN	DnaJ homolog subfamily C member 7 (Tetratricopeptide repeat protein 2) (TPR repeat protein 2)
Q9Y3Z3	-0.355791615	0.784267974	NA	SAMH1_HUMAN	SAM domain and HD domain-containing protein 1 (EC 3.1.4.-)

Protein	log2FC	adj.pvalue	issue	Protein_name	Protein_desc
Q9ULX6	-0.169141975	0.839290579	NA	AKP8L_HUMAN	A-kinase anchor protein 8-like (AKAP8-like protein) (Helicase A-binding protein 95) (HAP95) (Homologous to AKAP95 protein) (HA95) (Neighbor of A-kinase-anchoring protein 95) (Neighbor of AKAP95)
P28331	-0.402330498	0.846432468	NA	NDUS1_HUMAN	NADH-ubiquinone oxidoreductase 75 kDa subunit, mitochondrial (EC 1.6.5.3) (EC 1.6.99.3) (Complex I-75kD) (CI-75kD)
O95071	0.220039394	0.857166099	NA	UBR5_HUMAN	E3 ubiquitin-protein ligase UBR5 (EC 6.3.2.-) (E3 ubiquitin-protein ligase, HECT domain-containing 1) (Hyperplastic discs protein homolog) (hHYD) (Progestin-induced protein)
O95831	-0.12592353	0.857166099	NA	AIFM1_HUMAN	Apoptosis-inducing factor 1, mitochondrial (EC 1.-.-.-) (Programmed cell death protein 8)
P30837	-0.224127563	0.857166099	NA	AL1B1_HUMAN	Aldehyde dehydrogenase X, mitochondrial (EC 1.2.1.3) (Aldehyde dehydrogenase 5) (Aldehyde dehydrogenase family 1 member B1)
P52272	0.198538025	0.857166099	NA	HNRPM_HUMAN	Heterogeneous nuclear ribonucleoprotein M (hnRNP M)
Q13509	0.305360532	0.857166099	NA	TBB3_HUMAN	Tubulin beta-3 chain (Tubulin beta-4 chain) (Tubulin beta-III)
Q16891	-0.763881383	0.857166099	NA	IMMT_HUMAN	Mitochondrial inner membrane protein (Cell proliferation-inducing gene 4/52 protein) (Mitofilin) (p87/89)
Q96PK6	0.532749746	0.857166099	NA	RBM14_HUMAN	RNA-binding protein 14 (Paraspeckle protein 2) (PSP2) (RNA-binding motif protein 14) (RRM-containing coactivator activator/modulator) (Synaptotagmin-interacting protein) (SYT-interacting protein)
Q9Y5V3	0.158386738	0.857166099	NA	MAGD1_HUMAN	Melanoma-associated antigen D1 (MAGE tumor antigen CCF) (MAGE-D1 antigen) (Neurotrophin receptor-interacting MAGE homolog)

Protein	log2FC	adj.pvalue	issue	Protein_name	Protein_desc
Q9BRX2	-0.148405711	0.865681066	NA	PELO_HUMAN	Protein pelota homolog (EC 3.1.-.-)
P04792	0.128237554	0.872152513	NA	HSPB1_HUMAN	Heat shock protein beta-1 (HspB1) (28 kDa heat shock protein) (Estrogen-regulated 24 kDa protein) (Heat shock 27 kDa protein) (HSP 27) (Stress-responsive protein 27) (SRP27)
Q9NXW2	0.157485477	0.88619116	NA	DJB12_HUMAN	DnaJ homolog subfamily B member 12
Q9NZ01	0.178887018	0.917888291	NA	TECR_HUMAN	Very-long-chain enoyl-CoA reductase (EC 1.3.1.93) (Synaptic glycoprotein SC2) (Trans-2,3-enoyl-CoA reductase) (TER)
O14545	-0.10091593	0.933744853	NA	TRAD1_HUMAN	TRAF-type zinc finger domain-containing protein 1 (Protein FLN29)
O95394	0.212225084	0.933744853	NA	AGM1_HUMAN	Phosphoacetylglucosamine mutase (PAGM) (EC 5.4.2.3) (Acetylglucosamine phosphomutase) (N-acetylglucosamine-phosphate mutase) (Phosphoglucomutase-3) (PGM 3)
P04350	-0.30373301	0.933744853	NA	TBB4A_HUMAN	Tubulin beta-4A chain (Tubulin 5 beta) (Tubulin beta-4 chain)
P09543	-0.112995638	0.933744853	NA	CN37_HUMAN	2',3'-cyclic-nucleotide 3'-phosphodiesterase (CNP) (CNPase) (EC 3.1.4.37)
P25685	-0.137429281	0.933744853	NA	DNJB1_HUMAN	DnaJ homolog subfamily B member 1 (DnaJ protein homolog 1) (Heat shock 40 kDa protein 1) (HSP40) (Heat shock protein 40) (Human DnaJ protein 1) (hDj-1)
P49411	0.067338432	0.933744853	NA	EFTU_HUMAN	Elongation factor Tu, mitochondrial (EF-Tu) (P43)
P53007	-0.077969416	0.933744853	NA	TXTP_HUMAN	Tricarboxylate transport protein, mitochondrial (Citrate transport protein) (CTP) (Solute carrier family 25 member 1) (Tricarboxylate carrier protein)
P61962	0.094698961	0.933744853	NA	DCAF7_HUMAN	DDB1- and CUL4-associated factor 7 (WD repeat-containing protein 68) (WD repeat-containing protein An11 homolog)
P78318	0.0806507	0.933744853	NA	IGBP1_HUMAN	Immunoglobulin-binding protein 1

Protein	log2FC	adj.pvalue	issue	Protein_name	Protein_desc
Q13951	-0.093781391	0.933744853	NA	PEBB_HUMAN	Core-binding factor subunit beta (CBF-beta) (Polyomavirus enhancer-binding protein 2 beta subunit) (PEA2-beta) (PEBP2-beta) (SL3-3 enhancer factor 1 subunit beta) (SL3/AKV core-binding factor beta subunit)
Q3ZCQ8	0.051242153	0.933744853	NA	TIM50_HUMAN	Mitochondrial import inner membrane translocase subunit TIM50
Q6P4A7	0.147589388	0.933744853	NA	SFXN4_HUMAN	Sideroflexin-4 (Breast cancer resistance marker 1)
Q8N163	0.13552819	0.933744853	NA	K1967_HUMAN	DBIRD complex subunit KIAA1967 (Deleted in breast cancer gene 1 protein) (DBC-1) (DBC.1) (p30 DBC)
Q8N4Q1	-0.165402612	0.933744853	NA	MIA40_HUMAN	Mitochondrial intermembrane space import and assembly protein 40 (Coiled-coil-helix-coiled-coil-helix domain-containing protein 4)
Q8WWC4	0.081980242	0.933744853	NA	CB047_HUMAN	Uncharacterized protein C2orf47, mitochondrial
Q8WXK3	0.41276049	0.933744853	NA	ASB13_HUMAN	Ankyrin repeat and SOCS box protein 13 (ASB-13)
Q92900	-0.090893233	0.933744853	NA	RENT1_HUMAN	Regulator of nonsense transcripts 1 (EC 3.6.4.-) (ATP-dependent helicase RENT1) (Up-frameshift suppressor 1 homolog) (hUpf1)
Q96D09	0.068264843	0.933744853	NA	GASP2_HUMAN	G-protein coupled receptor-associated sorting protein 2 (GASP-2)
Q9BPW8	0.072468872	0.933744853	NA	NIPS1_HUMAN	Protein NipSnap homolog 1 (NipSnap1)
Q9BSD7	-0.10011589	0.933744853	NA	NTPCR_HUMAN	Cancer-related nucleoside-triphosphatase (NTPase) (EC 3.6.1.15) (Nucleoside triphosphate phosphohydrolase)
Q9BW92	-0.05540429	0.933744853	NA	SYTM_HUMAN	Threonine--tRNA ligase, mitochondrial (EC 6.1.1.3) (Threonyl-tRNA synthetase) (ThrRS)
Q9HCN8	0.165654206	0.933744853	NA	SDF2L_HUMAN	Stromal cell-derived factor 2-like protein 1 (SDF2-like protein 1) (PWP1-interacting protein 8)
Q9UNE7	-0.076993277	0.933744853	NA	CHIP_HUMAN	E3 ubiquitin-protein ligase CHIP (EC 6.3.2.-) (Antigen NY-CO-7)

Protein	log2FC	adj.pvalue	issue	Protein_name	Protein_desc
P12236	0.124751323	0.954931165	NA	ADT3_HUMAN	ADP/ATP translocase 3 (ADP,ATP carrier protein 3) (ADP,ATP carrier protein, isoform T2) (ANT 2) (Adenine nucleotide translocator 3) (ANT 3) (Solute carrier family 25 member 6)
P35244	0.097068264	0.964129809	NA	RFA3_HUMAN	Replication protein A 14 kDa subunit (RP-A p14) (Replication factor A protein 3) (RF-A protein 3)
P46379	0.047822516	0.973019988	NA	BAG6_HUMAN	Large proline-rich protein BAG6 (BAG family molecular chaperone regulator 6) (BCL2-associated athanogene 6) (BAG-6) (BAG6) (HLA-B-associated transcript 3) (Protein G3) (Protein Scythe)
P61289	0.023906841	0.973019988	NA	PSME3_HUMAN	Proteasome activator complex subunit 3 (11S regulator complex subunit gamma) (REG-gamma) (Activator of multicatalytic protease subunit 3) (Ki nuclear autoantigen) (Proteasome activator 28 subunit gamma) (PA28g) (PA28gamma)
P63167	0.016276951	0.973019988	NA	DYL1_HUMAN	Dynein light chain 1, cytoplasmic (8 kDa dynein light chain) (DLC8) (Dynein light chain LC8-type 1) (Protein inhibitor of neuronal nitric oxide synthase) (PIN)
Q13015	0.016273406	0.973019988	NA	AF1Q_HUMAN	Protein AF1q
Q93008	0.033388955	0.973019988	NA	USP9X_HUMAN	Probable ubiquitin carboxyl-terminal hydrolase FAF-X (EC 3.4.19.12) (Deubiquitinating enzyme FAF-X) (Fat facets in mammals) (hFAM) (Fat facets protein-related, X-linked)
Q9C0C7	-0.080493241	0.973019988	NA	AMRA1_HUMAN	Activating molecule in BECN1-regulated autophagy protein 1
Q9NZL4	0.010267721	0.973757633	NA	HPBP1_HUMAN	Hsp70-binding protein 1 (HspBP1) (Heat shock protein-binding protein 1) (Hsp70-binding protein 2) (HspBP2) (Hsp70-interacting protein 1) (Hsp70-interacting protein 2)

Table 3.2. Label-free quantitative proteomic data comparing the WT and ΔH22 AMBRA1 mutant in the presence of VIF

Protein	log2FC	adj.pvalue	issue	Protein_name	Protein_desc
O14641	Inf	0	oneConditionMissing	DVL2_HUMAN	Segment polarity protein dishevelled homolog DVL-2 (Dishevelled-2) (DSH homolog 2)
Q13619	-Inf	0	oneConditionMissing	CUL4A_HUMAN	Cullin-4A (CUL-4A)
Q13620	-Inf	0	oneConditionMissing	CUL4B_HUMAN	Cullin-4B (CUL-4B)
Q5TA31	Inf	0	oneConditionMissing	RN187_HUMAN	E3 ubiquitin-protein ligase RNF187 (EC 6.3.2.-) (RING domain AP1 coactivator 1) (RACO-1) (RING finger protein 187)
Q9BW61	-6.041388617	1.41E-12	NA	DDA1_HUMAN	DET1- and DDB1-associated protein 1 (Placenta cross-immune reaction antigen 1) (PCIA-1)
Q16531	-5.429240156	3.72E-11	NA	DDB1_HUMAN	DNA damage-binding protein 1 (DDB p127 subunit) (DNA damage-binding protein a) (DDBa) (Damage-specific DNA-binding protein 1) (HBV X-associated protein 1) (XAP-1) (UV-damaged DNA-binding factor) (UV-damaged DNA-binding protein 1) (UV-DDB 1) (XPE-binding factor) (XPE-BF) (Xeroderma pigmentosum group E-complementing protein) (XPCe)
Q13098	-1.822168446	0.000580641	NA	CSN1_HUMAN	COP9 signalosome complex subunit 1 (SGN1) (Signalosome subunit 1) (G protein pathway suppressor 1) (GPS-1) (JAB1-containing signalosome subunit 1) (Protein MFH)
Q9BT78	-1.806847992	0.007035769	NA	CSN4_HUMAN	COP9 signalosome complex subunit 4 (SGN4) (Signalosome subunit 4)
Q9H078	1.063345629	0.017821057	NA	CLPB_HUMAN	Caseinolytic peptidase B protein homolog (Suppressor of potassium transport defect 3)
O15027	1.04979692	0.029175486	NA	SC16A_HUMAN	Protein transport protein Sec16A (SEC16 homolog A)
P61201	-2.005224447	0.029175486	NA	CSN2_HUMAN	COP9 signalosome complex subunit 2 (SGN2) (Signalosome subunit 2) (Alien homolog)

Protein	log2FC	adj.pvalue	issue	Protein_name	Protein_desc
P62877	-1.884880224	0.031394867	NA	RBX1_HUMAN	E3 ubiquitin-protein ligase RBX1 (EC 6.3.2.-) (Protein ZYP) (RING finger protein 75) (RING-box protein 1) (Rbx1) (Regulator of cullins 1)
Q9UNS2	-1.716888164	0.037335651	NA	CSN3_HUMAN	COP9 signalosome complex subunit 3 (SGN3) (Signalosome subunit 3)
Q15773	1.152396183	0.052778563	NA	MLF2_HUMAN	Myeloid leukemia factor 2 (Myelodysplasia-myeloid leukemia factor 2)
Q9H3G5	-0.668971516	0.069252085	NA	CPVL_HUMAN	Probable serine carboxypeptidase CPVL (EC 3.4.16.-) (Carboxypeptidase, vitellogenic-like) (Vitellogenic carboxypeptidase-like protein) (VCP-like protein) (hVLP)
Q15369	0.675021548	0.081617242	NA	ELOC_HUMAN	Transcription elongation factor B polypeptide 1 (Elongin 15 kDa subunit) (Elongin-C) (EloC) (RNA polymerase II transcription factor SIII subunit C) (SIII p15)
O43164	0.915964239	0.086684631	NA	PJA2_HUMAN	E3 ubiquitin-protein ligase Praja-2 (Praja2) (EC 6.3.2.-) (RING finger protein 131)
O15294	1.161396988	0.088159598	NA	OGT1_HUMAN	UDP-N-acetylglucosamine--peptide N-acetylglucosaminyltransferase 110 kDa subunit (EC 2.4.1.255) (O-GlcNAc transferase subunit p110)
Q8IWZ3	1.061321544	0.09385505	NA	ANKH1_HUMAN	Ankyrin repeat and KH domain-containing protein 1 (HIV-1 Vpr-binding ankyrin repeat protein) (Multiple ankyrin repeats single KH domain) (hMASK)
O14654	0.528828106	0.182592222	NA	IRS4_HUMAN	Insulin receptor substrate 4 (IRS-4) (160 kDa phosphotyrosine protein) (py160) (Phosphoprotein of 160 kDa) (pp160)
Q9UJC3	1.50675048	0.182592222	NA	HOOK1_HUMAN	Protein Hook homolog 1 (h-hook1) (hHK1)
vifprotein	0.697945277	0.182592222	NA	NA	NA
P04792	0.49423233	0.218867547	NA	HSPB1_HUMAN	Heat shock protein beta-1 (HspB1) (28 kDa heat shock protein) (Estrogen-regulated 24 kDa protein) (Heat shock 27 kDa protein) (HSP 27) (Stress-responsive protein 27) (SRP27)

Protein	log2FC	adj.pvalue	issue	Protein_name	Protein_desc
P49411	-0.576950255	0.244948411	NA	EFTU_HUMAN	Elongation factor Tu, mitochondrial (EF-Tu) (P43)
O60220	0.532533547	0.267974243	NA	TIM8A_HUMAN	Mitochondrial import inner membrane translocase subunit Tim8 A (Deafness dystonia protein 1) (X-linked deafness dystonia protein)
P09543	-0.544322945	0.267974243	NA	CN37_HUMAN	2',3'-cyclic-nucleotide 3'-phosphodiesterase (CNP) (CNPase) (EC 3.1.4.37)
Q14257	-0.606241212	0.267974243	NA	RCN2_HUMAN	Reticulocalbin-2 (Calcium-binding protein ERC-55) (E6-binding protein) (E6BP)
Q9Y5V3	0.508367623	0.267974243	NA	MAGD1_HUMAN	Melanoma-associated antigen D1 (MAGE tumor antigen CCF) (MAGE-D1 antigen) (Neurotrophin receptor-interacting MAGE homolog)
O60762	0.494059551	0.295573466	NA	DPM1_HUMAN	Dolichol-phosphate mannosyltransferase (EC 2.4.1.83) (Dolichol-phosphate mannose synthase) (DPM synthase) (Dolichyl-phosphate beta-D-mannosyltransferase) (Mannose-P-dolichol synthase) (MPD synthase)
P51784	-1.186615756	0.34608675	NA	UBP11_HUMAN	Ubiquitin carboxyl-terminal hydrolase 11 (EC 3.4.19.12) (Deubiquitinating enzyme 11) (Ubiquitin thioesterase 11) (Ubiquitin-specific-processing protease 11)
Q5QP82	0.501342489	0.347456056	NA	DCA10_HUMAN	DDB1- and CUL4-associated factor 10 (WD repeat-containing protein 32)
Q96D09	0.416388207	0.489568189	NA	GASP2_HUMAN	G-protein coupled receptor-associated sorting protein 2 (GASP-2)
Q92900	0.530497147	0.491506044	NA	RENT1_HUMAN	Regulator of nonsense transcripts 1 (EC 3.6.4.-) (ATP-dependent helicase RENT1) (Nonsense mRNA reducing factor 1) (NORF1) (Up-frameshift suppressor 1 homolog) (hUpf1)
P21953	-0.658793971	0.559027015	NA	ODBB_HUMAN	2-oxoisovalerate dehydrogenase subunit beta, mitochondrial (EC 1.2.4.4) (Branched-chain alpha-keto acid dehydrogenase E1 component beta chain) (BCKDE1B) (BCKDH E1-beta)

Protein	log2FC	adj.pvalue	issue	Protein_name	Protein_desc
P10809	-1.136157658	0.560936706	NA	CH60_HUMAN	60 kDa heat shock protein, mitochondrial (60 kDa chaperonin) (Chaperonin 60) (CPN60) (Heat shock protein 60) (HSP-60) (Hsp60) (HuCHA60) (Mitochondrial matrix protein P1) (P60 lymphocyte protein)
P25685	0.517121239	0.560936706	NA	DNJB1_HUMAN	DnaJ homolog subfamily B member 1 (DnaJ protein homolog 1) (Heat shock 40 kDa protein 1) (HSP40) (Heat shock protein 40) (Human DnaJ protein 1) (hDj-1)
P55786	-0.436873175	0.560936706	NA	PSA_HUMAN	Puromycin-sensitive aminopeptidase (PSA) (EC 3.4.11.14) (Cytosol alanyl aminopeptidase) (AAP-S)
Q3ZCQ8	0.203388135	0.560936706	NA	TIM50_HUMAN	Mitochondrial import inner membrane translocase subunit TIM50
Q8WWC4	0.443398984	0.560936706	NA	CB047_HUMAN	Uncharacterized protein C2orf47, mitochondrial
Q9ULX6	-0.296629957	0.560936706	NA	AKP8L_HUMAN	A-kinase anchor protein 8-like (AKAP8-like protein) (Helicase A-binding protein 95) (HAP95) (Homologous to AKAP95 protein) (HA95) (Neighbor of A-kinase-anchoring protein 95) (Neighbor of AKAP95)
O95831	0.244695989	0.57752425	NA	AIFM1_HUMAN	Apoptosis-inducing factor 1, mitochondrial (EC 1.-.-.-) (Programmed cell death protein 8)
P36776	0.560084592	0.57752425	NA	LONM_HUMAN	Lon protease homolog, mitochondrial (EC 3.4.21.-) (LONHs) (Lon protease-like protein) (LONP)
P53007	0.436286867	0.57752425	NA	TXTP_HUMAN	Tricarboxylate transport protein, mitochondrial (Citrate transport protein) (CTP) (Solute carrier family 25 member 1)
Q5TAQ9	0.466588845	0.57752425	NA	DCAF8_HUMAN	DDB1- and CUL4-associated factor 8 (WD repeat-containing protein 42A)
Q93008	-0.3915942	0.57752425	NA	USP9X_HUMAN	Probable ubiquitin carboxyl-terminal hydrolase FAF-X (EC 3.4.19.12) (Deubiquitinating enzyme FAF-X) (Fat facets protein-related, X-linked) (Ubiquitin-specific protease 9, X chromosome)

Protein	log2FC	adj.pvalue	issue	Protein_name	Protein_desc
Q9NZ01	0.445878297	0.57752425	NA	TECR_HUMAN	Very-long-chain enoyl-CoA reductase (EC 1.3.1.93) (Synaptic glycoprotein SC2) (Trans-2,3-enoyl-CoA reductase) (TER)
Q9UL15	-0.504661641	0.57752425	NA	BAG5_HUMAN	BAG family molecular chaperone regulator 5 (BAG-5) (Bcl-2-associated athanogene 5)
Q13501	-0.5312127	0.700475543	NA	SQSTM_HUMAN	Sequestosome-1 (EBI3-associated protein of 60 kDa) (EBIAP) (p60) (Phosphotyrosine-independent ligand for the Lck SH2 domain of 62 kDa) (Ubiquitin-binding protein p62)
O15269	-0.35878183	0.709937505	NA	SPTC1_HUMAN	Serine palmitoyltransferase 1 (EC 2.3.1.50) (Long chain base biosynthesis protein 1) (LCB 1) (Serine-palmitoyl-CoA transferase 1) (SPT 1)
P35244	0.757141879	0.76017553	NA	RFA3_HUMAN	Replication protein A 14 kDa subunit (RP-A p14) (Replication factor A protein 3) (RF-A protein 3)
P63167	0.243468148	0.76017553	NA	DYL1_HUMAN	Dynein light chain 1, cytoplasmic (8 kDa dynein light chain) (DLC8) (Dynein light chain LC8-type 1) (Protein inhibitor of neuronal nitric oxide synthase) (PIN)
Q9BRX2	0.232395917	0.76017553	NA	PELO_HUMAN	Protein pelota homolog (EC 3.1.-.-)
Q9NXW2	0.274112423	0.76017553	NA	DJB12_HUMAN	DnaJ homolog subfamily B member 12
P51570	-0.282674923	0.761321624	NA	GALK1_HUMAN	Galactokinase (EC 2.7.1.6) (Galactose kinase)
P78318	0.334284844	0.761321624	NA	IGBP1_HUMAN	Immunoglobulin-binding protein 1 (B-cell signal transduction molecule alpha 4) (Protein alpha-4) (CD79a-binding protein 1) (Protein phosphatase 2/4/6 regulatory subunit)
Q13509	0.396538342	0.761321624	NA	TBB3_HUMAN	Tubulin beta-3 chain (Tubulin beta-4 chain) (Tubulin beta-III)
Q15370	0.821870279	0.761321624	NA	ELOB_HUMAN	Transcription elongation factor B polypeptide 2 (Elongin 18 kDa subunit) (Elongin-B) (EloB) (RNA polymerase II transcription factor SIII subunit B) (SIII p18)

Protein	log2FC	adj.pvalue	issue	Protein_name	Protein_desc
Q99615	0.165634888	0.761321624	NA	DNJC7_HUMAN	DnaJ homolog subfamily C member 7 (Tetratricopeptide repeat protein 2) (TPR repeat protein 2)
Q9BW92	-0.225371732	0.761321624	NA	SYTM_HUMAN	Threonine--tRNA ligase, mitochondrial (EC 6.1.1.3) (Threonyl-tRNA synthetase) (ThrRS) (Threonyl-tRNA synthetase-like 1)
Q9UJS0	-0.210429542	0.761321624	NA	CMC2_HUMAN	Calcium-binding mitochondrial carrier protein Aralar2 (Citrin) (Mitochondrial aspartate glutamate carrier 2)
P38606	0.246711739	0.77728949	NA	VATA_HUMAN	V-type proton ATPase catalytic subunit A (V-ATPase subunit A) (EC 3.6.3.14) (V-ATPase 69 kDa subunit) (Vacuolar ATPase isoform VA68) (Vacuolar proton pump subunit alpha)
Q9UNE7	-0.184977366	0.799747369	NA	CHIP_HUMAN	E3 ubiquitin-protein ligase CHIP (EC 6.3.2.-) (Antigen NY-CO-7) (CLL-associated antigen KW-8) (Carboxy terminus of Hsp70-interacting protein) (STIP1 homology and U box-containing protein 1)
Q9Y5L4	0.144073103	0.802657093	NA	TIM13_HUMAN	Mitochondrial import inner membrane translocase subunit Tim13
P30837	-0.241376078	0.832376591	NA	AL1B1_HUMAN	Aldehyde dehydrogenase X, mitochondrial (EC 1.2.1.3) (Aldehyde dehydrogenase 5) (Aldehyde dehydrogenase family 1 member B1)
O75306	-0.172848097	0.840606112	NA	NDUS2_HUMAN	NADH dehydrogenase [ubiquinone] iron-sulfur protein 2, mitochondrial (EC 1.6.5.3) (EC 1.6.99.3) (NADH-ubiquinone oxidoreductase 49 kDa subunit)
P28331	0.317552856	0.877680226	NA	NDUS1_HUMAN	NADH-ubiquinone oxidoreductase 75 kDa subunit, mitochondrial (EC 1.6.5.3) (EC 1.6.99.3)
Q13951	-0.288691829	0.877680226	NA	PEBB_HUMAN	Core-binding factor subunit beta (CBF-beta) (Polyomavirus enhancer-binding protein 2 beta subunit) (PEA2-beta) (PEBP2-beta) (SL3-3 enhancer factor 1 subunit beta) (SL3/AKV core-binding factor beta subunit)

Protein	log2FC	adj.pvalue	issue	Protein_name	Protein_desc
Q8TD19	0.137445389	0.877680226	NA	NEK9_HUMAN	Serine/threonine-protein kinase Nek9 (EC 2.7.11.1) (Nercc1 kinase) (Never in mitosis A-related kinase 9) (NimA-related protein kinase 9) (NimA-related kinase 8) (Nek8)
Q96PK6	0.491925379	0.877680226	NA	RBM14_HUMAN	RNA-binding protein 14 (Paraspeckle protein 2) (PSP2) (RNA-binding motif protein 14) (RRM-containing coactivator activator/modulator) (Synaptotagmin-interacting protein) (SYT-interacting protein)
Q9BUF5	0.131897521	0.877680226	NA	TBB6_HUMAN	Tubulin beta-6 chain
Q8NB90	0.179406316	0.906501929	NA	SPAT5_HUMAN	Spermatogenesis-associated protein 5 (ATPase family protein 2 homolog) (Spermatogenesis-associated factor protein)
O95071	-0.1518449	0.908070533	NA	UBR5_HUMAN	E3 ubiquitin-protein ligase UBR5 (EC 6.3.2.-) (E3 ubiquitin-protein ligase, HECT domain-containing 1) (Hyperplastic discs protein homolog) (hHYD) (Progestin-induced protein)
O95394	0.224323622	0.908070533	NA	AGM1_HUMAN	Phosphoacetylglucosamine mutase (PAGM) (EC 5.4.2.3) (Acetylglucosamine phosphomutase) (N-acetylglucosamine-phosphate mutase) (Phosphoglucomutase-3) (PGM 3)
P12236	0.376060201	0.908070533	NA	ADT3_HUMAN	ADP/ATP translocase 3 (ADP,ATP carrier protein 3) (ADP,ATP carrier protein, isoform T2) (ANT 2) (Adenine nucleotide translocator 3) (ANT 3)
Q9BPW8	0.158020874	0.908070533	NA	NIPS1_HUMAN	Protein NipSnap homolog 1 (NipSnap1)
A3KMH1	-0.108665661	0.919769172	NA	VWA8_HUMAN	von Willebrand factor A domain-containing protein 8
O00410	0.121987729	0.919769172	NA	IPO5_HUMAN	Importin-5 (Imp5) (Importin subunit beta-3) (Karyopherin beta-3) (Ran-binding protein 5) (RanBP5)
P04350	0.279874927	0.919769172	NA	TBB4A_HUMAN	Tubulin beta-4A chain (Tubulin 5 beta) (Tubulin beta-4 chain)

Protein	log2FC	adj.pvalue	issue	Protein_name	Protein_desc
P51617	0.211183503	0.919769172	NA	IRAK1_HUMAN	Interleukin-1 receptor-associated kinase 1 (IRAK-1) (EC 2.7.11.1)
Q15293	-0.128209354	0.919769172	NA	RCN1_HUMAN	Reticulocalbin-1
Q8WXK3	0.300353434	0.919769172	NA	ASB13_HUMAN	Ankyrin repeat and SOCS box protein 13 (ASB-13)
Q96EY1	-0.085565161	0.919769172	NA	DNJA3_HUMAN	DnaJ homolog subfamily A member 3, mitochondrial (DnaJ protein Tid-1) (hTid-1) (Hepatocellular carcinoma-associated antigen 57) (Tumorous imaginal discs protein Tid56 homolog)
Q9NZL4	0.104483458	0.919769172	NA	HPBP1_HUMAN	Hsp70-binding protein 1 (HspBP1) (Heat shock protein-binding protein 1) (Hsp70-binding protein 2) (HspBP2) (Hsp70-interacting protein 1) (Hsp70-interacting protein 2)
Q9Y3Z3	0.17509583	0.919769172	NA	SAMH1_HUMAN	SAM domain and HD domain-containing protein 1 (EC 3.1.4.-) (Dendritic cell-derived IFNG-induced protein) (DCIP) (Monocyte protein 5) (MOP-5)
P46379	0.147986407	0.944422669	NA	BAG6_HUMAN	Large proline-rich protein BAG6 (BAG family molecular chaperone regulator 6) (BCL2-associated athanogene 6) (BAG-6) (BAG6) (HLA-B-associated transcript 3) (Protein G3) (Protein Scythe)
P00367	-0.065679314	0.955069783	NA	DHE3_HUMAN	Glutamate dehydrogenase 1, mitochondrial (GDH 1) (EC 1.4.1.3)
O00165	0.024963992	0.958743542	NA	HAX1_HUMAN	HCLS1-associated protein X-1 (HS1-associating protein X-1) (HAX-1) (HS1-binding protein 1) (HSP1BP-1)
O14545	-0.045079183	0.958743542	NA	TRAD1_HUMAN	TRAF-type zinc finger domain-containing protein 1 (Protein FLN29)
O95816	0.037128526	0.958743542	NA	BAG2_HUMAN	BAG family molecular chaperone regulator 2 (BAG-2) (Bcl-2-associated athanogene 2)
P50402	0.031412692	0.958743542	NA	EMD_HUMAN	Emerin
P61289	0.115332759	0.958743542	NA	PSME3_HUMAN	Proteasome activator complex subunit 3 (11S regulator complex subunit gamma) (Proteasome activator 28 subunit gamma)

Protein	log2FC	adj.pvalue	issue	Protein_name	Protein_desc
P61962	0.046519732	0.958743542	NA	DCAF7_HUMAN	DDB1- and CUL4-associated factor 7 (WD repeat-containing protein 68) (WD repeat-containing protein An11 homolog)
Q04837	-0.057068014	0.958743542	NA	SSBP_HUMAN	Single-stranded DNA-binding protein, mitochondrial (Mt-SSB) (MtSSB) (PWP1-interacting protein 17)
Q13015	0.065212887	0.958743542	NA	AF1Q_HUMAN	Protein AF1q
Q16891	0.086052196	0.958743542	NA	IMMT_HUMAN	Mitochondrial inner membrane protein (Cell proliferation-inducing gene 4/52 protein) (Mitofilin) (p87/89)
Q6P4A7	0.069938718	0.958743542	NA	SFXN4_HUMAN	Sideroflexin-4 (Breast cancer resistance marker 1)
Q8N163	-0.03921333	0.958743542	NA	K1967_HUMAN	DBIRD complex subunit KIAA1967 (Deleted in breast cancer gene 1 protein) (DBC-1) (DBC.1) (p30 DBC)
Q8N4Q1	0.113106632	0.958743542	NA	MIA40_HUMAN	Mitochondrial intermembrane space import and assembly protein 40 (Coiled-coil-helix-coiled-coil-helix domain-containing protein 4)
Q9BSD7	0.02285201	0.958743542	NA	NTPCR_HUMAN	Cancer-related nucleoside-triphosphatase (NTPase) (EC 3.6.1.15) (Nucleoside triphosphate phosphohydrolase)
Q9C0C7	-0.143049013	0.958743542	NA	AMRA1_HUMAN	Activating molecule in BECN1-regulated autophagy protein 1
Q9H936	-0.040854876	0.958743542	NA	GHC1_HUMAN	Mitochondrial glutamate carrier 1 (GC-1) (Glutamate/H(+) symporter 1) (Solute carrier family 25 member 22)
P52272	-0.00494038	0.997411066	NA	HNRPM_HUMAN	Heterogeneous nuclear ribonucleoprotein M (hnRNP M)
Q9HCN8	-0.000911819	0.998566041	NA	SDF2L_HUMAN	Stromal cell-derived factor 2-like protein 1 (SDF2-like protein 1) (PWP1-interacting protein 8)

Table 3.3. Label-free quantitative proteomic data comparing the WT and ΔH43 AMBRA1 mutant (no VIF)

Protein	log2FC	adj.pvalue	issue	Protein_name	Protein_desc
Q13620	-Inf	0	oneConditionMissing	CUL4B_HUMAN	Cullin-4B (CUL-4B)
vifprotein	-Inf	0	oneConditionMissing	NA	NA
Q9BW61	-5.995484731	1.58E-12	NA	DDA1_HUMAN	DET1- and DDB1-associated protein 1 (Placenta cross-immune reaction antigen 1) (PCIA-1)
Q16531	-4.760867631	2.53E-10	NA	DDB1_HUMAN	DNA damage-binding protein 1 (DDB p127 subunit) (DNA damage-binding protein a) (DDBa) (Damage-specific DNA-binding protein 1) (HBV X-associated protein 1) (XAP-1) (UV-damaged DNA-binding factor) (UV-damaged DNA-binding protein 1) (UV-DDB 1) (XPE-binding factor) (XPE-BF) (Xeroderma pigmentosum group E-complementing protein) (XPCe)
Q5QP82	4.141696745	2.90E-06	NA	DCA10_HUMAN	DDB1- and CUL4-associated factor 10 (WD repeat-containing protein 32)
O00410	2.467467589	1.87E-05	NA	IPO5_HUMAN	Importin-5 (Imp5) (Importin subunit beta-3) (Karyopherin beta-3) (Ran-binding protein 5) (RanBP5)
Q13098	-1.838491334	0.000318919	NA	CSN1_HUMAN	COP9 signalosome complex subunit 1 (SGN1) (Signalosome subunit 1) (G protein pathway suppressor 1) (GPS-1) (Protein MFH)
Q13619	-1.255237081	0.001044868	NA	CUL4A_HUMAN	Cullin-4A (CUL-4A)
P61962	1.148995248	0.001664932	NA	DCAF7_HUMAN	DDB1- and CUL4-associated factor 7 (WD repeat-containing protein 68) (WD repeat-containing protein An11 homolog)
Q15369	1.036068834	0.004422254	NA	ELOC_HUMAN	Transcription elongation factor B polypeptide 1 (Elongin 15 kDa subunit) (Elongin-C) (EloC) (RNA polymerase II transcription factor SIII subunit C) (SIII p15)
Q96D09	-1.315243908	0.004422254	NA	GASP2_HUMAN	G-protein coupled receptor-associated sorting protein 2 (GASP-2)

Protein	log2FC	adj.pvalue	issue	Protein_name	Protein_desc
Q9BT78	-1.858970829	0.005478928	NA	CSN4_HUMAN	COP9 signalosome complex subunit 4 (SGN4) (Signalosome subunit 4) (JAB1-containing signalosome subunit 4)
Q13501	-2.374846545	0.005500936	NA	SQSTM_HUMAN	Sequestosome-1 (EBI3-associated protein of 60 kDa) (EBIAP) (p60) (Phosphotyrosine-independent ligand for the Lck SH2 domain of 62 kDa) (Ubiquitin-binding protein p62)
O15294	1.677473278	0.007901589	NA	OGT1_HUMAN	UDP-N-acetylglucosamine--peptide N-acetylglucosaminyltransferase 110 kDa subunit (EC 2.4.1.255) (O-GlcNAc transferase subunit p110) (O-linked N-acetylglucosamine transferase 110 kDa subunit) (OGT)
Q5TAQ9	1.547751455	0.009663659	NA	DCAF8_HUMAN	DDB1- and CUL4-associated factor 8 (WD repeat-containing protein 42A)
Q8TD19	0.966015786	0.009663659	NA	NEK9_HUMAN	Serine/threonine-protein kinase Nek9 (EC 2.7.11.1) (Nercc1 kinase) (Never in mitosis A-related kinase 9) (NimA-related protein kinase 9) (NimA-related kinase 8) (Nek8)
P62877	-1.559200311	0.026738297	NA	RBX1_HUMAN	E3 ubiquitin-protein ligase RBX1 (EC 6.3.2.-) (Protein ZYP) (RING finger protein 75) (RING-box protein 1) (Rbx1) (Regulator of cullins 1)
Q3ZCQ8	0.516923385	0.026738297	NA	TIM50_HUMAN	Mitochondrial import inner membrane translocase subunit TIM50
P61201	-1.452179818	0.049150305	NA	CSN2_HUMAN	COP9 signalosome complex subunit 2 (SGN2) (Signalosome subunit 2) (Alien homolog) (JAB1-containing signalosome subunit 2) (Thyroid receptor-interacting protein 15) (TR-interacting protein 15) (TRIP-15)
P04792	-0.623197546	0.070396943	NA	HSPB1_HUMAN	Heat shock protein beta-1 (HspB1) (28 kDa heat shock protein) (Heat shock 27 kDa protein) (HSP 27) (Stress-responsive protein 27) (SRP27)

Protein	log2FC	adj.pvalue	issue	Protein_name	Protein_desc
P78318	1.139597888	0.070396943	NA	IGBP1_HUMAN	Immunoglobulin-binding protein 1 (B-cell signal transduction molecule alpha 4) (Protein alpha-4) (CD79a-binding protein 1) (Protein phosphatase 2/4/6 regulatory subunit) (Renal carcinoma antigen NY-REN-16)
Q9H936	0.648498954	0.094549876	NA	GHC1_HUMAN	Mitochondrial glutamate carrier 1 (GC-1) (Glutamate/H(+) symporter 1) (Solute carrier family 25 member 22)
Q9UJC3	1.447381931	0.176295833	NA	HOOK1_HUMAN	Protein Hook homolog 1 (h-hook1) (hHK1)
Q8WWC4	0.718934035	0.188969016	NA	CB047_HUMAN	Uncharacterized protein C2orf47, mitochondrial
Q9H3G5	0.451037896	0.232829213	NA	CPVL_HUMAN	Probable serine carboxypeptidase CPVL (EC 3.4.16.-) (Carboxypeptidase, vitellogenic-like) (Vitellogenic carboxypeptidase-like protein) (VCP-like protein) (hVLP)
O14654	0.461725311	0.234663485	NA	IRS4_HUMAN	Insulin receptor substrate 4 (IRS-4) (160 kDa phosphotyrosine protein) (py160) (Phosphoprotein of 160 kDa) (pp160)
Q9UNS2	-0.743403754	0.236580657	NA	CSN3_HUMAN	COP9 signalosome complex subunit 3 (SGN3) (Signalosome subunit 3) (JAB1-containing signalosome subunit 3)
O95394	0.969935351	0.248969228	NA	AGM1_HUMAN	Phosphoacetylglucosamine mutase (PAGM) (EC 5.4.2.3) (Acetylglucosamine phosphomutase) (N-acetylglucosamine-phosphate mutase) (Phosphoglucomutase-3) (PGM 3)
Q13015	-0.688663168	0.248969228	NA	AF1Q_HUMAN	Protein AF1q
Q9Y5L4	0.390201037	0.248969228	NA	TIM13_HUMAN	Mitochondrial import inner membrane translocase subunit Tim13
P09543	-0.511465148	0.279123572	NA	CN37_HUMAN	2',3'-cyclic-nucleotide 3'-phosphodiesterase (CNP) (CNPase) (EC 3.1.4.37)
Q5TA31	1.514101453	0.295572998	NA	RN187_HUMAN	E3 ubiquitin-protein ligase RNF187 (EC 6.3.2.-) (RING domain AP1 coactivator 1) (RACO-1) (RING finger protein 187)

Protein	log2FC	adj.pvalue	issue	Protein_name	Protein_desc
Q9UJS0	0.43716457	0.330467692	NA	CMC2_HUMAN	Calcium-binding mitochondrial carrier protein Aralar2 (Citrin) (Mitochondrial aspartate glutamate carrier 2) (Solute carrier family 25 member 13)
Q9UNE7	-0.426487806	0.335559529	NA	CHIP_HUMAN	E3 ubiquitin-protein ligase CHIP (EC 6.3.2.-) (Antigen NY-CO-7) (CLL-associated antigen KW-8) (Carboxy terminus of Hsp70-interacting protein) (STIP1 homology and U box-containing protein 1)
Q9Y3Z3	0.736386658	0.335559529	NA	SAMH1_HUMAN	SAM domain and HD domain-containing protein 1 (EC 3.1.4.-) (Dendritic cell-derived IFNG-induced protein) (DCIP) (Monocyte protein 5) (MOP-5)
Q8N163	0.671179186	0.339444739	NA	K1967_HUMAN	DBIRD complex subunit KIAA1967 (Deleted in breast cancer gene 1 protein) (DBC-1) (DBC.1) (p30 DBC)
O43164	0.445149921	0.35355712	NA	PJA2_HUMAN	E3 ubiquitin-protein ligase Praja-2 (Praja2) (EC 6.3.2.-) (RING finger protein 131)
O60220	0.424450486	0.360752851	NA	TIM8A_HUMAN	Mitochondrial import inner membrane translocase subunit Tim8 A (Deafness dystonia protein 1) (X-linked deafness dystonia protein)
O60762	0.398383159	0.387061014	NA	DPM1_HUMAN	Dolichol-phosphate mannosyltransferase (EC 2.4.1.83) (Dolichol-phosphate mannose synthase) (DPM synthase) (Mannose-P-dolichol synthase)
O95831	-0.29119488	0.422159305	NA	AIFM1_HUMAN	Apoptosis-inducing factor 1, mitochondrial (EC 1.-.-.-) (Programmed cell death protein 8)
Q92900	0.550491697	0.422159305	NA	RENT1_HUMAN	Regulator of nonsense transcripts 1 (EC 3.6.4.-) (ATP-dependent helicase RENT1) (Nonsense mRNA reducing factor 1) (NORF1) (Up-frameshift suppressor 1 homolog) (hUpf1)
Q93008	0.468995767	0.422159305	NA	USP9X_HUMAN	Probable ubiquitin carboxyl-terminal hydrolase FAF-X (EC 3.4.19.12) (Deubiquitinating enzyme FAF-X) (Fat facets in mammals) (hFAM) (Ubiquitin thioesterase FAF-X) (Ubiquitin-specific protease 9, X chromosome)

Protein	log2FC	adj.pvalue	issue	Protein_name	Protein_desc
Q9ULX6	0.322522451	0.422159305	NA	AKP8L_HUMAN	A-kinase anchor protein 8-like (AKAP8-like protein) (Helicase A-binding protein 95) (HAP95) (Homologous to AKAP95 protein) (HA95) (Neighbor of A-kinase-anchoring protein 95) (Neighbor of AKAP95)
O75306	0.365225586	0.433681304	NA	NDUS2_HUMAN	NADH dehydrogenase [ubiquinone] iron-sulfur protein 2, mitochondrial (EC 1.6.5.3) (EC 1.6.99.3) (Complex I-49kD) (CI-49kD) (NADH-ubiquinone oxidoreductase 49 kDa subunit)
P10809	-1.14336234	0.435732562	NA	CH60_HUMAN	60 kDa heat shock protein, mitochondrial (60 kDa chaperonin) (Chaperonin 60) (CPN60) (Heat shock protein 60) (HSP-60) (Hsp60) (HuCHA60) (Mitochondrial matrix protein P1) (P60 lymphocyte protein)
Q96PK6	0.951281616	0.51258213	NA	RBM14_HUMAN	RNA-binding protein 14 (Paraspeckle protein 2) (PSP2) (RNA-binding motif protein 14) (RRM-containing coactivator activator/modulator) (Synaptotagmin-interacting protein)
P63167	0.334844378	0.513133551	NA	DYL1_HUMAN	Dynein light chain 1, cytoplasmic (8 kDa dynein light chain) (DLC8) (Dynein light chain LC8-type 1) (Protein inhibitor of neuronal nitric oxide synthase) (PIN)
Q8NB90	0.348014334	0.527329321	NA	SPAT5_HUMAN	Spermatogenesis-associated protein 5 (ATPase family protein 2 homolog) (Spermatogenesis-associated factor protein)
P35244	-0.861232978	0.547000526	NA	RFA3_HUMAN	Replication protein A 14 kDa subunit (RP-A p14) (Replication factor A protein 3)
Q15370	1.118564446	0.548746835	NA	ELOB_HUMAN	Transcription elongation factor B polypeptide 2 (Elongin 18 kDa subunit) (Elongin-B) (EloB) (RNA polymerase II transcription factor SIII subunit B) (SIII p18)

Protein	log2FC	adj.pvalue	issue	Protein_name	Protein_desc
Q9BW92	-0.31555699	0.56186199	NA	SYTM_HUMAN	Threonine--tRNA ligase, mitochondrial (EC 6.1.1.3) (Threonyl-tRNA synthetase) (ThrRS) (Threonyl-tRNA synthetase-like 1)
O15269	-0.39062153	0.566594718	NA	SPTC1_HUMAN	Serine palmitoyltransferase 1 (EC 2.3.1.50) (Long chain base biosynthesis protein 1) (LCB 1) (Serine-palmitoyl-CoA transferase 1) (SPT 1) (SPT1)
P50402	0.172519088	0.572096948	NA	EMD_HUMAN	Emerin
Q14257	0.309672846	0.624642293	NA	RCN2_HUMAN	Reticulocalbin-2 (Calcium-binding protein ERC-55) (E6-binding protein) (E6BP)
Q9Y5V3	0.249926014	0.634505053	NA	MAGD1_HUMAN	Melanoma-associated antigen D1 (MAGE tumor antigen CCF) (MAGE-D1 antigen) (Neurotrophin receptor-interacting MAGE homolog)
P00367	-0.235505561	0.646912497	NA	DHE3_HUMAN	Glutamate dehydrogenase 1, mitochondrial (GDH 1) (EC 1.4.1.3)
Q8N4Q1	0.503171733	0.697491614	NA	MIA40_HUMAN	Mitochondrial intermembrane space import and assembly protein 40 (Coiled-coil-helix-coiled-coil-helix domain-containing protein 4)
P51570	0.252063041	0.731673971	NA	GALK1_HUMAN	Galactokinase (EC 2.7.1.6) (Galactose kinase)
P51784	0.344319598	0.731673971	NA	UBP11_HUMAN	Ubiquitin carboxyl-terminal hydrolase 11 (EC 3.4.19.12) (Deubiquitinating enzyme 11) (Ubiquitin thioesterase 11) (Ubiquitin-specific-processing protease 11)
Q9BUF5	0.194143187	0.731673971	NA	TBB6_HUMAN	Tubulin beta-6 chain
O95071	0.285650745	0.741215142	NA	UBR5_HUMAN	E3 ubiquitin-protein ligase UBR5 (EC 6.3.2.-) (E3 ubiquitin-protein ligase, HECT domain-containing 1) (Hyperplastic discs protein homolog) (hHYD) (Progestin-induced protein)
P25685	-0.317191232	0.748996804	NA	DNJB1_HUMAN	DnaJ homolog subfamily B member 1 (DnaJ protein homolog 1) (Heat shock 40 kDa protein 1) (HSP40) (Heat shock protein 40)
Q8WXK3	0.440657649	0.784971861	NA	ASB13_HUMAN	Ankyrin repeat and SOCS box protein 13 (ASB-13)
Q9UL15	-0.285216396	0.864568264	NA	BAG5_HUMAN	BAG family molecular chaperone regulator 5 (BAG-5)

Protein	log2FC	adj.pvalue	issue	Protein_name	Protein_desc
Q6P4A7	0.402625633	0.911627774	NA	SFXN4_HUMAN	Sideroflexin-4 (Breast cancer resistance marker 1)
Q9BRX2	0.139401165	0.911627774	NA	PELO_HUMAN	Protein pelota homolog (EC 3.1.-.-)
P04350	0.351416669	0.913141109	NA	TBB4A_HUMAN	Tubulin beta-4A chain (Tubulin 5 beta) (Tubulin beta-4 chain)
O95816	0.077591055	0.927749118	NA	BAG2_HUMAN	BAG family molecular chaperone regulator 2 (BAG-2) (Bcl-2-associated athanogene 2)
P30837	0.139401661	0.927749118	NA	AL1B1_HUMAN	Aldehyde dehydrogenase X, mitochondrial (EC 1.2.1.3) (Aldehyde dehydrogenase 5) (Aldehyde dehydrogenase family 1 member B1)
P38606	-0.139600074	0.927749118	NA	VATA_HUMAN	V-type proton ATPase catalytic subunit A (V-ATPase subunit A) (EC 3.6.3.14) (V-ATPase 69 kDa subunit) (Vacuolar ATPase isoform VA68) (Vacuolar proton pump subunit alpha)
P46379	0.209891769	0.927749118	NA	BAG6_HUMAN	Large proline-rich protein BAG6 (BAG family molecular chaperone regulator 6) (BCL2-associated athanogene 6) (BAG-6) (BAG6) (HLA-B-associated transcript 3) (Protein G3) (Protein Scythe)
P51617	0.215768626	0.927749118	NA	IRAK1_HUMAN	Interleukin-1 receptor-associated kinase 1 (IRAK-1) (EC 2.7.11.1)
P55786	0.134784795	0.927749118	NA	PSA_HUMAN	Puromycin-sensitive aminopeptidase (PSA) (EC 3.4.11.14) (Cytosol alanyl aminopeptidase) (AAP-S)
Q13509	0.185737174	0.927749118	NA	TBB3_HUMAN	Tubulin beta-3 chain (Tubulin beta-4 chain)
Q15773	0.162119438	0.927749118	NA	MLF2_HUMAN	Myeloid leukemia factor 2 (Myelodysplasia-myeloid leukemia factor 2)
Q8IWZ3	0.152189132	0.927749118	NA	ANKH1_HUMAN	Ankyrin repeat and KH domain-containing protein 1 (HIV-1 Vpr-binding ankyrin repeat protein)
Q96EY1	0.108258635	0.927749118	NA	DNJA3_HUMAN	DnaJ homolog subfamily A member 3, mitochondrial (DnaJ protein Tid-1) (hTid-1) (Hepatocellular carcinoma-associated antigen 57) (Tumorous imaginal discs protein Tid56 homolog)

Protein	log2FC	adj.pvalue	issue	Protein_name	Protein_desc
Q9BPW8	0.13562525	0.927749118	NA	NIPS1_HUMAN	Protein NipSnap homolog 1 (NipSnap1)
O14641	0.11987223	0.93678578	NA	DVL2_HUMAN	Segment polarity protein dishevelled homolog DVL-2 (Dishevelled-2) (DSH homolog 2)
P12236	0.250788527	0.93678578	NA	ADT3_HUMAN	ADP/ATP translocase 3 (ADP,ATP carrier protein 3) (ADP,ATP carrier protein, isoform T2) (ANT 2) (Adenine nucleotide translocator 3) (ANT 3) (Solute carrier family 25 member 6)
Q15293	-0.113310567	0.93678578	NA	RCN1_HUMAN	Reticulocalbin-1
Q16891	0.387133121	0.93678578	NA	IMMT_HUMAN	Mitochondrial inner membrane protein (Cell proliferation-inducing gene 4/52 protein) (Mitofilin) (p87/89)
Q9BSD7	0.088693395	0.93678578	NA	NTPCR_HUMAN	Cancer-related nucleoside-triphosphatase (NTPase) (EC 3.6.1.15) (Nucleoside triphosphate phosphohydrolase)
Q9NZL4	0.111250132	0.93678578	NA	HPBP1_HUMAN	Hsp70-binding protein 1 (HspBP1) (Heat shock protein-binding protein 1) (Hsp70-binding protein 2) (HspBP2) (Hsp70-interacting protein 1) (Hsp70-interacting protein 2)
O00165	0.065454916	0.945877652	NA	HAX1_HUMAN	HCLS1-associated protein X-1 (HS1-associating protein X-1) (HAX-1) (HS1-binding protein 1) (HSP1BP-1)
Q99615	0.051510845	0.945877652	NA	DNJC7_HUMAN	DnaJ homolog subfamily C member 7 (Tetratricopeptide repeat protein 2) (TPR repeat protein 2)
O14545	-0.078372968	0.951743435	NA	TRAD1_HUMAN	TRAF-type zinc finger domain-containing protein 1 (Protein FLN29)
P28331	0.087441218	0.951743435	NA	NDUS1_HUMAN	NADH-ubiquinone oxidoreductase 75 kDa subunit, mitochondrial (EC 1.6.5.3) (EC 1.6.99.3) (Complex I-75kD) (CI-75kD)
P36776	-0.088490744	0.951743435	NA	LONM_HUMAN	Lon protease homolog, mitochondrial (EC 3.4.21.-) (LONHs) (Lon protease-like protein) (LONP) (Mitochondrial ATP-dependent protease Lon)

Protein	log2FC	adj.pvalue	issue	Protein_name	Protein_desc
P49411	-0.060000891	0.951743435	NA	EFTU_HUMAN	Elongation factor Tu, mitochondrial (EF-Tu) (P43)
P52272	0.052051178	0.951743435	NA	HNRPM_HUMAN	Heterogeneous nuclear ribonucleoprotein M (hnRNP M)
Q9C0C7	0.155025279	0.951743435	NA	AMRA1_HUMAN	Activating molecule in BECN1-regulated autophagy protein 1
Q9H078	0.053204503	0.951743435	NA	CLPB_HUMAN	Caseinolytic peptidase B protein homolog (Suppressor of potassium transport defect 3)
Q9HCN8	-0.075616415	0.951743435	NA	SDF2L_HUMAN	Stromal cell-derived factor 2-like protein 1 (SDF2-like protein 1) (PWP1-interacting protein 8)
Q9NXW2	0.056640174	0.951743435	NA	DJB12_HUMAN	DnaJ homolog subfamily B member 12
P61289	-0.056591732	0.952486085	NA	PSME3_HUMAN	Proteasome activator complex subunit 3 (11S regulator complex subunit gamma) (REG-gamma) (Activator of multicatalytic protease subunit 3) (Ki nuclear autoantigen) (Proteasome activator 28 subunit gamma) (PA28g) (PA28gamma)
Q04837	-0.04751047	0.952486085	NA	SSBP_HUMAN	Single-stranded DNA-binding protein, mitochondrial (Mt-SSB) (MtSSB) (PWP1-interacting protein 17)
Q9NZ01	-0.038763251	0.952486085	NA	TECR_HUMAN	Very-long-chain enoyl-CoA reductase (EC 1.3.1.93) (Synaptic glycoprotein SC2) (Trans-2,3-enoyl-CoA reductase) (TER)
P21953	0.032798215	0.964872105	NA	ODBB_HUMAN	2-oxoisovalerate dehydrogenase subunit beta, mitochondrial (EC 1.2.4.4) (Branched-chain alpha-keto acid dehydrogenase E1 component beta chain) (BCKDE1B) (BCKDH E1-beta)
A3KMH1	0.014230657	0.976247039	NA	VWA8_HUMAN	von Willebrand factor A domain-containing protein 8
O15027	0.011028377	0.976247039	NA	SC16A_HUMAN	Protein transport protein Sec16A (SEC16 homolog A)
P53007	0.00912413	0.979917644	NA	TXTP_HUMAN	Tricarboxylate transport protein, mitochondrial (Citrate transport protein) (CTP) (Solute carrier family 25 member 1

Protein	log2FC	adj.pvalue	issue	Protein_name	Protein_desc
Q13951	NA	NA	completeMissing	PEBB_HUMAN	Core-binding factor subunit beta (CBF-beta) (Polyomavirus enhancer-binding protein 2 beta subunit) (PEA2-beta) (PEBP2-beta) (SL3-3 enhancer factor 1 subunit beta) (SL3/AKV core-binding factor beta subunit)

Table 3.4. Label-free quantitative proteomic data comparing the WT and ΔH22 AMBRA1 mutant (no VIF)

Protein	log2FC	adj.pvalue	issue	Protein_name	Protein_desc
O95071	-Inf	0	oneConditionMissing	UBR5_HUMAN	E3 ubiquitin-protein ligase UBR5 (EC 6.3.2.-) (E3 ubiquitin-protein ligase, HECT domain-containing 1) (Hyperplastic discs protein homolog) (hHYD) (Progestin-induced protein)
Q13619	-Inf	0	oneConditionMissing	CUL4A_HUMAN	Cullin-4A (CUL-4A)
vifprotein	-Inf	0	oneConditionMissing	NA	NA
Q9BW61	-6.228905294	4.62E-12	NA	DDA1_HUMAN	DET1- and DDB1-associated protein 1 (Placenta cross-immune reaction antigen 1) (PCIA-1)
Q16531	-5.050485923	5.35E-10	NA	DDB1_HUMAN	DNA damage-binding protein 1 (DDB p127 subunit) (DNA damage-binding protein a) (DDBa) (Damage-specific DNA-binding protein 1) (HBV X-associated protein 1) (XAP-1) (UV-damaged DNA-binding factor) (UV-damaged DNA-binding protein 1) (UV-DDB 1) (XPE-binding factor) (XPE-BF) (Xeroderma pigmentosum group E-complementing protein) (XPCe)
Q13098	-1.609682209	0.004999901	NA	CSN1_HUMAN	COP9 signalosome complex subunit 1 (SGN1) (Signalosome subunit 1) (G protein pathway suppressor 1) (GPS-1) (JAB1-containing signalosome subunit 1) (Protein MFH)
Q5QP82	1.892095106	0.004999901	NA	DCA10_HUMAN	DDB1- and CUL4-associated factor 10 (WD repeat-containing protein 32)
P61962	1.161434121	0.00504042	NA	DCAF7_HUMAN	DDB1- and CUL4-associated factor 7 (WD repeat-containing protein 68) (WD repeat-containing protein An11 homolog)
Q8TD19	1.303961689	0.00504042	NA	NEK9_HUMAN	Serine/threonine-protein kinase Nek9 (EC 2.7.11.1) (Nercc1 kinase) (Never in mitosis A-related kinase 9) (NimA-related protein kinase 9)
Q13620	-2.271170135	0.006070581	NA	CUL4B_HUMAN	Cullin-4B (CUL-4B)

Protein	log2FC	adj.pvalue	issue	Protein_name	Protein_desc
Q9UNS2	-1.420989144	0.031805313	NA	CSN3_HUMAN	COP9 signalosome complex subunit 3 (SGN3) (Signalosome subunit 3) (JAB1-containing signalosome subunit 3)
Q15369	0.894157286	0.035640707	NA	ELOC_HUMAN	Transcription elongation factor B polypeptide 1 (Elongin 15 kDa subunit) (Elongin-C) (EloC) (RNA polymerase II transcription factor SIII subunit C) (SIII p15)
P10809	-2.815993538	0.036828542	NA	CH60_HUMAN	60 kDa heat shock protein, mitochondrial (60 kDa chaperonin) (Chaperonin 60) (CPN60) (Heat shock protein 60) (HSP-60) (Hsp60) (HuCHA60) (Mitochondrial matrix protein P1) (P60 lymphocyte protein)
Q9BT78	-1.71942324	0.043614521	NA	CSN4_HUMAN	COP9 signalosome complex subunit 4 (SGN4) (Signalosome subunit 4) (JAB1-containing signalosome subunit 4)
Q9Y5L4	0.725458334	0.048559117	NA	TIM13_HUMAN	Mitochondrial import inner membrane translocase subunit Tim13
O15294	1.409738375	0.057916797	NA	OGT1_HUMAN	UDP-N-acetylglucosamine--peptide N-acetylglucosaminyltransferase 110 kDa subunit (EC 2.4.1.255) (O-GlcNAc transferase subunit p110) (O-linked N-acetylglucosamine transferase 110 kDa subunit) (OGT)
P61201	-2.041160176	0.061280852	NA	CSN2_HUMAN	COP9 signalosome complex subunit 2 (SGN2) (Signalosome subunit 2) (Alien homolog) (JAB1-containing signalosome subunit 2) (Thyroid receptor-interacting protein 15) (TRIP-15)
Q13501	-1.742233049	0.065141416	NA	SQSTM_HUMAN	Sequestosome-1 (EBI3-associated protein of 60 kDa) (EBIAP) (p60) (Phosphotyrosine-independent ligand for the Lck SH2 domain of 62 kDa) (Ubiquitin-binding protein p62)
Q9UJC3	2.061617666	0.070017057	NA	HOOK1_HUMAN	Protein Hook homolog 1 (h-hook1) (hHK1)

Protein	log2FC	adj.pvalue	issue	Protein_name	Protein_desc
O14654	0.70084183	0.076199813	NA	IRS4_HUMAN	Insulin receptor substrate 4 (IRS-4) (160 kDa phosphotyrosine protein) (py160) (Phosphoprotein of 160 kDa) (pp160)
P62877	-1.428662556	0.076199813	NA	RBX1_HUMAN	E3 ubiquitin-protein ligase RBX1 (EC 6.3.2.-) (Protein ZYP) (RING finger protein 75) (RING-box protein 1) (Rbx1) (Regulator of cullins 1)
O60220	0.735836805	0.13663586	NA	TIM8A_HUMAN	Mitochondrial import inner membrane translocase subunit Tim8 A (Deafness dystonia protein 1) (X-linked deafness dystonia protein)
Q9H936	0.671382055	0.136999732	NA	GHC1_HUMAN	Mitochondrial glutamate carrier 1 (GC-1) (Glutamate/H(+) symporter 1) (Solute carrier family 25 member 22)
Q9Y3Z3	1.146066383	0.161916425	NA	SAMH1_HUMAN	SAM domain and HD domain-containing protein 1 (EC 3.1.4.-) (Dendritic cell-derived IFNG-induced protein) (DCIP) (Monocyte protein 5) (MOP-5)
Q5TAQ9	0.974278368	0.178737965	NA	DCAF8_HUMAN	DDB1- and CUL4-associated factor 8 (WD repeat-containing protein 42A)
O43164	0.688495996	0.182547223	NA	PJA2_HUMAN	E3 ubiquitin-protein ligase Praja-2 (Praja2) (EC 6.3.2.-)
P28331	-1.142508667	0.212528559	NA	NDUS1_HUMAN	NADH-ubiquinone oxidoreductase 75 kDa subunit, mitochondrial (EC 1.6.5.3) (EC 1.6.99.3) (Complex I-75kD) (CI-75kD)
Q96D09	-0.629574059	0.212528559	NA	GASP2_HUMAN	G-protein coupled receptor-associated sorting protein 2 (GASP-2)
O95394	1.108025616	0.246214932	NA	AGM1_HUMAN	Phosphoacetylglucosamine mutase (PAGM) (EC 5.4.2.3) (Acetylglucosamine phosphomutase) (N-acetylglucosamine-phosphate mutase) (Phosphoglucomutase-3)
P09543	-0.572086244	0.29636086	NA	CN37_HUMAN	2',3'-cyclic-nucleotide 3'-phosphodiesterase (CNP) (CNPase) (EC 3.1.4.37)
P25685	-0.83738278	0.301758269	NA	DNJB1_HUMAN	DnaJ homolog subfamily B member 1 (DnaJ protein homolog 1) (Heat shock 40 kDa protein 1) (HSP40) (Heat shock protein 40) (Human DnaJ protein 1) (hDj-1)

Protein	log2FC	adj.pvalue	issue	Protein_name	Protein_desc
Q9NXW2	0.579604923	0.309266781	NA	DJB12_HUMAN	DnaJ homolog subfamily B member 12
P51784	0.87056221	0.313846719	NA	UBP11_HUMAN	Ubiquitin carboxyl-terminal hydrolase 11 (EC 3.4.19.12) (Deubiquitinating enzyme 11) (Ubiquitin thioesterase 11) (Ubiquitin-specific-processing protease 11)
O00165	0.453450293	0.331465348	NA	HAX1_HUMAN	HCLS1-associated protein X-1 (HS1-associating protein X-1) (HAX-1) (HS1-binding protein 1) (HSP1BP-1)
Q9UJS0	0.481595836	0.331465348	NA	CMC2_HUMAN	Calcium-binding mitochondrial carrier protein Aralar2 (Citrin) (Mitochondrial aspartate glutamate carrier 2) (Solute carrier family 25 member 13)
Q9C0C7	-1.763743973	0.342970868	NA	AMRA1_HUMAN	Activating molecule in BECN1-regulated autophagy protein 1
Q3ZCQ8	0.276365536	0.370721011	NA	TIM50_HUMAN	Mitochondrial import inner membrane translocase subunit TIM50
P12236	-1.192190146	0.424925602	NA	ADT3_HUMAN	ADP/ATP translocase 3 (ADP,ATP carrier protein 3) (ADP,ATP carrier protein, isoform T2) (ANT 2) (Adenine nucleotide translocator 3) (ANT 3)
P35244	-1.234934617	0.424925602	NA	RFA3_HUMAN	Replication protein A 14 kDa subunit (RP-A p14) (Replication factor A protein 3) (RF-A protein 3)
Q9UL15	-0.677694917	0.424925602	NA	BAG5_HUMAN	BAG family molecular chaperone regulator 5 (BAG-5) (Bcl-2-associated athanogene 5)
P04792	-0.358632017	0.430601226	NA	HSPB1_HUMAN	Heat shock protein beta-1 (HspB1) (28 kDa heat shock protein) (Heat shock 27 kDa protein) (HSP 27) (Stress-responsive protein 27) (SRP27)
Q13015	-0.561837314	0.430601226	NA	AF1Q_HUMAN	Protein AF1q
O00410	-0.462616315	0.43941473	NA	IPO5_HUMAN	Importin-5 (Imp5) (Importin subunit beta-3) (Ran-binding protein 5) (RanBP5)
P63167	0.420578264	0.43941473	NA	DYL1_HUMAN	Dynein light chain 1, cytoplasmic (8 kDa dynein light chain) (DLC8) (Dynein light chain LC8-type 1) (Protein inhibitor of neuronal nitric oxide synthase) (PIN)

Protein	log2FC	adj.pvalue	issue	Protein_name	Protein_desc
Q8N163	0.571695046	0.524055338	NA	K1967_HUMAN	DBIRD complex subunit KIAA1967 (Deleted in breast cancer gene 1 protein) (DBC-1) (DBC.1) (p30 DBC)
Q14257	-0.41466806	0.543544048	NA	RCN2_HUMAN	Reticulocalbin-2 (Calcium-binding protein ERC-55) (E6-binding protein) (E6BP)
Q9H078	0.348033268	0.543544048	NA	CLPB_HUMAN	Caseinolytic peptidase B protein homolog (Suppressor of potassium transport defect 3)
A3KMH1	-0.366792973	0.643933901	NA	VWA8_HUMAN	von Willebrand factor A domain-containing protein 8
P52272	-0.369985934	0.643933901	NA	HNRPM_HUMAN	Heterogeneous nuclear ribonucleoprotein M (hnRNP M)
Q9BPW8	0.372187924	0.654728893	NA	NIPS1_HUMAN	Protein NipSnap homolog 1 (NipSnap1)
Q9NZ01	0.396998262	0.68567409	NA	TECR_HUMAN	Very-long-chain enoyl-CoA reductase (EC 1.3.1.93) (Synaptic glycoprotein SC2) (Trans-2,3-enoyl-CoA reductase) (TER)
Q92900	0.409060941	0.695930472	NA	RENT1_HUMAN	Regulator of nonsense transcripts 1 (EC 3.6.4.-) (ATP-dependent helicase RENT1) (Nonsense mRNA reducing factor 1) (NORF1) (Up-frameshift suppressor 1 homolog) (hUpf1)
Q8WWC4	0.330024845	0.733000473	NA	CB047_HUMAN	Uncharacterized protein C2orf47, mitochondrial
P36776	-0.470310013	0.736083749	NA	LONM_HUMAN	Lon protease homolog, mitochondrial (EC 3.4.21.-) (LONHs) (Lon protease-like protein) (LONP) (Mitochondrial ATP-dependent protease Lon) (Serine protease 15)
Q96EY1	0.227345761	0.736083749	NA	DNJA3_HUMAN	DnaJ homolog subfamily A member 3, mitochondrial (DnaJ protein Tid-1) (hTid-1) (Hepatocellular carcinoma-associated antigen 57)
P53007	0.34509677	0.738813691	NA	TXTP_HUMAN	Tricarboxylate transport protein, mitochondrial (Citrate transport protein) (CTP) (Solute carrier family 25 member 1) (Tricarboxylate carrier protein)
Q9BW92	-0.267806475	0.738813691	NA	SYTM_HUMAN	Threonine--tRNA ligase, mitochondrial (EC 6.1.1.3) (Threonyl-tRNA synthetase) (ThrRS)

Protein	log2FC	adj.pvalue	issue	Protein_name	Protein_desc
Q9BRX2	0.234014397	0.743889705	NA	PELO_HUMAN	Protein pelota homolog (EC 3.1.-.-)
P51570	0.278257599	0.744665435	NA	GALK1_HUMAN	Galactokinase (EC 2.7.1.6) (Galactose kinase)
Q8N4Q1	-0.615545492	0.766483669	NA	MIA40_HUMAN	Mitochondrial intermembrane space import and assembly protein 40 (Coiled-coil-helix-coiled-coil-helix domain-containing protein 4)
Q9BUF5	-0.206507132	0.766483669	NA	TBB6_HUMAN	Tubulin beta-6 chain
O75306	0.17106912	0.769603418	NA	NDUS2_HUMAN	NADH dehydrogenase [ubiquinone] iron-sulfur protein 2, mitochondrial (EC 1.6.5.3) (EC 1.6.99.3) (Complex I-49kD) (CI-49kD) (NADH-ubiquinone oxidoreductase 49 kDa subunit)
O95831	-0.140202629	0.769603418	NA	AIFM1_HUMAN	Apoptosis-inducing factor 1, mitochondrial (EC 1.-.-.-) (Programmed cell death protein 8)
P30837	-0.239388426	0.769603418	NA	AL1B1_HUMAN	Aldehyde dehydrogenase X, mitochondrial (EC 1.2.1.3) ((Aldehyde dehydrogenase family 1 member B1)
P38606	-0.254312268	0.769603418	NA	VATA_HUMAN	V-type proton ATPase catalytic subunit A (V-ATPase subunit A) (EC 3.6.3.14) (V-ATPase 69 kDa subunit) (Vacuolar ATPase isoform VA68) (Vacuolar proton pump subunit alpha)
P46379	-0.346715158	0.769603418	NA	BAG6_HUMAN	Large proline-rich protein BAG6 (BAG family molecular chaperone regulator 6) (BCL2-associated athanogene 6) (BAG-6) (BAG6) (HLA-B-associated transcript 3)
P50402	-0.117134329	0.769603418	NA	EMD_HUMAN	Emerin
P51617	0.448011057	0.769603418	NA	IRAK1_HUMAN	Interleukin-1 receptor-associated kinase 1 (IRAK-1) (EC 2.7.11.1)
P61289	-0.313498799	0.769603418	NA	PSME3_HUMAN	Proteasome activator complex subunit 3 (11S regulator complex subunit gamma) (REG-gamma) (Activator of multicatalytic protease subunit 3) (Proteasome activator 28 subunit gamma) (PA28g)

Protein	log2FC	adj.pvalue	issue	Protein_name	Protein_desc
P78318	0.333682434	0.769603418	NA	IGBP1_HUMAN	Immunoglobulin-binding protein 1 (B-cell signal transduction molecule alpha 4) (Protein alpha-4) (CD79a-binding protein 1) (Protein phosphatase 2/4/6 regulatory subunit) (Renal carcinoma antigen NY-REN-16)
Q15370	-0.61819153	0.769603418	NA	ELOB_HUMAN	Transcription elongation factor B polypeptide 2 (Elongin 18 kDa subunit) (Elongin-B) (EloB) (RNA polymerase II transcription factor SIII subunit B) (SIII p18)
Q15773	0.242786616	0.769603418	NA	MLF2_HUMAN	Myeloid leukemia factor 2 (Myelodysplasia-myeloid leukemia factor 2)
Q6P4A7	-0.430475379	0.769603418	NA	SFXN4_HUMAN	Sideroflexin-4 (Breast cancer resistance marker 1)
Q93008	-0.239728574	0.769603418	NA	USP9X_HUMAN	Probable ubiquitin carboxyl-terminal hydrolase FAF-X (EC 3.4.19.12) (Deubiquitinating enzyme FAF-X) (Fat facets in mammals) (hFAM) (Fat facets protein-related, X-linked) (Ubiquitin-specific protease 9, X chromosome) (Ubiquitin-specific-processing protease FAF-X)
Q99615	0.142111646	0.769603418	NA	DNJC7_HUMAN	DnaJ homolog subfamily C member 7 (Tetratricopeptide repeat protein 2) (TPR repeat protein 2)
Q9UNE7	-0.191495193	0.769603418	NA	CHIP_HUMAN	E3 ubiquitin-protein ligase CHIP (EC 6.3.2.-) (Antigen NY-CO-7) (CLL-associated antigen KW-8) (Carboxy terminus of Hsp70-interacting protein) (STIP1 homology and U box-containing protein 1)
O14545	-0.144080208	0.820461412	NA	TRAD1_HUMAN	TRAF-type zinc finger domain-containing protein 1
O15027	-0.085698534	0.820461412	NA	SC16A_HUMAN	Protein transport protein Sec16A (SEC16 homolog A)
O15269	0.199204453	0.820461412	NA	SPTC1_HUMAN	Serine palmitoyltransferase 1 (EC 2.3.1.50) (Long chain base biosynthesis protein 1) (LCB 1) (Serine-palmitoyl-CoA transferase 1) (SPT 1)
O95816	0.073670551	0.820461412	NA	BAG2_HUMAN	BAG family molecular chaperone regulator 2 (BAG-2) (Bcl-2-associated athanogene 2)

Protein	log2FC	adj.pvalue	issue	Protein_name	Protein_desc
P04350	0.287128387	0.820461412	NA	TBB4A_HUMAN	Tubulin beta-4A chain (Tubulin 5 beta) (Tubulin beta-4 chain)
P21953	-0.212591691	0.820461412	NA	ODBB_HUMAN	2-oxoisovalerate dehydrogenase subunit beta, mitochondrial (EC 1.2.4.4) (Branched-chain alpha-keto acid dehydrogenase E1 component beta chain) (BCKDH E1-beta)
P49411	-0.092381499	0.820461412	NA	EFTU_HUMAN	Elongation factor Tu, mitochondrial (EF-Tu) (P43)
P55786	0.15087721	0.820461412	NA	PSA_HUMAN	Puromycin-sensitive aminopeptidase (PSA) (EC 3.4.11.14) (Cytosol alanyl aminopeptidase) (AAP-S)
Q04837	-0.137241209	0.820461412	NA	SSBP_HUMAN	Single-stranded DNA-binding protein, mitochondrial (Mt-SSB) (MtSSB) (PWP1-interacting protein 17)
Q13509	-0.208486851	0.820461412	NA	TBB3_HUMAN	Tubulin beta-3 chain (Tubulin beta-4 chain) (Tubulin beta-III)
Q15293	-0.155317677	0.820461412	NA	RCN1_HUMAN	Reticulocalbin-1
Q16891	0.374676776	0.820461412	NA	IMMT_HUMAN	Mitochondrial inner membrane protein (Cell proliferation-inducing gene 4/52 protein) (Mitofilin) (p87/89)
Q5TA31	0.350975425	0.820461412	NA	RN187_HUMAN	E3 ubiquitin-protein ligase RNF187 (EC 6.3.2.-) (RING domain AP1 coactivator 1) (RACO-1) (RING finger protein 187)
Q8NB90	-0.159480949	0.820461412	NA	SPAT5_HUMAN	Spermatogenesis-associated protein 5 (ATPase family protein 2 homolog) (Spermatogenesis-associated factor protein)
Q8WXK3	0.282478559	0.820461412	NA	ASB13_HUMAN	Ankyrin repeat and SOCS box protein 13 (ASB-13)
Q96PK6	-0.290055912	0.820461412	NA	RBM14_HUMAN	RNA-binding protein 14 (Paraspeckle protein 2) (PSP2) (RNA-binding motif protein 14) (RRM-containing coactivator activator/modulator) (Synaptotagmin-interacting protein)
Q9BSD7	0.107155465	0.820461412	NA	NTPCR_HUMAN	Cancer-related nucleoside-triphosphatase (EC 3.6.1.15) (Nucleoside triphosphate phosphohydrolase)

Protein	log2FC	adj.pvalue	issue	Protein_name	Protein_desc
Q9H3G5	-0.117229046	0.820461412	NA	CPVL_HUMAN	Probable serine carboxypeptidase CPVL (EC 3.4.16.-) (Carboxypeptidase, vitellogenic-like) (Vitellogenic carboxypeptidase-like protein) (VCP-like protein) (hVLP)
Q9NZL4	-0.120614013	0.820461412	NA	HPBP1_HUMAN	Hsp70-binding protein 1 (HspBP1) (Heat shock protein-binding protein 1) (Hsp70-binding protein 2) (HspBP2) (Hsp70-interacting protein 1) (Hsp70-interacting protein 2)
Q9ULX6	0.081235332	0.820461412	NA	AKP8L_HUMAN	A-kinase anchor protein 8-like (AKAP8-like protein) (Helicase A-binding protein 95) (HAP95) (Homologous to AKAP95 protein) (HA95) (Neighbor of A-kinase-anchoring protein 95) (Neighbor of AKAP95)
Q9HCN8	0.107150753	0.89548947	NA	SDF2L_HUMAN	Stromal cell-derived factor 2-like protein 1 (SDF2-like protein 1) (PWP1-interacting protein 8)
O60762	0.037267372	0.926959221	NA	DPM1_HUMAN	Dolichol-phosphate mannosyltransferase (EC 2.4.1.83) (Dolichol-phosphate mannose synthase) (DPM synthase) (Dolichyl-phosphate beta-D-mannosyltransferase)
P00367	-0.037204596	0.926959221	NA	DHE3_HUMAN	Glutamate dehydrogenase 1, mitochondrial (GDH 1) (EC 1.4.1.3)
O14641	0.03559104	0.937940159	NA	DVL2_HUMAN	Segment polarity protein dishevelled homolog DVL-2 (Dishevelled-2) (DSH homolog 2)
Q8IWZ3	-0.034780493	0.937940159	NA	ANKH1_HUMAN	Ankyrin repeat and KH domain-containing protein 1 (HIV-1 Vpr-binding ankyrin repeat protein) (Multiple ankyrin repeats single KH domain) (hMASK)
Q9Y5V3	-0.022215121	0.937940159	NA	MAGD1_HUMAN	Melanoma-associated antigen D1 (MAGE tumor antigen CCF) (MAGE-D1 antigen)
Q13951	NA	NA	completeMissing	PEBB_HUMAN	Core-binding factor subunit beta (CBF-beta) (Polyomavirus enhancer-binding protein 2 beta subunit) (PEA2-beta) (PEBP2-beta)

Table 4. Key resources table (antibodies, chemicals, cell lines, recombinant DNA, sequence-based reagents, and softwares)

REAGENT or RESOURCE	SOURCE	IDENTIFIER
Antibodies		
Rabbit polyclonal anti-AMBRA1	EMD-Millipore	ABC131
Rabbit polyclonal anti-AMBRA1	Bethyl	A302
Mouse monoclonal anti-ELOC	BD Biosciences	#610761
Rabbit monoclonal anti-ELOB	Abcam	ab154854
Rabbit monoclonal anti-CUL4A	Abcam	ab92554
Mouse monoclonal anti-DDB1	Thermo Fisher	#39-9901
Mouse monoclonal anti-STAT3	Cell Signaling Technology	#9139
Rabbit monoclonal anti-Phospho-STAT3 (Tyr705)	Cell Signaling Technology	#9145
Rabbit polyclonal anti-SOCS3	Cell Signaling Technology	#2932
Rabbit polyclonal anti-GAPDH	Cell Signaling Technology	#2118
Mouse monoclonal anti-GAPDH	Thermo Fisher	MA5-15738
Rabbit polyclonal anti-GFP	Abcam	ab6556
Mouse monoclonal anti-GFP	Santa Cruz	sc9996
Mouse monoclonal anti-HA	Cell Signaling Technology	#2367
Rabbit polyclonal anti-Myc	Abcam	ab9106
Guinea pig polyclonal anti-p62/SQSTM1	Progen	GP62-C
Mouse monoclonal anti-p62/SQSTM1	Novus	#2C11
Rabbit polyclonal anti-LC3	EMD-Millipore	ABC232
Goat polyclonal anti-ATG7	Santa Cruz	sc8668
Rabbit polyclonal anti-ATG12	Cell Signaling Technology	#4180
Chemicals, Peptides, and Recombinant Proteins		
Bafilomycin A1	Calbiochem	196000
IL-6	EMD-Millipore	IL006
3X FLAG peptides	Elimbio	NA
RapiGest SF surfactant	Waters	NA
DUB inhibitor PR-619	Lifesensors	SI9619
Experimental Models: Cell Lines		
SupT11-A3G	[95]	
HEK293	UCSF Cell Culture Facility	
293T/17	UCSF Cell Culture Facility	
Jurkat E6-1	UCSF Cell Culture Facility	
HeLa	ATCC	CCL-2
Hep3B	Rik Derynck Lab/UCSF	
Recombinant DNA		
pCDH-EF1-MCS-IRES-GFP FLAG-ELOC	This paper	NA

Recombinant DNA		
pCDH-EF1-MCS-IRES-GFP FLAG-SKP1	This paper	NA
Tet-On 3G ZeoR SOCS3-GFP	This paper	NA
Tet-On 3G ZeoR VIF-GFP	This paper	NA
Tet-On 3G ZeoR VHL-GFP	This paper	NA
Tet-On 3G ZeoR PPIL5-GFP	This paper	NA
Tet-On 3G ZeoR AMBRA1-FLAG	This paper	NA
AMBRA1 ZeoR Δ34H-FLAG	This paper	NA
pCDH-EF1-MCS-T2A-HygroR mCherry-FLAG	This paper	NA
pCDH-EF1-MCS-T2A-HygroR AMBRA1-FLAG	This paper	NA
Sequence-Based Reagents		
pLKO.1 Control sh-NT	Sigma-Aldrich	SHC002
pLKO.1 sh-AMBRA1 #1; target GGCTTGGCCTATGGTACTAAC	Sigma-Aldrich	TRCN0000417120
pLKO.1 sh-AMBRA1 #2; target GGCCACTGGGAAAGAATTTAC	Sigma-Aldrich	TRCN0000441636
pLKO.1 sh-AMBRA1 #3; target CCCACTTTCTCCTAGTAACAT	Sigma-Aldrich	TRCN0000167886
si-AMBRA1; UUUGUUAGUACCAUAGGCCAAGCCA	Thermo	pre-designed Stealth#3156
si-ELOB; GCUGUACAAGGAUGACCAAtt	This paper	NA
si-ELOC; CGAACUUCUUAGAUUGUUAtt	This paper	NA
si-CUL5; AGCUGAUUCAGUUAAUAUAtt	This paper	NA
si-SOCS3	Sigma-Aldrich	pre-designed SASI_Hs01_00179195
si-Control	Thermo	Stealth siRNA negative control medium GC, Cat#12935300
SpCas9-P2A-GFP AMBRA1 sgRNA TGGTAGAAGATAAAACCCGG	This paper	NA
SpCas9-P2A-puro ATG7 ATAGCTGGGCAGCAACGGGC	This paper	NA
SpCas9-P2A-puro ATG12 GAAACTGCAGCGGAAGACGG	This paper	NA
AMBRA1 genotyping forward primer tagaactagtggatccCTTCTCGTTGCAGAAGTCGT	This paper	NA
AMBRA1 genotyping reverse primer gcttgatatcgaattcCAGATATGTCAACTCTCCCACACA	This paper	NA
ATG7 genotyping forward primer caccg TGGGGGACAGTAGAACAGCA	This paper	NA
ATG7 genotyping reverse primer aaac CCTGGATGTCCTCTCCCTGA	This paper	NA
ATG12 genotyping forward primer caccgAGCCGGGAACACCAAGTTT	This paper	NA
ATG12 genotyping reverse primer aaacGTGGCAGCCAAGTATCAGGC	This paper	NA
Software and Algorithms		
Image Studio Lite software	LI-COR	
Cytoscape	[88]	
R	[89]	

References

1. Bonifacino, J.S. and A.M. Weissman, *Ubiquitin and the control of protein fate in the secretory and endocytic pathways*. Annu Rev Cell Dev Biol, 1998. **14**: p. 19-57.

2. Frescas, D. and M. Pagano, *Deregulated proteolysis by the F-box proteins SKP2 and beta-TrCP: tipping the scales of cancer*. Nat Rev Cancer, 2008. **8**(6): p. 438-49.

3. Reavie, L., et al., *Regulation of hematopoietic stem cell differentiation by a single ubiquitin ligase-substrate complex*. Nat Immunol, 2010. **11**(3): p. 207-15.

4. Petroski, M.D. and R.J. Deshaies, *Function and regulation of cullin–RING ubiquitin ligases*. Nature Reviews Molecular Cell Biology, 2005. **6**(1): p. 9-20.

5. Hua, Z. and R.D. Vierstra, *The Cullin-RING Ubiquitin-Protein Ligases*. Annual Review of Plant Biology, 2011. **62**(1): p. 299-334.

6. Duda, D.M., et al., *Structural Insights into NEDD8 Activation of Cullin-RING Ligases: Conformational Control of Conjugation*. Cell, 2008. **134**(6): p. 995-1006.

7. Zhou, P. and P.M. Howley, *Ubiquitination and degradation of the substrate recognition subunits of SCF ubiquitin–protein ligases*. Molecular cell, 1998. **2**(5): p. 571-580.

8. Galan, J.-M. and M. Peter, *Ubiquitin-dependent degradation of multiple F-box proteins by an autocatalytic mechanism*. Proceedings of the National Academy of Sciences, 1999. **96**(16): p. 9124-9129.

9. Wee, S., et al., *CSN facilitates Cullin–RING ubiquitin ligase function by counteracting autocatalytic adapter instability*. Nature Cell Biology, 2005. **7**(4): p. 387-391.

10. Schmidt, M.W., et al., *F-Box-Directed CRL Complex Assembly and Regulation by the CSN and CAND1*. Molecular Cell, 2009. **35**(5): p. 586-597.

11. Tron, Adriana E., et al., *The Glomuvenous Malformation Protein Glomulin Binds Rbx1 and Regulates Cullin RING Ligase-Mediated Turnover of Fbw7*. Molecular Cell, 2012. **46**(1): p. 67-78.

12. Duda, David M., et al., *Structure of a Glomulin-RBX1-CUL1 Complex: Inhibition of a RING E3 Ligase through Masking of Its E2-Binding Surface*. Molecular Cell, 2012. **47**(3): p. 371-382.

13. Wei, W., et al., *Degradation of the SCF component Skp2 in cell-cycle phase G1 by the anaphase-promoting complex*. Nature, 2004. **428**(6979): p. 194-198.

14. Bashir, T., et al., *Control of the SCF(Skp2-Cks1) ubiquitin ligase by the APC/C(Cdh1) ubiquitin ligase*. Nature, 2004. **428**(6979): p. 190-193.

15. Abbas, T., et al., *CRL1-FBXO11 Promotes Cdt2 Ubiquitylation and Degradation and Regulates Pr-Set7/Set8-Mediated Cellular Migration*. Molecular Cell, 2013. **49**(6): p. 1147-1158.

16. Rossi, M., et al., *Regulation of the CRL4Cdt2 Ubiquitin Ligase and Cell-Cycle Exit by the SCFFbxo11 Ubiquitin Ligase*. Molecular Cell, 2013. **49**(6): p. 1159-1166.

17. Maria Fimia, G., et al., *Ambra1 regulates autophagy and development of the nervous system*. Nature, 2007.

18. Bartolomeo, S.D., et al., *The dynamic interaction of AMBRA1 with the dynein motor complex regulates mammalian autophagy*. The Journal of Cell Biology, 2010. **191**(1): p. 155-168.

19. Nazio, F., et al., *mTOR inhibits autophagy by controlling ULK1 ubiquitylation, self-association and function through AMBRA1 and TRAF6*. Nat Cell Biol, 2013. **15**(4): p. 406-16.

20. Cianfanelli, V., et al., *AMBRA1 links autophagy to cell proliferation and tumorigenesis by promoting c-Myc dephosphorylation and degradation*. Nat Cell Biol, 2015. **17**(1): p. 20-30.

21. Strappazzon, F., et al., *Mitochondrial BCL-2 inhibits AMBRA1-induced autophagy*. Embo j, 2011. **30**(7): p. 1195-208.

22. Jin, J., et al., *A Family of Diverse Cul4-Ddb1-Interacting Proteins Includes Cdt2, which Is Required for S Phase Destruction of the Replication Factor Cdt1*. Molecular Cell, 2006. **23**(5): p. 709-721.

23. Sugasawa, K., et al., *UV-induced ubiquitylation of XPC protein mediated by UV-DDB-ubiquitin ligase complex*. Cell, 2005. **121**(3): p. 387-400.

24. Fischer, E.S., et al., *The molecular basis of CRL4DDB2/CSA ubiquitin ligase architecture, targeting, and activation*. Cell, 2011. **147**(5): p. 1024-39.

25. Sansam, C.L., et al., *DTL/CDT2 is essential for both CDT1 regulation and the early G2/M checkpoint*. Genes & Development, 2006. **20**(22): p. 3117-3129.

26. Jackson, S. and Y. Xiong, *CRL4s: the CUL4-RING E3 ubiquitin ligases*. Trends Biochem Sci, 2009. **34**(11): p. 562-70.

27. Fischer, E.S., et al., *Structure of the DDB1-CRBN E3 ubiquitin ligase in complex with thalidomide*. Nature, 2014. **512**(7512): p. 49-53.

28. Petzold, G., E.S. Fischer, and N.H. Thoma, *Structural basis of lenalidomide-induced CK1alpha degradation by the CRL4(CRBN) ubiquitin ligase*. Nature, 2016. **532**(7597): p. 127-30.

29. Xia, P., et al., *WASH inhibits autophagy through suppression of Beclin 1 ubiquitination*. The EMBO journal, 2013. **32**(20): p. 2685-2696.

30. Shi, C.S. and J.H. Kehrl, *TRAF6 and A20 regulate lysine 63-linked ubiquitination of Beclin-1 to control TLR4-induced autophagy*. Sci Signal, 2010. **3**(123): p. ra42.

31. Jäger, S., et al., *Global landscape of HIV–human protein complexes*. Nature, 2011.

32. Yu, X., et al., *Induction of APOBEC3G ubiquitination and degradation by an HIV-1 Vif-Cul5-SCF complex*. Science (New York, N.Y.), 2003. **302**(5647): p. 1056-1060.

33. Marin, M., et al., *HIV-1 Vif protein binds the editing enzyme APOBEC3G and induces its degradation*. Nature Medicine, 2003. **9**(11): p. 1398-1403.

34. Mehle, A., *Phosphorylation of a novel SOCS-box regulates assembly of the HIV-1 Vif-Cul5 complex that promotes APOBEC3G degradation*. Genes & Development, 2004. **18**(23): p. 2861-2866.

35. Luo, Y., et al., *HIV–host interactome revealed directly from infected cells*. Nature Microbiology, 2016. **1**(7): p. 16068.

36. Antonioli, M., et al., *AMBRA1 interplay with cullin E3 ubiquitin ligases regulates autophagy dynamics*. Dev Cell, 2014. **31**(6): p. 734-746.

37. Mangeat, B., et al., *HIV-1 Vpu Neutralizes the Antiviral Factor Tetherin/BST-2 by Binding It and Directing Its Beta-TrCP2-Dependent Degradation*. PLOS Pathog, 2009. **5**(9): p. e1000574.

38. Margottin, F., et al., *A novel human WD protein, h-beta TrCp, that interacts with HIV-1 Vpu connects CD4 to the ER degradation pathway through an F-box motif*. Molecular Cell, 1998. **1**(4): p. 565-574.

39. Berger, G., et al., *G2/M Cell Cycle Arrest Correlates with Primate Lentiviral Vpr Interaction with the SLX4 Complex*. Journal of Virology, 2015. **89**(1): p. 230-240.

40. Schwefel, D., et al., *Structural basis of lentiviral subversion of a cellular protein degradation pathway*. Nature, 2014. **505**(7482): p. 234-8.

41. Weissman, A.M., N. Shabek, and A. Ciechanover, *The predator becomes the prey: regulating the ubiquitin system by ubiquitylation and degradation*. Nat Rev Mol Cell Biol, 2011. **12**(9): p. 605-20.

42. He, Y.J., et al., *DDB1 functions as a linker to recruit receptor WD40 proteins to CUL4-ROC1 ubiquitin ligases*. Genes & Development, 2006. **20**(21): p. 2949-2954.

43. Decorsière, A., et al., *Hepatitis B virus X protein identifies the Smc5/6 complex as a host restriction factor*. Nature, 2016. **531**(7594): p. 386-380.

44. Angers, S., et al., *Molecular architecture and assembly of the DDB1–CUL4A ubiquitin ligase machinery*. Nature, 2006.

45. Notredame, C., D.G. Higgins, and J. Heringa, *T-coffee: a novel method for fast and accurate multiple sequence alignment*. Journal of Molecular Biology, 2000. **302**(1): p. 205-217.

46. Robert, X. and P. Gouet, *Deciphering key features in protein structures with the new ENDscript server*. Nucleic Acids Research, 2014. **42**(W1): p. W320-W324.

47. Olma, M.H., et al., *An interaction network of the mammalian COP9 signalosome identifies Dda1 as a core subunit of multiple Cul4-based E3 ligases*. J Cell Sci, 2009. **122**(Pt 7): p. 1035-1044.

48. Enchev, Radoslav I., et al., *Structural Basis for a Reciprocal Regulation between SCF and CSN*. Cell Reports, 2012. **2**(3): p. 616-627.

49. Lingaraju, G.M., et al., *Crystal structure of the human COP9 signalosome*. Nature, 2014. **512**(7513): p. 161-165.

50. Fischer, E.S., et al., *The molecular basis of CRL4DDB2/CSA ubiquitin ligase architecture, targeting, and activation*. Cell, 2011. **147**(5): p. 1024-39.

51. Choi, M., et al., *MSstats: an R package for statistical analysis of quantitative mass spectrometry-based proteomic experiments*. Bioinformatics, 2014. **30**(17): p. 2524-6.

52. Biasini, M., et al., *SWISS-MODEL: modelling protein tertiary and quaternary structure using evolutionary information*. Nucleic Acids Res, 2014. **42**(Web Server issue): p. W252-8.

53. Klionsky, D.J., et al., *Guidelines for the use and interpretation of assays for monitoring autophagy (3rd edition)*. Autophagy, 2016. **12**(1): p. 1-222.

54. Stebbins, C.E., *Structure of the VHL-ElonginC-ElonginB Complex: Implications for VHL Tumor Suppressor Function*. Science, 1999. **284**(5413): p. 455-461.

55. Kim, W., et al., *Systematic and quantitative assessment of the ubiquitin-modified proteome*. Mol Cell, 2011. **44**(2): p. 325-40.

56. Listovsky, T., et al., *Mammalian Cdh1/Fzr mediates its own degradation*. The EMBO Journal, 2004. **23**(7): p. 1619-1626.

57. Foe, Ian T., et al., *Ubiquitination of Cdc20 by the APC Occurs through an Intramolecular Mechanism*. Current Biology, 2011. **21**(22): p. 1870-1877.

58. Geyer, R., et al., *BTB/POZ domain proteins are putative substrate adaptors for cullin 3 ubiquitin ligases*. Molecular cell, 2003. **12**(3): p. 783-790.

59. Lang, R., et al., *SOCS3 regulates the plasticity of gp130 signaling*. Nat Immunol, 2003. **4**(6): p. 546-50.

60. Croker, B.A., et al., *SOCS3 negatively regulates IL-6 signaling in vivo*. Nat Immunol, 2003. **4**(6): p. 540-5.

61. Boyle, K., et al., *The SOCS box of suppressor of cytokine signaling-3 contributes to the control of G-CSF responsiveness in vivo*. Blood, 2007. **110**(5): p. 1466-1474.

62. Lecossier, D., et al., *Hypermutation of HIV-1 DNA in the Absence of the Vif Protein*. Science, 2003. **300**(5622): p. 1112-1112.

63. Mangeat, B., et al., *Broad antiretroviral defence by human APOBEC3G through lethal editing of nascent reverse transcripts*. Nature, 2003. **424**(6944): p. 99-103.

64. Yu, H., D. Pardoll, and R. Jove, *STATs in cancer inflammation and immunity: a leading role for STAT3*. Nature Reviews Cancer, 2009. **9**(11): p. 798-809.

65. Bosu, D.R. and E.T. Kipreos, *Cullin-RING ubiquitin ligases: global regulation and activation cycles*. Cell Division, 2008. **3**: p. 7.

66. Lisztwan, J., et al., *The von Hippel-Lindau tumor suppressor protein is a component of an E3 ubiquitin-protein ligase activity*. Genes Dev, 1999. **13**(14): p. 1822-33.

67. Welcker, M., et al., *Fbw7 dimerization determines the specificity and robustness of substrate degradation*. Genes & Development, 2013. **27**(23): p. 2531-2536.

68. Koepp, D.M., et al., *Phosphorylation-dependent ubiquitination of cyclin E by the SCFFbw7 ubiquitin ligase*. Science, 2001. **294**(5540): p. 173-7.

69. Hao, B., et al., *Structure of a Fbw7-Skp1-Cyclin E Complex: Multisite-Phosphorylated Substrate Recognition by SCF Ubiquitin Ligases*. Molecular Cell, 2007. **26**(1): p. 131-143.

70. Shao, Q., et al., *Polyubiquitination of APOBEC3G Is Essential for Its Degradation by HIV-1 Vif*. Journal of Virology, 2010. **84**(9): p. 4840-4844.

71. de Bie, P. and A. Ciechanover, *Ubiquitination of E3 ligases: self-regulation of the ubiquitin system via proteolytic and non-proteolytic mechanisms*. Cell Death Differ, 2011. **18**(9): p. 1393-402.

72. Bennett, E.J., et al., *Dynamics of Cullin-RING Ubiquitin Ligase Network Revealed by Systematic Quantitative Proteomics*. Cell, 2010. **143**(6): p. 951-965.

73. Pierce, Nathan W., et al., *Cand1 Promotes Assembly of New SCF Complexes through Dynamic Exchange of F Box Proteins*. Cell, 2013. **153**(1): p. 206-215.

74. McClellan, A.J., M.D. Scott, and J. Frydman, *Folding and quality control of the VHL tumor suppressor proceed through distinct chaperone pathways*. Cell, 2005. **121**(5): p. 739-48.

75. Guo, Y., et al., *Structural basis for hijacking CBF-β and CUL5 E3 ligase complex by HIV-1 Vif*. Nature, 2014. **505**(7482): p. 229-33.

76. Babon, J.J., et al., *The SOCS Box Encodes a Hierarchy of Affinities for Cullin5: Implications for Ubiquitin Ligase Formation and Cytokine Signalling Suppression*. Journal of Molecular Biology, 2009. **387**(1): p. 162-174.

77. Xia, P., et al., *RNF2 is recruited by WASH to ubiquitinate AMBRA1 leading to downregulation of autophagy*. Cell Research, 2014. **24**(8): p. 943-958.

78. Murray, P.J., *The JAK-STAT Signaling Pathway: Input and Output Integration*. The Journal of Immunology, 2007. **178**(5): p. 2623-2629.

79. White, C.A. and N.A. Nicola, *SOCS3: An essential physiological inhibitor of signaling by interleukin-6 and G-CSF family cytokines*. JAK-STAT, 2013. **2**(4): p. e25045.

80. Kershaw, N.J., et al., *Reconstruction of an active SOCS3-based E3 ubiquitin ligase complex in vitro : identification of the active components and JAK2 and gp130 as substrates*. Growth Factors, 2014. **32**(1): p. 1-10.

81. Yoshimura, A., T. Naka, and M. Kubo, *SOCS proteins, cytokine signalling and immune regulation*. Nature Reviews. Immunology, 2007. **7**(6): p. 454-465.

82. Zhang, J.-G., et al., *The SOCS box of suppressor of cytokine signaling-1 is important for inhibition of cytokine action in vivo*. Proceedings of the National Academy of Sciences, 2001. **98**(23): p. 13261-13265.

83. Brinkman, E.K., et al., *Easy quantitative assessment of genome editing by sequence trace decomposition*. Nucleic Acids Res, 2014. **42**(22): p. e168.

84. Cox, J. and M. Mann, *MaxQuant enables high peptide identification rates, individualized p.p.b.-range mass accuracies and proteome-wide protein quantification*. Nature Biotechnology, 2008. **26**(12): p. 1367-1372.

85. Sowa, M.E., et al., *Defining the Human Deubiquitinating Enzyme Interaction Landscape*. Cell, 2009. **138**(2): p. 389-403.

86. Choi, H., et al., *SAINT: probabilistic scoring of affinity purification–mass spectrometry data*. Nature Methods, 2011. **8**(1): p. 70-73.

87. Choi, M., et al., *MSstats: an R package for statistical analysis of quantitative mass spectrometry-based proteomic experiments*. Bioinformatics, 2014: p. btu305.

88. Shannon, P., et al., *Cytoscape: a software environment for integrated models of biomolecular interaction networks*. Genome research, 2003. **13**(11): p. 2498-2504.

89. Team, R.C., *R: A Language and Environment for Statistical Computing*. 2015, Vienna, Austria: R Foundation for Statistical Computing.

90. Muller, B., et al., *Construction and characterization of a fluorescently labeled infectious human immunodeficiency virus type 1 derivative*. J Virol, 2004. **78**(19): p. 10803-13.

91. Holmes, M., F. Zhang, and P.D. Bieniasz, *Single-Cell and Single-Cycle Analysis of HIV-1 Replication*. PLOS Pathogens, 2015. **11**(6): p. e1004961.

92. Dettenhofer, M. and X.-F. Yu, *Highly purified human immunodeficiency virus type 1 reveals a virtual absence of Vif in virions*. Journal of virology, 1999. **73**(2): p. 1460-1467.

93. Platt, E.J., et al., *Infectious properties of human immunodeficiency virus type 1 mutants with distinct affinities for the CD4 receptor*. J Virol, 1997. **71**(2): p. 883-90.

94. Eekels, J.J., et al., *Inhibition of HIV-1 replication with stable RNAi-mediated knockdown of autophagy factors*. Virol J, 2012. **9**: p. 69.

95. Hultquist, J.F., et al., *Human and Rhesus APOBEC3D, APOBEC3F, APOBEC3G, and APOBEC3H Demonstrate a Conserved Capacity To Restrict Vif-Deficient HIV-1*. Journal of Virology, 2011. **85**(21): p. 11220-11234.

Publishing Agreement

It is the policy of the University to encourage the distribution of all theses, dissertations, and manuscripts. Copies of all UCSF theses, dissertations, and manuscripts will be routed to the library via the Graduate Division. The library will make all theses, dissertations, and manuscripts accessible to the public and will preserve these to the best of their abilities, in perpetuity.

Please sign the following statement:

I hereby grant permission to the Graduate Division of the University of California, San Francisco to release copies of my thesis, dissertation, or manuscript to the Campus Library to provide access and preservation, in whole or in part, in perpetuity.

Gillian Chen

Author Signature

01103/2017

Date